145 pages

NASA TECHNICAL MEMORANDUM NASA TM- 88403

N - 15341

AERODYNAMICS OF THE VIGGEN 37 AIRCRAFT

Part 1: General - Characteristics at Low Speed

Krister Karling
SAAB-Scania, Linkoeping, Sweden

Translation of "FLYGPLAN 37:s Aerodynamik - Del 1: Allmaent - egenskaper vid Laaga farter", Compendium, SAAB-Scania, Linkoeping, Sweden, 1975, 96 pp.

(NASA-TM-88403) AERODYNAMICS OF THE VIGGEN 37 AIRCRAFT. PART 1: GENERAL CHARACTERISTICS AT LOW SPEED (National Aeronautics and Space Administration) 145 p CSCL 01A

N86-28925

G3/02 Unclas 43472

NATIONAL AERONAUTICS AND SPACE ADMINISTRATION
WASHINGTON, D.C. 20546 JUNE 1986

STANDARD TITLE PAGE

1. Report No. NASA TM-88403	2. Government Accession No.	3. Recipient's Catalog No.
4. Title and Subtitle AERODYNAMICS OF AIRCRAFT 37 - Part 1: General Characteristics at Low Speed		5. Report Date June 1986 6. Performing Organization Code
7. Author(s) Krister Karling, SAAB-Scania, Linkoeping, Sweden		8. Performing Organization Report No. 10. Work Unit No.
9. Performing Organization Name and Address Leo Kanner Associates, Redwood City, California 94063		11. Contract or Grant No. NASw-4005 13. Type of Report and Period Covered Translation
12. Sponsoring Agency Name and Address National Aeronautics and Space Administration, Washington, D.C. 20546		14. Sponsoring Agency Code

15. Supplementary Notes

Translation of "Flygplan 37:s Aerodynamik - Part 1: Allmaent - egenskaper vid laaga farter". A compendium from SAAB-Scania, Linkoeping, Sweden, 1975, 96 pp.

16. Abstract

A description of the aerodynamics of FPL (aircraft) 37, the Viggen, and its performance, especially at low speeds. The aerodynamic requirements for the design of the Viggen 37 aircraft are given, including the basic design, performance requirements, aerodynamic characteristics, static and dynamic load test results and flight test results. The Viggen 37 aircraft is designed to be used for air attack, surveilance, pursuit and training applications; it is shown that this aircraft is suitable for short runways, and has good manuevering, acceleration and climbing characteristics. The design objectives for this aircraft were met by utilizing the effect produced by the interference between two triagular wings, positioned in tandem.

17. Key Words (Selected by Author(s))	18. Distribution Statement Unlimited-Unclassified		
19. Security Classif. (of this report) Unclassified	20. Security Classif. (of this page) Unclassified	21. No. of Pages 96	22.

AERODYNAMICS OF AIRCRAFT 37

Part 1: General Characteristics at Low Speed

Krister Karling

SAAB-Scania, Linkoeping, Sweden

LIST OF CONTENTS

		Orig. page	Transl. page
A.	GENERAL - SPECIFICATION OF DEMANDS	4	1
B.	AERODYNAMIC BACKGROUND FOR THE DESIGN OF FPL 37 - CHARACTERISTICS AT LOW SPEED	5	2
1.	LIFT AT LOW SPEED - GENERAL	5	2
1.1	Introduction - The Idea Behind the Design of FPL 37	5	2
1.2	Concept of Lift - Definition of C_L	5	3
1.3	Lift of Two-dimensional Wings - Dependency of the Angle of Attack on the Lift	6	3
1.4	Lift of Three-dimensional Wings - Effect of the Aspect Ratio	8	7
1.5	Dependency of the Lift on the Angle of Attack at Narrow Angles of Attack - Stalling of Conventional Wings	10	10
1.6	Wings with a Small Aspect Ration at Wide Angles of Attack	13	16
1.7	Principle of Leading Edge Separation - the Air Flow Around the Delta Wing	14	17
1.8	Interference Between Fuselage and Wing During An Air Flow Separated by the Leading Edge	19	25
1.9	Interference Between Two Delta Wings in Tandem Formation During An Air Flow Separated by the Leading Edge - Principle Behind FPL 37	20	27
2.	LIFT AND PITCHING MOMENT OF THE FPL 37 CONFIGURATION AT LOW SPEED	27	36
2.1	Introduction	27	36
2.2	Definition of Symmetric Forces and Moments in Respect to FPL 37	28	37
2.3	Characteristics of Normal Force	29	39
2.4	Longitudinal Stability, Pitching Moment and Margin of Stability	32	43
2.5	Effect of Modification of the Leading Edges of the Wing and the Canard on the Pitch Moment	39	52
	a) Cambering	40	53
	b) Partitioning of the Vortex Layer - the "Sawtooth"	41	54

/1*

*Numbers in the Margin indicate pagination in the foreign text.

		Orig. page	Transl. page
2.6	Characteristics of the Pitching Moment of FPL 37 in Comparison With That of Other Aircrafts	42	57
2.7	External Aerodynamic Factors Affecting the Longitudinal Stability of the Basic Aircraft at Low Speed	43	58
	a) Ground Effect	43	58
	b) Air Intake Factor	44	60
2.8	Problems of Longitudinal Stability When Deflecting the Flaps of the Canard	46	62
2.9	Problems of Longitudinal Stability When deflecting the Elevator	47	64
2.10	Problems of Longitudinal Stability in Connection With an External Load	48	65
2.11	Zero Moment, Effect of the Canard Flap	49	68
2.12	Effects of the Elevator	51	71
2.13	Effect of the Elevator in Association with the Ground Effect	54	75
2.14	Pitch Damping, Dynamic Longitudinal Stability	55	76 /2
3.	DRAG AT LOW SPEED	56	79
3.1	Drag on an Untrimmed Aircraft	56	81
3.2	Drag During Trimmed Flying	56	81
3.3	Induction of Induced Drag by Cambering	59	83
3.4	Drag and Tractive Force - Flying in the "Second Regime"	60	84
4.	THE AIRCRAFT IN RELATION TO AN OBLIQUE AIR FLOW, ASYMMETRIC FORCES AND MOMENTS: YAW RESISTANCE AND RUDDER EFFECT	61	86
4.1	General - Definition of Asymmetric Forces and Moments	61	86
4.2	Component Force, Efficiency of the Tail Fin Depending on the Interference Between Fuselage and Wing	62	88
	a) General	62	88
	b) Wing/Tail Fin Interference Due to an Oblique Air Flow - Principle	63	90
	c) Canard/Tail Fin Interference - Principle	65	92
4.3	Variation in Component Force and Yawing Moment in Relation to the Angle of an Oblique Air flow	65	92
4.4	Component Force and Variation in Yawing Moment in Relation to the Angle of Attack - Wing/Tail Interference. - Effect	66	93
4.5	Effect of Tail Fin at Wide Angles of Attack	66	93
4.6	Effect of Tail Fin at Wide Angels of an Oblique Air Flow - Measures Toward Increasing the β Maximum of the Tail Fin	66	94
4.7	Efficiency of the Tail Fin of FPL 37 - Effect Exerted by the Canard	68	96

		Orig. page	Transl. page
4.8	Asymmetric Forces During Extreme Angles of Attack and Symmetric Oblique Air Flow	69	98
4.9	Characteristics of the Component Force and the Yawing Moment of FPL 37 at Low Speed	70	99
	a) Component Force	70	99
	b) Yawing Moment	71	101
4.10	Effect of External Load	74	106
4.11	Yaw Resistance of FPL 37 in Comparison With That of Other Aircrafts	75	108
4.12	Rudder Effect	76	109
4.13	Yaw Damping, Dynamic Yaw Resistance	76	109
5.	ROLLING MOMENT, ROLL RESISTANCE	78	112
5.1	General	78	112
5.2	Effect of Sweep-back Angle	78	112
5.3	Effect of Fuselage/Wing Interference	79	113
5.4	Effect of the V-positioning of the Wing	79	115
5.5	Contribution of the Wing to the Roll Resistance at Wide Angles of Attack	80	115
5.6	Influence of the Ground Effect	80	116
5.7	Contribution of the Tail Fin	81	117
5.8	Contributions of Stabilizer, Canard, Etc., on the Roll Resistance of FPL 37	83	120
5.9	Comparison Between the Roll Resistance of FPL 37 and that of Other Aircrafts	84	121
5.10	Roll Resistance in Relation to an External Load	85	125 /3
5.11	Effect of the Ailerons	86	127
5.12	Dynamic Roll Resistance - Roll Damping	89	130
SELECTED REFERENCES		93	136
APPENDIX NO. 1.	Geometric Data of FPL 37	—	138
APPENDIX NO. 2.	Definitions of the Positive Directions of Forces and Moments	—	139
APPENDIX NO. 3.	Conversion Formulas from Fuselage-related into Wind-related Systems and Vice Versa [1]	—	—

[1] Translator's note: Appendix 3 is not included in the translation.

A. GENERAL - SPECIFICATION OF DEMANDS

Aircraft 37, the "Viggen", is constructed as a standard aircraft, i.e., a basic aircraft which following relatively few alterations of its design can be built as different versions for use during

- attack,
- surveillance,
- pursuit, and
- training.

It was essential for the construction that the aircraft should be able to take off from and land on short run ways (ca. 500 m long) under field conditions. Because of this, the aeronautic envelop of this aircraft (speed, altitude and range of load factors; Fig. 1) is more comprehensive than that of any other Swedish Combat aircraft. A review of the demands on the performance characteristics is illustrated in the following figure.

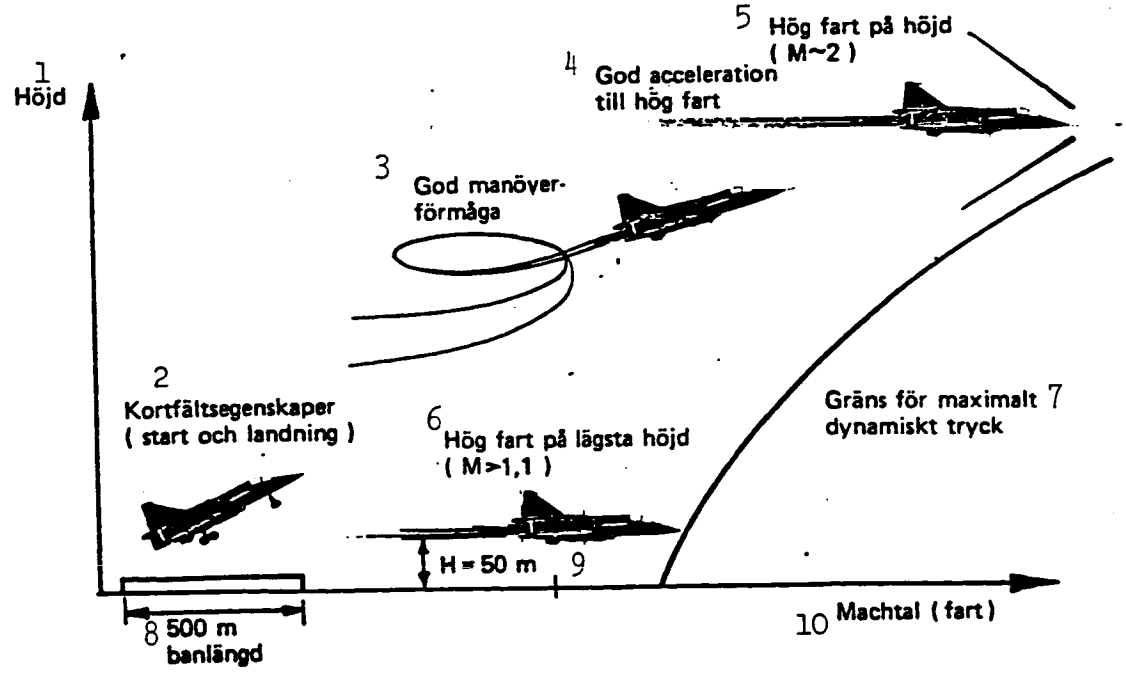

Fig. A. Key: see p. 2.

Key to Fig. A:

1. Altitude.
2. Properties in relations to a short runway (during start and landing.
3. Satisfactory maneuverability.
4. Satisfactory acceleration to high speed.
5. High speed at high altitude ($M \sim 2$).
6. High speed at lowest altitude ($M > 1.1$).
7. Limit of maximum dynamic pressure.
8. Runway, 500 m long.
9. Altitude = 50 meters.
10. Mach number (Speed).

The comprehensive aeronautic envelop resulted in that a characteristic design, developed in Sweden, was selected for FPL 37[1], i.e., one with two delta wings closely positioned in tandem (a canard lay-out).

B. THE AERODYNAMIC BACKGROUND FOR FPL 37 - CHARACTERISTICS AT LOW SPEED /5

1. LIFT AT LOW SPEED - GENERAL

1.1 Introduction - The Idea Behind the Design of FPL 37

The objective during the developmental work on the design of FPL 37 was to create a slender configuration which should also have a highly trimmed lift, especially at low speed. In addition it was desirable to avoid - as far as possible - any heavy and expensive mechanical complications such as wings with a variable swept-back angle and advanced, mobile arrangements for high lift. In short, as far as possible a simple yet effective design for active service should be attempted.

These objectives were reached in respect to FPL 37 by utilizing the effect produced by the interference between two triangular wings, suitably positioned in tandem.

The experiences thereby utilized are to a great extent based on Swedish research over many years and are in many cases unique.

In order to explain the characteristics of the lifting force of the 37-configuration we must start with a brief review of the concept of lift.

---

[1] Translator's note: FPL (Swedish: aircraft) 37 is used throughout the translation in conformity with the original.

Following a general review we will enter into detail upon the problems existing when flying at low speed and especially thos in respect to slender delta wings where the separation by the leading edge can be utilized, "something which seems to clash with the conventional philosophy of classic aerodynamics according to which a contact airflow is the ultimate ideal and the ace of the craft" (H. Behrbom, one of the originators of the 37-design during the previous set-up at SAAB. and at that time head of the SAAB Aerodynamics Office at the beginning of the 1960s).

1.2 Concept of Lift - Definition of C_L.

The most important factors determinint the lifting force of a wing can be compiled into the formula

$$L = qSC_L$$

Where q is the so-called aerodynamic pressure, proportional to the density of the air and the square of the flying speed, S is the syrface area of the wing and C_L a non-dimensional number, i.e., the lift coefficient, which for a given wing depends mainly on the angle of attack, α, i.e., the angle between the reference plane of the wing and the direction of the movement. Since the drag when flying at high speed puts a limit on the size of the wing surface, the efforts toward satisfactory characteristics at low speed must be directed at raising the C_L value, which can be utilized for flying.

At low speed the characteristics of the correlation between the angle of attack and the lift coefficient, especially the aspect ratio, i.e., the correlation between the wing span and the man of the wings chords, are determined by the planar shape of the wing.

1.3 Lift of Two-dimensional Wings - Dependency of the Angle of Attack on the Lift

/6

Let us first consider a wing with an endless span (a so-called two-dimensional wing).

We assume that

- o the compressibility of the air is negligible;
- o the flow speed of the air is negligibly small in comparison that of the speed of sound (the mach number, i.e., M = 0);
- o the friction of the air against the wing is neglible and that the air flow around the contour of the wing is smooth and elegant.

This ideal condition is called a non-compressible potential circulation. If the wing is placed at an angle of attack (i.e., obliquely in relation to the air flow) and the direction of the air flow is illustrated by flow lines, the following idealized picture is obtained:

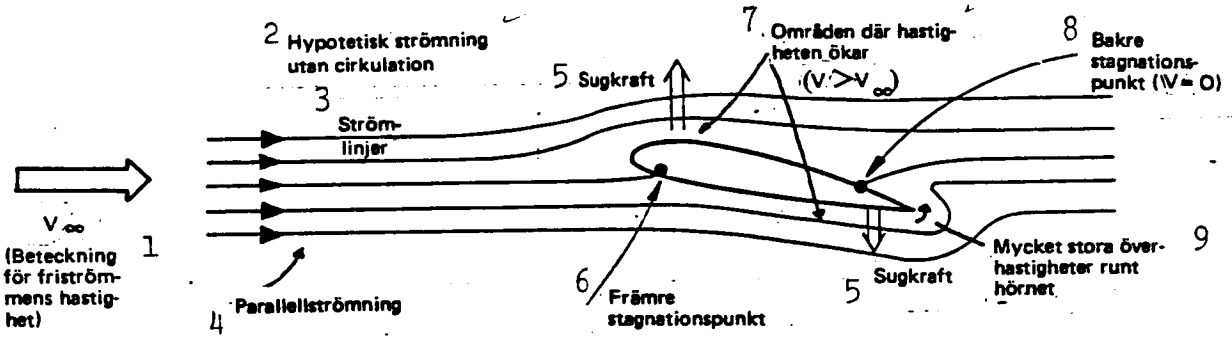

Fig. 1. Idealized potential air circulation without lift.
Key: 1. V_∞ (symbol of the speed of free air flow).
2. Hypothetic non-circulating air flow.
3. Flow lines.
4. Parallel flow.
5. Suction
6. Stagnation point at leading edge.
7. Areas where the speed increases.
8. Stagnation point at trailing edge (V = 0).
9. Very high excessive speed around the corner.

If we sum up the forces which appear when the air circulates around the profile, they will be exactly equal to zero in the case of an idealization of this kind.

The ideal picture above presumes that the air particles are weightless and, thus, able to flow smoothly around a sharp corner without anything happening.

However, forces related to mass and friction change this ideal picture. According to the well known law of Bernouilli any increase in speed means a reduction in pressure (or vice versa). Sudden, sharp changes in the contour will lead to very great changes in speed and pressure, resulting in that a regular flow cannot be maintained. A laminar air flow occurs only if the air is allowed to follow an even and rounded contour. However, in reality the air particles become separated from the surface of the profile at its trailing edge (Fig. 2).

/7

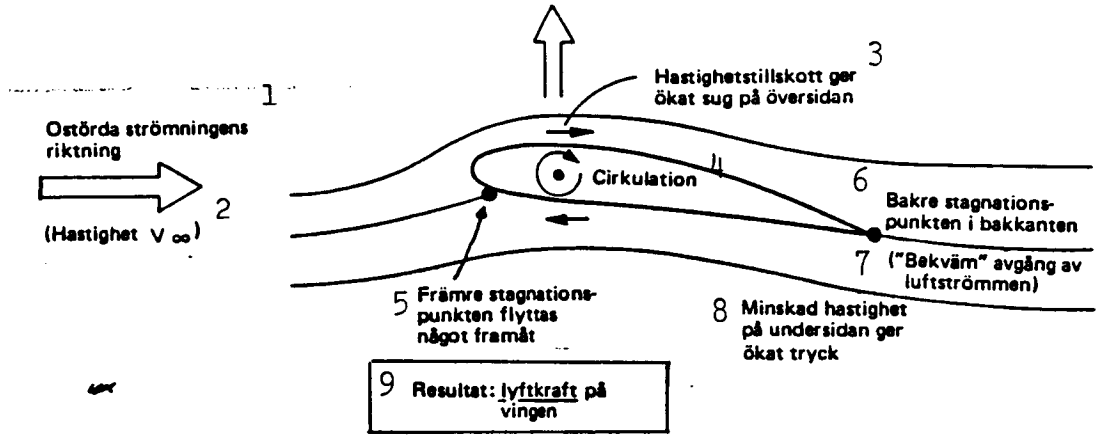

Fig. 2. Potential air circulation producing lift.
Key: 1. Direction of the undisturbed air flow.
2. Speed = V_∞)
3. Excess speed means increased suction on the upper surface.
4. Circulation
5. The leading edge stagnation point is moved slightly forward.
6. Rear stagnation point at the trailing edge.
7. "Smooth" separation of the air flow.
8. Reduced speed below the lower surface produces increased pressure.
9. Result: the wing is lifted.

The points on the surface of the profile where the flow lines separate or meet, respectively, are called stagnation points. In Fig. 2 the rear stagnation point is moved to the trailing edge. In order to fulfill this condition, the excess speed on the top of the wing must be increased and a corresponding reduction in speed must occur below the lower surface of the wing profile.

One way to achieve these local changes in speed in the case of a schematic flow model like the one in Fig. 2 is to superimpose a turbulent flow together with a distribution of speed like that illustrated in Fig. 3a (and marked by circling symbols in Figures 2 and 3b). If we imagine the turbulence in a position like that in Fig. 2, we obtain a model which satisfactorily represents the "separation" of the flow caused by a wing with an acute trailing edge, placed within the flow. The turbulence adds just a small amount of speed to the flow above the upper surface and an equally small reduction in the speed occurs below the lower surface. A distribution of the speed around the wing profile is obtained which fairly well resembles that which occurs in reality. In comparison with Fig. 1, we have now a further increased excess speed over the upper face which causes a reduction in pressure while, simultaneously, the suction on the lower side disappears. We have instead obtained a resultant lift of the wing

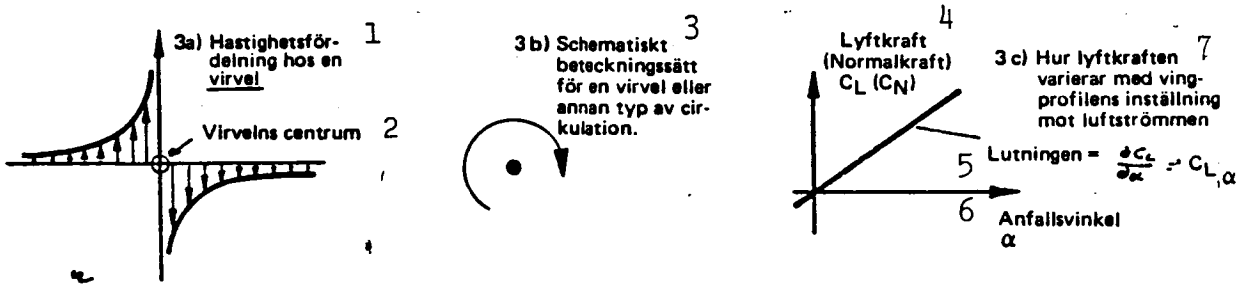

Fig. 3. Turbulent air circulation. Dependency of the lift on the angle of attack.

Key: 1. Distribution of speed within a vortex.
2. Center of the vortex.
3. Schematic symbol of a vortex or any other type of air circulation.
4. Lift (normal force), C_L (or C_N).
5. Gradient = ...
6. Angle of attack, α.
7. How lift varies in relation to the slant of the wing profile in relation to the air flow.

It is mathematically feasible to balance the magnitude of the turbulence so that the trailing edge stagnation point will become fixed at the trailing edge while simultaneously posing the condition at a check point on the wing /8

profile where the flow shall be tangential along the contour of the wing. In such a manner a simply constructed model can be obtained which actually agrees satisfactorily with the real conditions and which can be used for illustrating several of the phenomenons occuring when the air flows around aircrafts. The lift resulting in Fig. 2 is at narrow angles of attack mainly linearly dependent on the angle of attack (Fig. 3c). (The more obliquely the wing is positioned the wing is positioned, the more excess speed is required on the upper side in order to deflect the air flow correctly so that it will leave the trailing edge smoothly.)

1.4 Lift of Three-dimensional Wings - Effect of the Aspect Ratio

So far we have studied a single wing section only, which can be imagined as a cross section through a wing with an endless span (a two-dimensional wing). We shall see that the reasoning, according to which the excess speed above the upper face of the wing (and, thus, the lift) is created by vortices, can also be applied to a real wing with a limited span (i.e., to a three-dimensional wing).

First, a definition of aspect ratio and trapezoidal ratio. The shape of the wing is of great importance for its efficiency when creating lift. In order to quickly and simply characterize the shape of the wing, we use the terms:

- aspect ratio, $A = \frac{(\text{wing span})^2}{\text{wing surface}}$ or $\frac{b^2}{S}$, and
- trapezoidal ratio = $\frac{\text{the chord of the wing tip}}{\text{the chord at the wing root}}$.

The concepts of wing span and wing chord are illustrated in Fig. 4. In the case of a rectangular wing or a wing with a constant chord, it is valid that the aspect ratio = $\frac{(\text{wing span})}{\text{wing chord}}$ and that the trapezoidal ratio = 1.

A two-dimensional wing can be considered a wing with an endless aspect ratio.

In the case of a wing at an angle of attack and a finite aspect ratio it is possible to similarly imagine a model of the circulation where both turbulent and laminar flow are superimposed on each other. This three-dimensional model will then look as follows (Fig. 4):

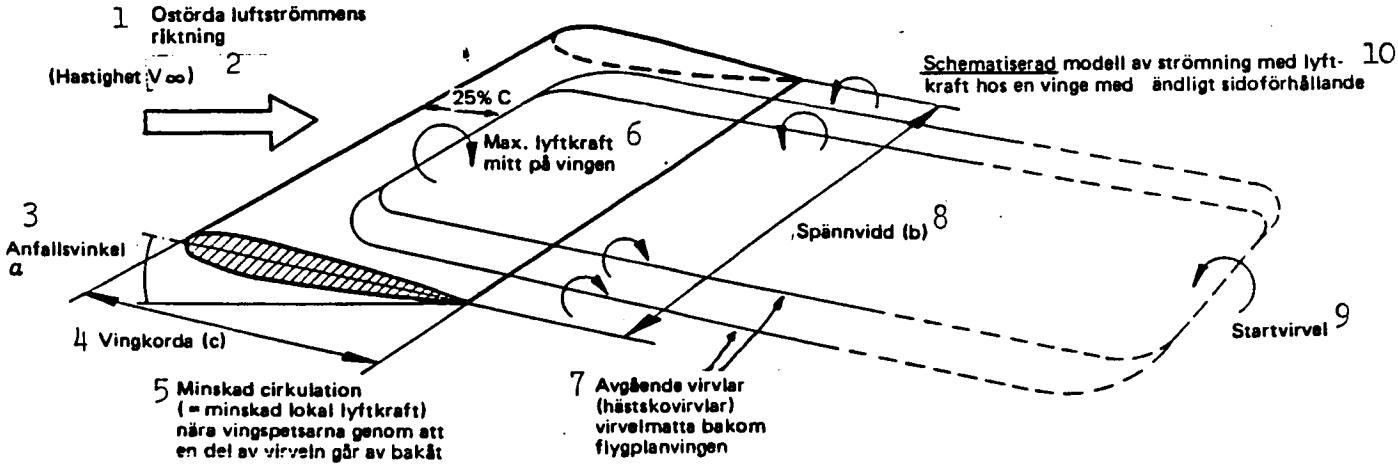

Fig. 4. Rectangular wing with a finite aspect ratio and an angle of attack at low speed.

Key: 1. Direction of the unperturbed air flow.
2. Speed, V_∞.
3. Angle of attack, α.
4. Wing chord (c)
5. Reduced circulation (= locally reduced lift) close to the wing tips because a part of the vortex is separated rearward.
6. Maximum lift at the center of the wing.
7. Separating vortices ("horse-shoe vortices"), train of vortices behind the wing of the aircraft.
8. Wing span (b).
9. Initial vortex.
10. Schematic model of circulation producing lift of a wing with a finite aspect ratio.

/9

The circulation around the wing tip causes a reduction in lift close to the tip. In our model this is caused by the filament of the vortex being deflected and separated from the wing close to its tip. This type of circulation is called a "horse-shoe vortex" in Sweden. More of such vortices than the single one shown in the figure would produce an even better model of the flow.

By gradually reducing the strength of the vortices along the wing span an increased leveling of the pressure is actually achieved. A distribution of the liftin the direction of the wing span, looking like in Fig. 5, will be produced.

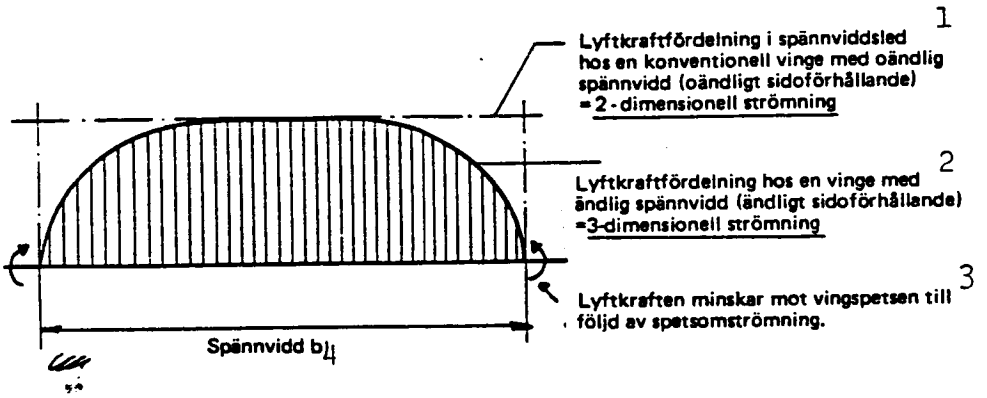

Fig. 5. Key: 1. Distribution of lift in the direction of the wing span of a conventional wing with an endless span (an endless Aspect ratio) = a two-dimensional air flow.
2. Distribution of lift in the case of a wing with a finite span (a finite aspect ratio) = a three-dimensional air flow.
3. The lift decreases in the direction of the wing tip due to circulation around the tip.
4. Wing span, b.

The smaller the aspect ratio, the greater the amount of lift lost due to the circulation around the tip. Figure 6 illustrates how the efficiency varies in relation to the aspect ratio from the point of view of lift.

A reduction of the aspect ratio (i.e., a greater loss due to the circulation around the wing tip) will also increase the drag, which induced lift (that is, the quotient of lift/drag changes for the worse).

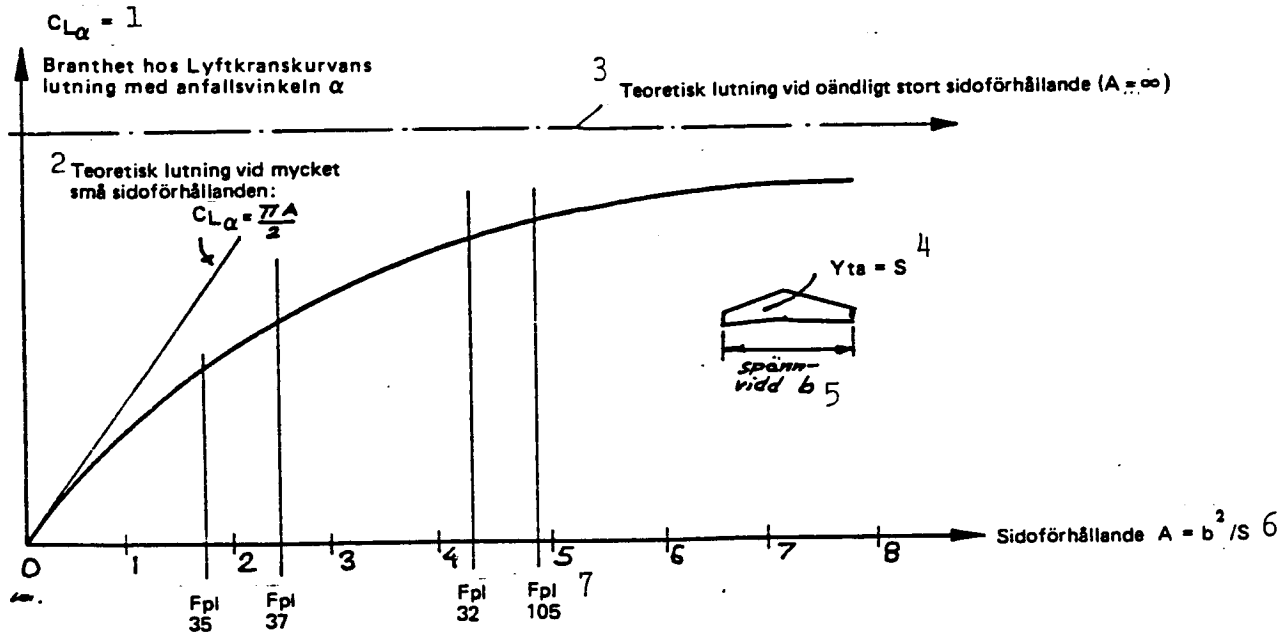

Fig. 6. Key: 1. $C_{L_\alpha} = 1$. The steepness of the gradient illustrating lift in relation to the angle of attack.
2. Theoretical gradient at very small aspcet ratios: ...
3. Theoretical gradient at infinitely large aspect ratios (A =).
4. Surface = S
5. Wing span, b.
6. Aspect ratio $A = b^2 / S$

1.5 Dependency of the Lift on the Angle of Attack at Narrow Angles of Attack - Stalling of Conventional Wings

/10

The lift of conventional aircraft configurations is approximately linearily dependent on the angle of attack at narrow to moderately wide angles. Saturation will gradually develop at wider angles of attack. At a given angle of attack, the lift will reach its maximum value (i.e., $C_{L\ max}$); see Fig. 7.

It is evident from Fig. 7 that a slender delta wing requires a considerably wider angle of attack in relation to a certain C_L than a conventional wing and that it reaches the saturation point only at very wide angles of attack. However, for aircrafts with a large aspect ratio, there is a more rapid increase in lift when the angle of attack widens and, thus, the saturation occurs rather quickly. It appears also that the types of

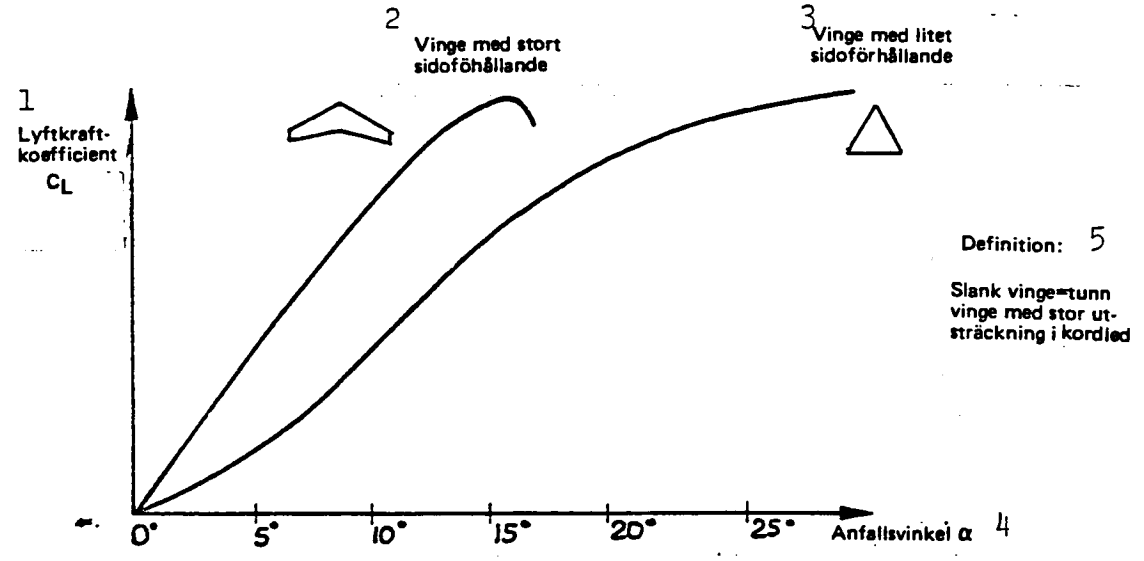

Fig. 7. Shapes of graphs illustrating the lift of wings with large and small aspect ratios at low speed.
Key: 1. Lift coefficient, C_L
2. Wing with a large aspect ratio.
3. Wing with a small aspect ratio.
4. Angle of attack, α.
5. Definition: Slender wing = thin wing with large extension in the direction of the chord.

flow at moderate to wide angles of attack differ considerably between the two wing types. In order to explain the differences it is worth while to consider at first what happens in the case of a straight, conventional wing.

At narrow angles of attack the air flow keeps in contact with the wings of most aircraft configurations presently used, i.e., in principle looking like those in Fig. 2 and 4. The graph illustrating lift is linear and the effect of the viscosity of the air is in that case limited to a thin boundary layer close to the surface of the wing. When increasing the angle of attack the following happens: when the angle of attack has reached a certain limit, some form of collapse of the air flow takes place. This can involve local separation of the boundary layer which at a further increased angle of attack quickly spreads across the upper surface of the wing. What happens is usually called "stalling of the wing". The course of stalling varies in relation to the different types of the wings. Factors affecting the course of stalling are, among others, the magnitude of the tractive force on the upper surface of the wing and the appearance of a corresponding distri-

bution of pressure. In order to describe what happens in the case of a conventional wing, we shall study the process in respect to a two-dimensional wing. The distribution of pressure on the upper surface of such a wing is illustrated in Fig. 8.

/11

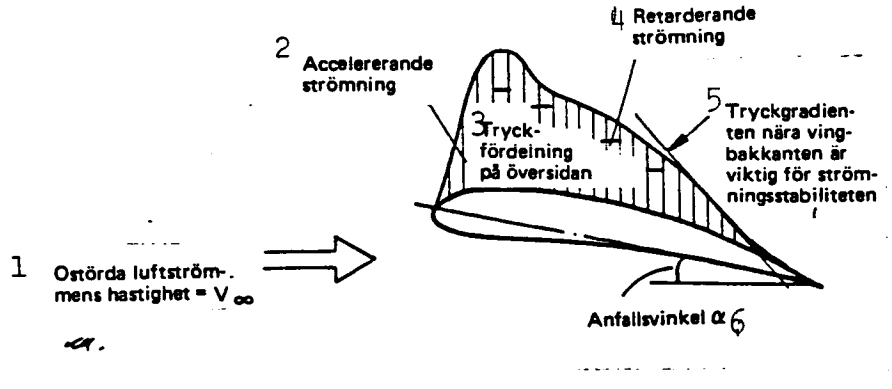

Fig. 8. Distribution of pressure in the direction of the chord of a conventional wing.
Key: 1. Speed of an unperturbed air flow, V_∞.
2. Accelerating air flow.
3. Pressure distribution on the upper side.
4. Retarding air flow.
5. The pressure gradient at the trailing edge of the wing is important for the stability of the flow.
6. Angle of attack, α.
7. The pressure changes are largest on the upper side of the wing.
The pressure gradient = the gradient of the pressure distribution graph.
The pressure gradient increases close to the trailing edge when the angle of incidence increases. The maximum pressure gradient attainable before the flow collapses is called the critical pressure gradient and the corresponding angle of attack is the critical angle of attack.

When the angle of attack increases, the magnitude of excess speed above the upper side of the wing increases and, consequently, so does the suction. However, as long as the wing functions, there is a parallel flow, separating from the trailing edge. Thus, the pressure on the upper and the lower sides are balanced and, thus, the air stream has been braked. The more it is held back, the more "exhausted" the boundary layer becomes.

If the distribution of the suction is illustrated like in Fig. 8, it is easy to vizualize how the pressure varies along the chord. The "grade" behind the peak of suction becomes steeper, the more the angle of attack is increased.

The gradient of the pressure distribution graph is called a pressure gradient. When the speed of the air flow is reduced, the pressure increases (i.e., the suction is reduced). The pressure gradient becomes positive. It is evident that its magnitude and the position of its peak on the upper surfaee of the wing, where the pressure gradient is largest, is of major importance for how large an angle of attack the wing will be able to tolerate and also for how the stalling will proceed when the angle of attack is increased even further. A too steep pressure gradient means that the regular flow cannot be maintained but will be transformed into a disorderly air flow. which will collapse, whereby the suction above the wing decreases. This happens when the pressure gradient passes a critical level. The corresponding angle of attack is called the critical angle of attack of the profile.

The course of stalling of a two-dimensional wing can take different forms depending on the relative diameter and the type of the profile. (Relative diameter of the profile = the ratio between the diameter of the profile and that of the chord.) Briefly stated, it is possible to distinguish the following main types of the course of stalling:

The first one (called "trailing edge stall") applies to wings with a large relative diameter (ca. 12%), corresponding to that of a conventional subsonic aircraft wing with a large aspect ratio. There the separation starts close to the trailing edge and travels forward in relation to an increasing angle of attack (trailing edge stall). The characteristics of this flow and the graph illustrating it in such a case are evident from Fig. 9.

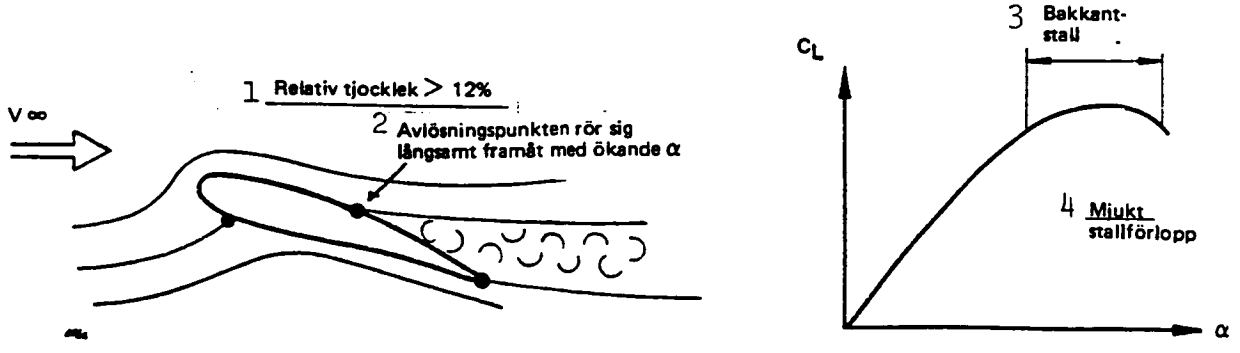

Fig. 9. Trailing edge separation of a conventional, thick wing.
Key: see p. 14.

Key to Fig. 9: 1. Relative diameter > 12%.
2. Point of separation moving slowly forward in relation to an increasing α.
3. Trailing edge stall.
4. Gentle course of stalling.

There is no longer any well defined stagnation point at the trailing edge. The flow type deviates from that in Fig. 2 and approaches that in Fig. 1 with a decrease in lift as a consequence. The gradient of the graph, illustrating lift, decreases slowly in relation to an increasing angle of attack without any sudden, large reduction in the lifting force. /12

Straight wings with a large aspect ratio and a small relative diameter (≤ 9%) experience a different, more abrupt course of stalling. In that case the detachment does not start close to the trailing edge but occurs near the leading edge of the wing profile. The large camber of the profile at this point cuases locally major excess speeds, resulting in significant changes in the pressure gradient. Initially a local separation is followed by reattachment of the flow; a so-called detachment bubble is formed. In the case of a slender wing, the length of the detachment bubble increases when the angle of attack is increased. Final separation occurs when the bubble reaches the trailing edge.

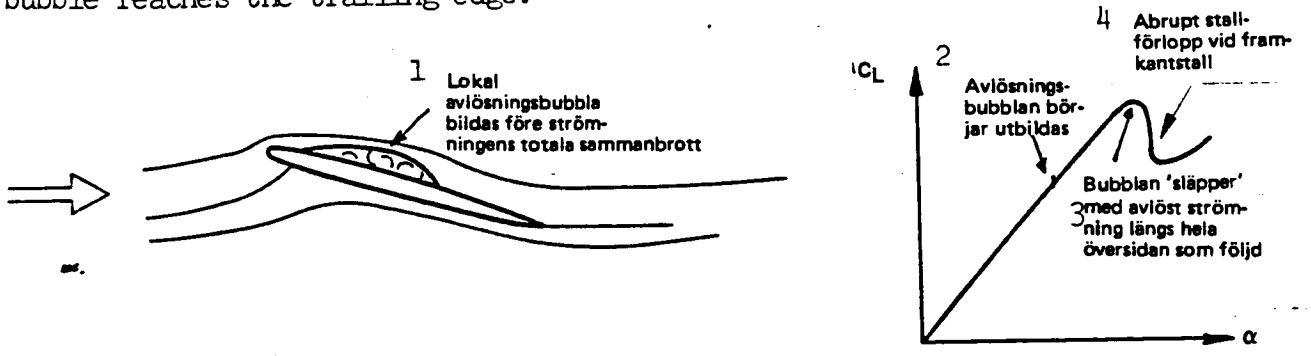

Fig. 10. Detachment bubble of a conventional slender wing at wide angles of attack. Relative diameter, < 9%.
Key: 1. Local detachment bubble formed before total collapse of the flow.
2. The detachment bubble starts to form.
3. The bubble is "released" with separated flow along the entire upper surface as a result.
4. Abrupt course of stalling due to leading edge stall.

In the case of a wing with a moderate diameter (10-12%), the course of stalling is more complicated. The detachment bubble no longer increases linearily in relation to the angle of attack. Instead there is a more or less abrupt course of separation, where the detachment of the flow starts close to the leading edge (leading edge stall). A combination of leading and trailing edges stalling is also feasible in the case of wings belonging to this order of dimensions. We will not continue to go into detail concerning those types of separation but will instead touch upon that of three-dimensional wings, which is of a greater importance in respect to FPL 37.

So far we have discussed separation in relation to wings with a large aspect ratio. In the case of wings with a moderate aspect ratio, the distribution of lift in the direction of the wing span affects the characteristics of the stall. By reducing the trapezoidal ratio of the wing (i.e., limiting the chord at the tip) the local load on the chord is increased and, thus, also the pressure gradient behind the pressure minimum. Due to this, the wing tip tends to stall before the base does so in spite of the fact that the inside portion of the wing in general carries the largest load. Conventional aircrafts with trapezoidal wings are, consequently, often designed sich a torsion (twist) of the wing so that the angle og attack will be reduced by 1 to 3° toward the tip. Increased cambering of the wing toward the tip can have a similar effect. By means of a suitable choice of trapezoidal ratio, torsion and the diameter of the cambering of the profile, it is possible to adjust the wing so that satisfactory stalling characteristics are achieved.

/13

We shall summarize the characteristics of the course of stalling:

Straight wings with a large aspect ratio: the course of stalling is is two-dimensional over the major portion of the wing. Different types of stalling depend on she shape and the relative diameter of the wing profile.

Straight wings with a moderate aspect ratio: What occurs at the wing acquires greater importance. The characteristics of the stall depend on the trapezoidal ratio; a varied geometry geometry

of the wing in the direction of its span is required for satisfactory characteristics of the stall.

What happens if, in addition, we sweep the wing rearward (increase the sweep-back angle) ? Then the boundary layer tends to flow outward and become thicker at wide angles of attack and, thus, to become more "exhausted" toward the wing tip. This means that the entire course of action becomes even more three-dimensional and that the stalling will preferably start at the wing tip.

The consequence is that the maximum lift diminishes if the wing is swept farther rearward. Since the wing tips are the first to "give up" in the case of sweep-back, only a slight asymmetry of the wing or of the air blowing against it are required in order that the stall shall also give rise to a major, rolling disturbance. Just that part of the lift of a wing, stalling at the tip, which is farthest away from the point of gravity will disappear and when stalling the aircraft suddenly becomes unstable in the pitching (longitudinal) direction (pitch-up, see below).

It is valid for all wing types (straight as well as moderately swept back, i.e., with a leading edge of the swept-back angle less than 55°) that following the collapse of the air flow, there is a more or less irregular type of circulation across the upper surface of the wing associated with a loss of lift, increased drag and buffeting as a consequence.

This is one of the reasons why a contact flow is always utilized for normal flying with conventional wings.

1.6 Wings With a Small Aspect Ratio at Wide Angles of Attack

We have seen that the picture of the air flow becomes increasingly three-dimensional the smaller the aspect ratio is. This is valid before as well as after reacing the point of a leading edge stall.

After having considered the conventional wing and seen how the aspect ratio and the sweep-back angle operate, we will now contemplate the extreme case of slender wings with a small aspect ratio.

It is just this type of a wing which is of current interest to us since it occurs in Sweden both on FPL 35 as well as on FPL 37.

This wing type differs from the conventional one by behaving quite differently when the angle of attack is increased. After seeing what happens to a swept-back wing, it could be expected that the problems concerning separation should become worse when the sweep-back angle is increased and when the local load on the chord close to the wing tip attains high magnitudes already at very narrow angles of attack. /14

It is also true that a contact flow in the conventional sense can be maintained only as far as up to narrow angles of attack (ca. 4° - 5°). If the angle of attack is increased beyond that value, something occurs which at first glance is not expected: the graph illustrating lift increases instead of showing tendencies toward saturation (Fig. 11c). Simultaneously the picture of the air flow is altered: a turbulent flow develops which is superficially similar to that close to the tip of a conventional wing. The stable condition of turbulent flow which develops in place of a collapsing flow is called a leading edge-separated flow. This type of air flow persists up to very wide angles of attack and results in that it becomes feasible to utilize a very high maximum lift without any exceptional increase in drag. This is exactly what has been applied for our aircrafts of models 35 and 37. FPL 35 utilizes the lift characteristics only to a limited extent, while FPL 37 is constructed for maximum utilization of the advantages of leading edge-separated flow.

In next section we shall try to explain what the picture of flow looks like in the case of a delta (or triangular) wing which is the wing type most commonly utilizing the leading edge separation.

1.7 Principle of Leading Edge Separation: Air Flow Around a Delta Wing

In order to explain in detail what happens we shall use the analogy which we applied previously when imagining the excess speed (providing lift) above the wing caused by trains of vortices in the plane of the wing. These will, as we have seen, be detached from the trailing edge of

the wing. (The wider the angle of attack, the greater the circulation within the vortex, i.e., the more powerful the lifting force created; cf. Fig. 4.) The detachment of the vortices rearward corresponds to a reduction in lift which is greater the closer to the wing tip we come. We shall first study what occurs at narrow angles of attack (Fig. 11). The "horseshoe" vortex model is similar to that in Fig. 4. In Fig. 11a we can see a model of this type of vortex, drawn schematically. In Fig. 11b the actual distribution of the lift created is shown. It corresponds to the distribution of the circulation (i.e., the vortices) in Fig. 11a. Finally, Fig. 11c illustrates the range of the lift where the flow type corresponding to a normal contact flow over a conventional wing is valid.

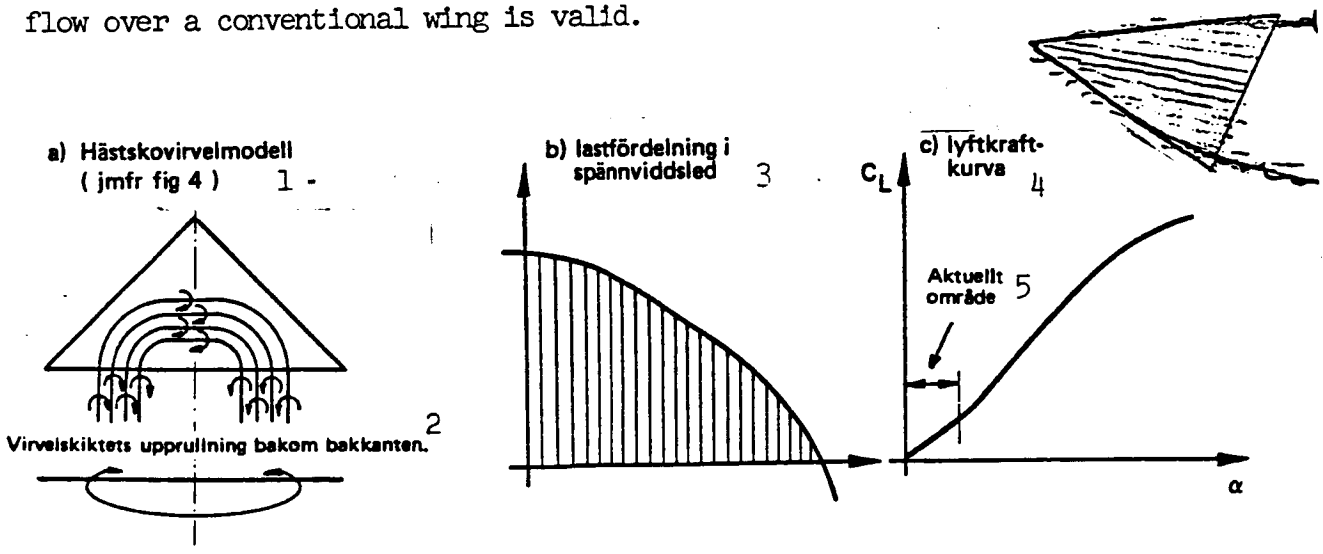

Fig. 11. Circulation around a delta wing at narrow angles of attack.
Key: 1. Model of "horseshoe" vortices (cf. Fig. 4).
2. Involution of the vortex layer behind the trailing edge.
3. Distribution of the load in the direction of the wing span.
4. Graph illustrating lift.
5. Area of concern.

The critical pressure gradient close to the leading edge of the tip is quickly reached in response to an increased angle of attack. However, instead of the usual collapse of the flow, which is normally expected, a new type of stable flow develops there. It is illustrated in Fig. 12. /15

It is characteristic of this new type of circulation (Fig. 13) that the train of vortices (and thus also the air flow) separates along the leading edge as well. How can this be?

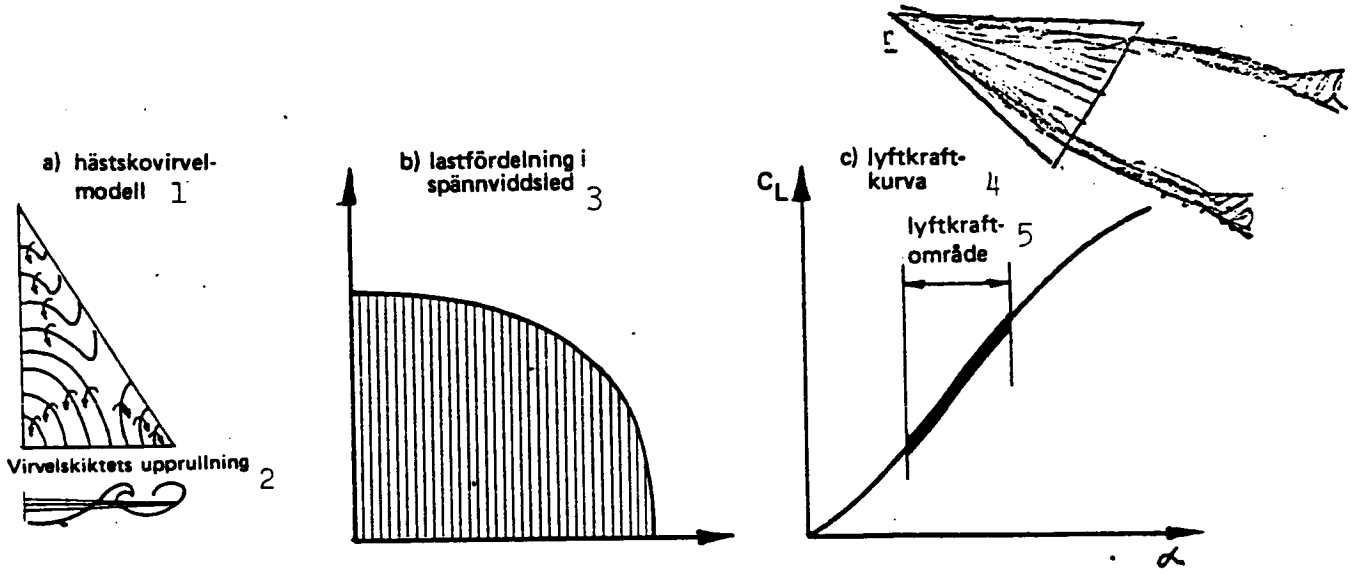

Fig. 12. Circulation around a delta wing at moderate angles of attack.
Key: 1. Model of horseshoe vortices.
2. Involution of the vortex layer.
3. Distribution of load in the direction of the wing span.
4. Graph illustrating lift.
5. Range of lift.

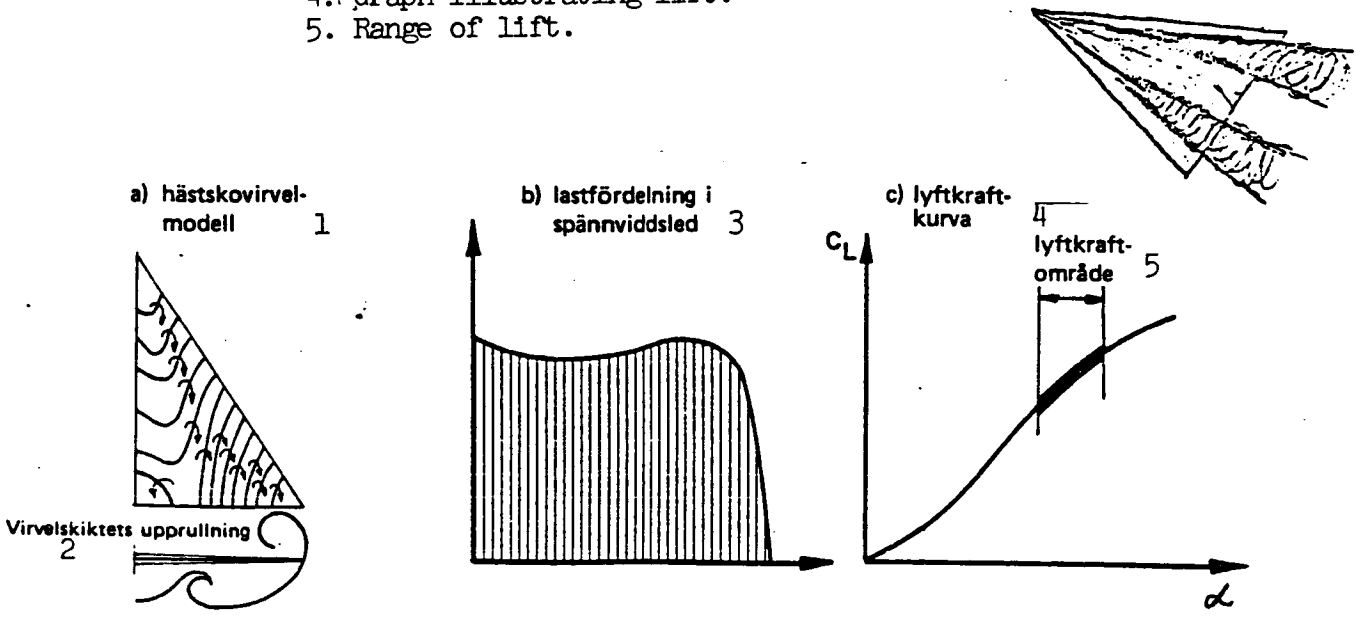

Fig. 13. Circulation around a delta wing at wide angles of attack.

Key: 1. Model of horseshoe vortices.
2. Involution of the vortex layer.
3. Distribution of load in the direction of the wing span.
4. Graph illustrating lift.
5. Range of lift.

If we observe what the flow around the wing actually looks like in this case, it becomes evident that a strong outward flow of the boundary layer takes place across the upper surface. (This flow pattern is also illustrated in Fig. 17 below.) It turns out that the air flow when encountering the wing becomes strongly deflected outward so that the air is separated obliquely rearward - outward from the leading edge (i.e., not only from the trailing edge). There is now two systems of vortices being detached instead of one (see also Fig. 14). The portion of the air flow separated by the leading edge increases when the angle of attack is further increased.

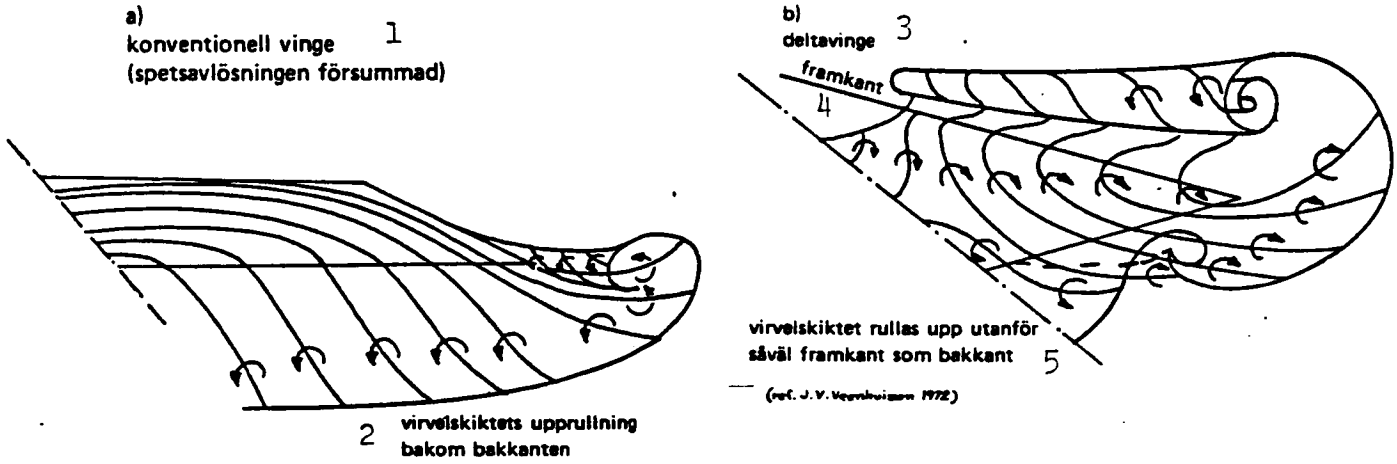

Fig. 14. Models of the flow of vortex layers around wings with and without leading edge separation.
Key: 1. Conventional wing (detachment at the tip ignored).
2. Involution of the vortec layer behind the trailing edge.
3. Delta wing.
4. Leading edge.
5. The vortex layer is involuted ourside the leading as well as the trailing edges.

A comparison between the models of the vortex layer flow around a conventional wing and a wing with the new type of air flow is evident from Fig. 14 where the phenomenon of involution can also be seen, i.e., the one which in the case of a conventional wing gives rise to trailing vortices. /16

The consequences of the new type of flow are as follows:

- The air flow separating along the leading edge (the leading edge vortex layer) is deflected rearward and curls up above the wing (Fig. 14). The involution occurs in a helical manner. The

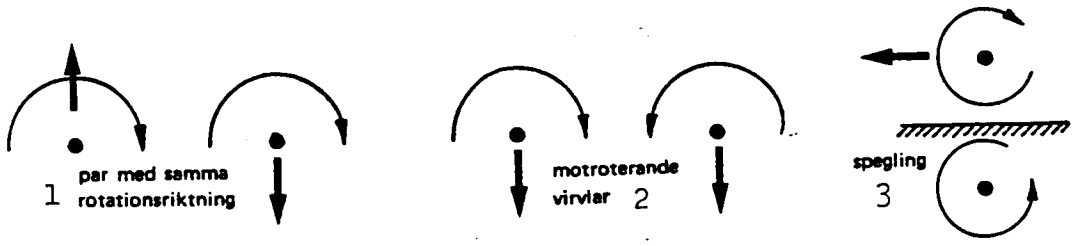

Fig. 15. Interference between a pair of vortices.
Key: 1. Pair rotating in the same direction.
2. Pair rotating in opposite directions.
3. Mirror image rotation.

explanation for this involution can be seen from the model of the vortex train: the individual vortices affect each other due to mutual interference which leads to a structure similar to a spiral. The principle according to which the individual eddies affect each other is illustrated in Fig. 15.

- The involution of the leading edge vortex layer results in forceful excess speed (directed outward and rearward) within an area close to the leading edge of the wing. A powerful peak of suction, widening toward the tip (i.e. rearward),develops near the leading edge.
- The pressure distribution changes character (Figs. 12b, 13b) and becomes more ample close to the leading edge.
- The new flow type increases the lifting force across the wing (the gradient of the graph, illustrating lift, is increased, cf. Fig. 12c).
- The air flowing outward across the upper surface sweeps away the boundary layer (Fig. 16a). The stagnation of the flow close to the leading edge outside the peak of the suction produces a local separation in a narrow band near the leading edge (secondary separation or the actual leading edge-separation). In certain cases there is also an orderly helical flow within this separating band; cf. Fig. 17. Notice that this separation is a relatively stable but very local separation. /17

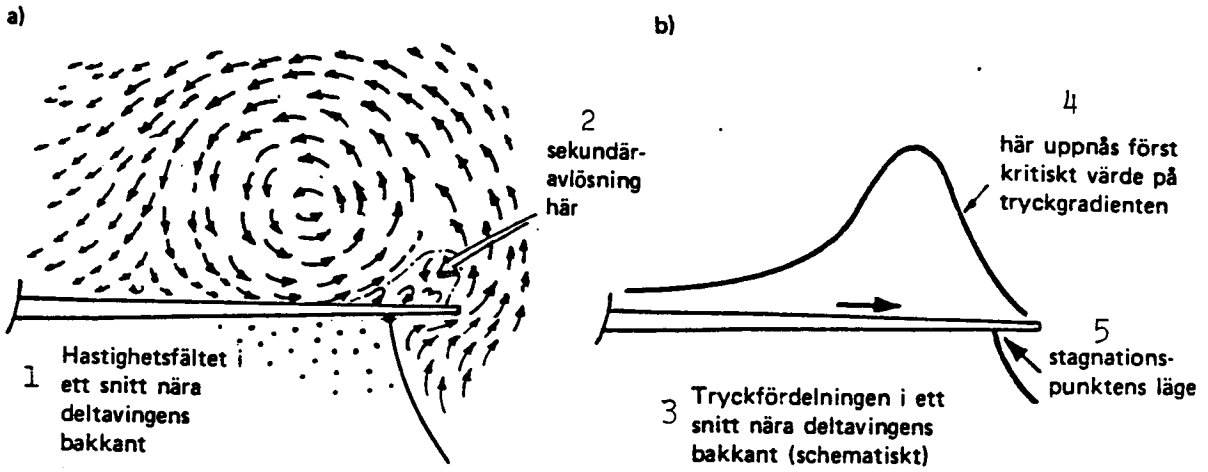

Fig. 16. Air flow around a leading edge-separated delta wing.
Key: 1. Velocity field within a cross section close to the trailing edge of a delta wing.
2. Secondary separation takes place here.
3. Pressure distribution within a section close to the trailing edge of a delta wing (diagram).
4. At this point the critical value of the pressure gradient is reached.
5. Position of the stagnation point.

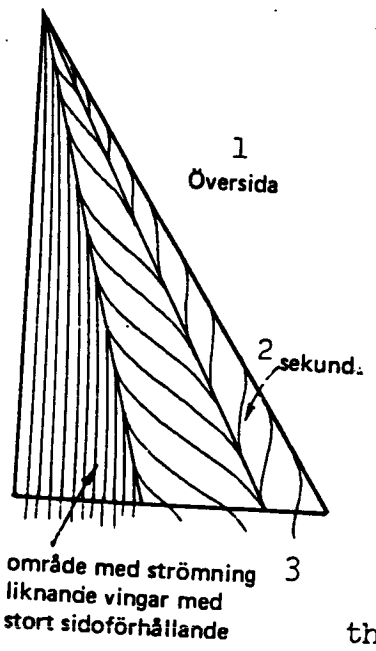

Fig. 17. The flow of the boundary layer in the case of a leading edge separated delta wing.
Key: 1. Upper surface.
2. Secondary separation.
3. area with an air flow similar to that of a wing with a large aspect ratio.
4. At increasing α the helix of the vortex layer is displaced inward and upward.

o A relatively large portion of the boundary layer on the upper surface disappears into the secondary vortex.

o The boundary layer surrounding the leading edge is thin since the line of stagnation runs along the lower surface of the wing close to the leading edge.

o The material in the boundary layer is swept up into the nuclei of the vortex systems.

When the angle of attack continues to widen further past the area of /18
the angle of attack related to leading edge separation, an actual collapse of the flow will gradually develop. This occurs in analogy with what is valid for wings with moderate aspect ratios, i.e., when the local pressure gradient has reached the critical value inside the narrow strip of secondary separation (cf. Figs. 8 and 16). The separation starts at the wing tip and continues foreward-inward (tip separation). It is felt like a successive increase of the buffeting level. The rear portion of the wing is unloaded, which means reduced longitudinal stability (see also further on). Something happens above the wing as well: the orderly helical structure above the wing collapses (vortex collapse). The vortex collapse can be easily observed by means of smoke in a wind tunnel or by means of bubbles in a water tunnel. In front of the point of collapse, the nucleus of the vortex cone is distinctly defined as a narrow filament originating from a point close to the top (or apex) of the delta wing. Within this narrow filament the air is transported downstrean with a speed considerably faster than that of the free flow.

At the point of collapse there is a sudden blockage of the axial flow (i.e., the transportation of the air downstream) within the nucleus of the vortex cone. The vortex filament widens to form a "funnel" within which there is a more or less disorderly flow. In English this is called a "vortex breakdown"; in Sweden we sometimes call it the "funnel phenomenon of delta wings." A vortex cone, the nucleus of which has broken down, is no longer an efficient producer of lift. When the angle of attack is still further widened, the breakdown of the vortex proceeds frontward (it started initially downstream just behind the wing), reaches the trailing edge of the wing and continues thereafter across the wing. Thereby a gradual decrease of the gradient of the $C_L(\alpha)$ graph occurs (cf. Fig. 7 and 13), and by time it results in that a maximum is reached also in the case of slender delta wings although not one as well defined as that of a wing with a large aspect ratio.

We shall summarize what is valid for a delta wing:

1. Conventional adherent flow occurs only at very narrow angles of attack.
2. A so-called leading edge-separated flow with vortex cones above the wing is the typical form of air flow within a very wide range of angles of attack. The gradient of the graph, illustrating lift, becomes steeper than at narrow angles of attack.
3. Maximum lift occurs only at very wide angles of attack.
4. The "saturation" of the graph, illustrating lift, is gentle at wide angles of attack.
5. The collapse of the leading edge-separated flow occurs in part in the form of successively increasing tip separation, in part due to the fact that a "funnel" travels across the wing during the breakdown of the vortex.

At what point in time the maximum lift will occur depends on the angle of the leading edge sweep-back. While a 50° delta wing experiences a flow collapse at $\alpha \cong 12 - 15°$, a 60° wing can tolerate up to 20 - 25° angles of attack. The stability of the flow can be advantageously affected by very /19
small, often local alterations of the leading edge of the wing such as its cambering, vertical guide rails (so-called vortex separators) or a "notch" in the leading edge, etc. The result is that in the case of this very simple type of wing, a large margin develops in respect to maximum lift at low and moderate speeds during normal flight. This fact in combination with the excellent characteristics of this wing type at high speed makes it expecially suitable for supersonic planes, where it is required that the load factor can be temporarily increased, e.g., during take-off and when turning. In addition the slight gradient of the lift graph at narrow angles of attack makes the aircraft relatively insensitive to [kytt = ? buffeting] when flying at high speed and at a low altitude.

It is evident from what has been stated above that the detailed appearance of the air flow across a delta wing at large angles of attack is relatively complicated. In practice a further simplified model of the delta wing is used, where the vortex layer, separated along the leading edge, is schematically illustrated as a single "leading-edge vortex". The corresponding range of excess speed does not deviate very much from what is illustrated in Figure 16.

The simplified model is illustrated in Fig. 18. Thus, from the point of view of interference, the "free" vortex layer, detached behind the wing, can be considered as a single vortex where the filament of the vortex corresponds to the narrow "nucleus", which is enveloped within the involute layer of the leading-edge vortex and can be observed during experiments with smoke.

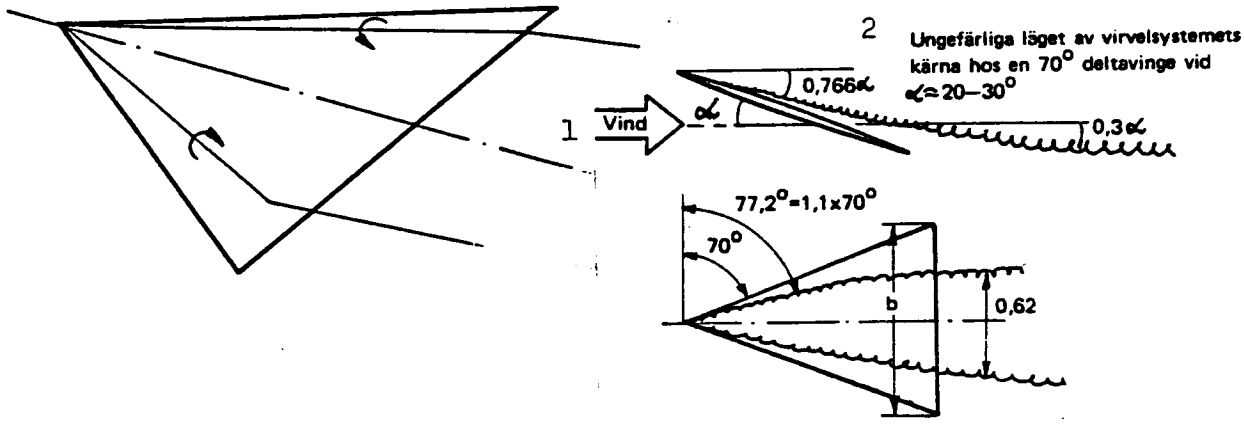

Fig. 18. Schematic description of the vortex system of a delta wing.
Key: 1. Wind.
2. Approximate position of the nucleus of the vortex system of a 70° delta wing at $\alpha = 20 - 30°$.

1.8. Interference Between Fuselage and Wing During an Air Flow Separated by the Leading Edge

The circulation described above is utilized for all delta-winged aircrafts, among others, FPL 35.

In the case of real aircrafts it is necessary to take the interference between the bow of the fuselage and the air intake as well into consideration. By using the simplified flow model described above, it is convenient to illustrate the process in the case of some common aircraft configurations with delta wings in the following manner:

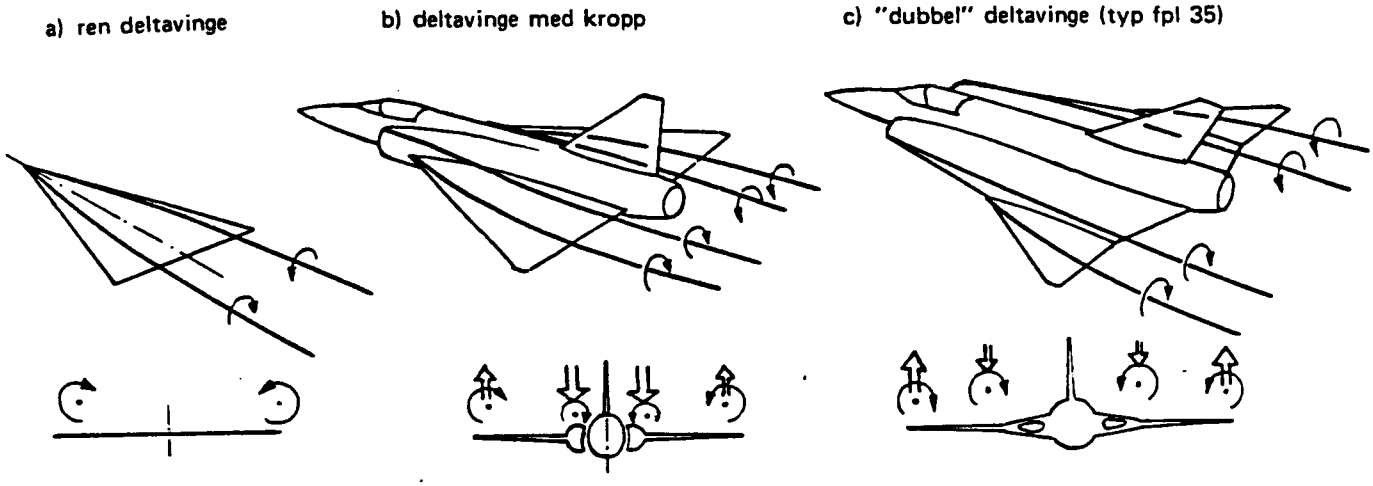

Fig. 19. Practical application of the delta wing principle.
Key: 1. "Pure" delta wing.
2. Delta wing with a fuselage.
3. "Tandem"delta wing (the type of FPL 35).

/20

In stead of a single system of leading-edge vortices, two or more systems can be seen, originating from the bow of the fuselage or from a portion of the air intake. These systems interfere mutually with each other so that the inner pair of vortices is forced down against the wing while the outer one tends to become elevated above the wing surface. Outside the inner vortex pair a field exists which is swept upward and contributes to an increase in the angle of attack locally around the starting point of the outer vortex pair, thus, increasing the force thereof locally. The fuselage, the wings and the portion of the air intake must be carefully adjusted mutually from an aerodynamic point of view. An optimal utilization of the characteristics of the leading-edge flow has also resulted in sophisticated solutions of aircraft designs, such as, e.g., in the case of the Concorde. This interference has also been applied for FPL 37, among others in order to make the outer wings effective as producers of lift at narrow and moderate angles of

attack. The disadvantage of this configuration lies in the fact that the circulation around the outer wing collapses relatively soon, resulting in "pitch-up" (cf. below).

1.9 Interference Between Two Delta Wings in Tandem Formation During An Air Flow Separated by the Leading Edge - Principle Behind FPL 37

This principle has been further developed in respect to FPL 37 by utilizing the mutual interference between slender delta wings in a tandem formation in order to achieve even further improved characteristics of the lift (Fig. 20).

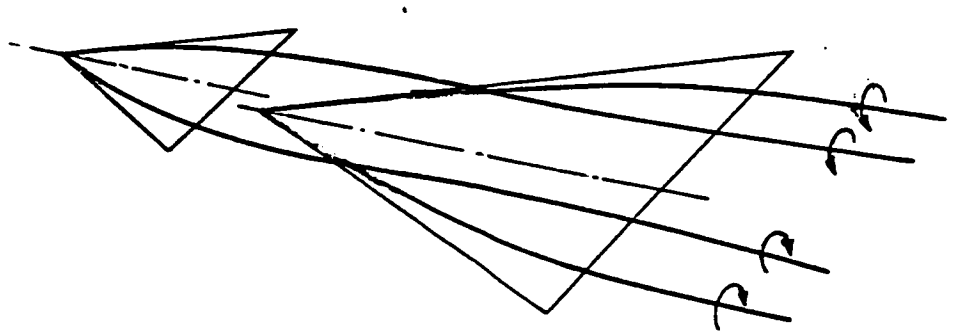

Fig. 20. Schematic illustration of the vortex systems of a tandem delta wing configuration.

The basic flow phenomena and the aerodynamic properties of the "Viggen" /21
configuration at low speed can most satisfactorily be demonstrated by the results of investigations concerning a strongly schematized model built at the start of the 1960s.[1] The model was simply made of two flat delta wings attached to a "fuselage" consisting of a thin, vertical piece of sheet metal. The front wing (i.e., the canard) could be rotated and the position of its axis of rotation could be varied vertically as well as horizontally. During the wind tunnel experiments, forces and moments in respect to both wings individually as well as in combination, forming one single unit, were measured. In addition, the air flow was made visible by means of smoke.

Figure 21b illustrates the lift coefficient, C_L, (referring to the surface of the canard) as a function of the angle of attack of the canard, i.e., $\alpha_S = \alpha \quad \delta$, where α is the angle of attack of the wing, and δ is the

[1] This and the following pages up to p. 32 are reproduced with minor changes from Holme's paper on"The Aerodynamic Background od the Viggen System of Wings", Cosmos 1980.

position of the canard in relation to that of the wing. The measurements were made in part with the wing removed, in part with the canard at vertically different positions, one above, the other below the plane of the wing but in both cases with the canard at a position of $\delta = 25°$. The longitudinal position of the canard was the same in both cases. Without the wing, the graph will assume the character, which in Fig. 7 was given as typical for a slender delta wing.

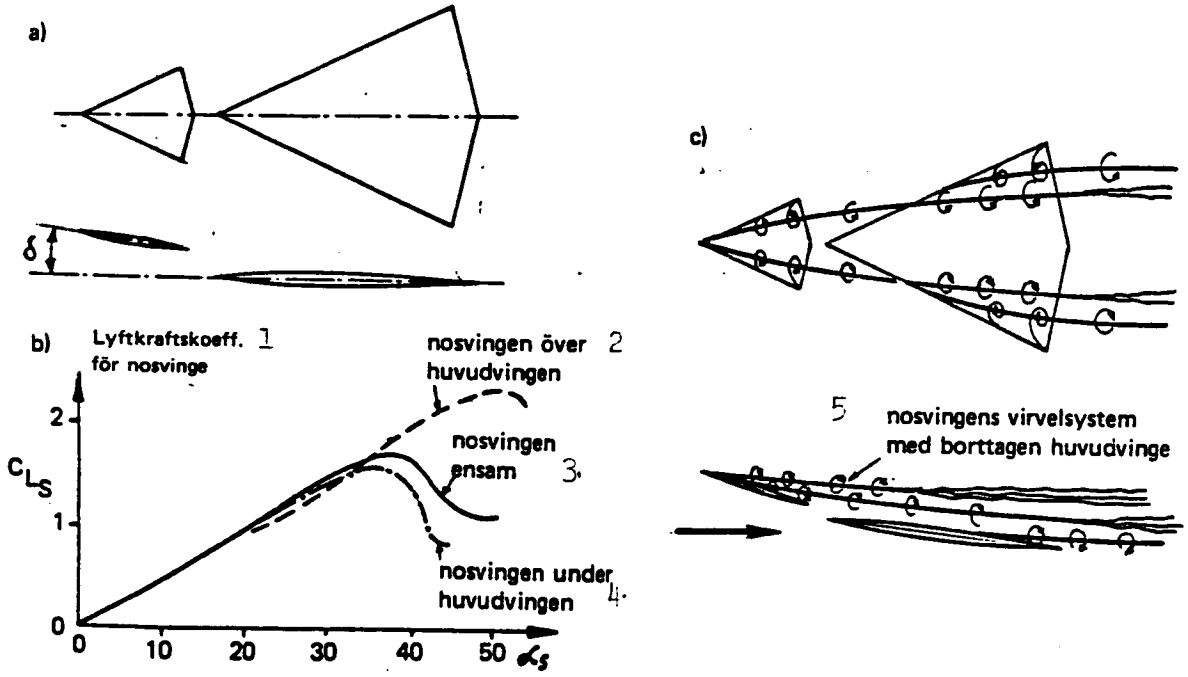

Fig. 21. Effect of the canard on the lifting force of a delta tandem configuration.
Key: 1. Lift coefficient of the canard.
2. The canard above the wing.
3. The canard exclusively.
4. The canard below the wing.
5. Vortex system of the canard when the wing is removed.

When the canard was in a low position the presence of the wing had a disadvantageous effect from the point of view of lift, but in an upper position of the canard this had a remarkably improved effect on the lift which resulted in that the C_{L_S} increased by ca. 40% and was moved to a ca. 12° wider angle of attack. /22

This desirable effect on a frontally placed canard is caused by the interference between the vortex systems of the canard and those of the wing. Figure 21c, drawn on the basis of experiments with smoke, illustrates how the vortices of the canard when in the upper position are forced by the vortices of the wing to pass across the upper surface at a lesser distance than when the main wing is removed. Due to this the low pressure below the vortices, which produces lift, is enhanced. However, it is even more important that the collapse of the forward-progressing canard vortices is delayed by the accelerating flow and by the accompanying favorable pressure gradient, present on the upper surface of the wing. When the canard is in the lower position, the vortices pass below the wing, where they encounter a retardant flow with an unfavorable pressure gradient which accelerates the forward progression of the vortex breakdown (Cf. Figs. 8, 16 and 17).

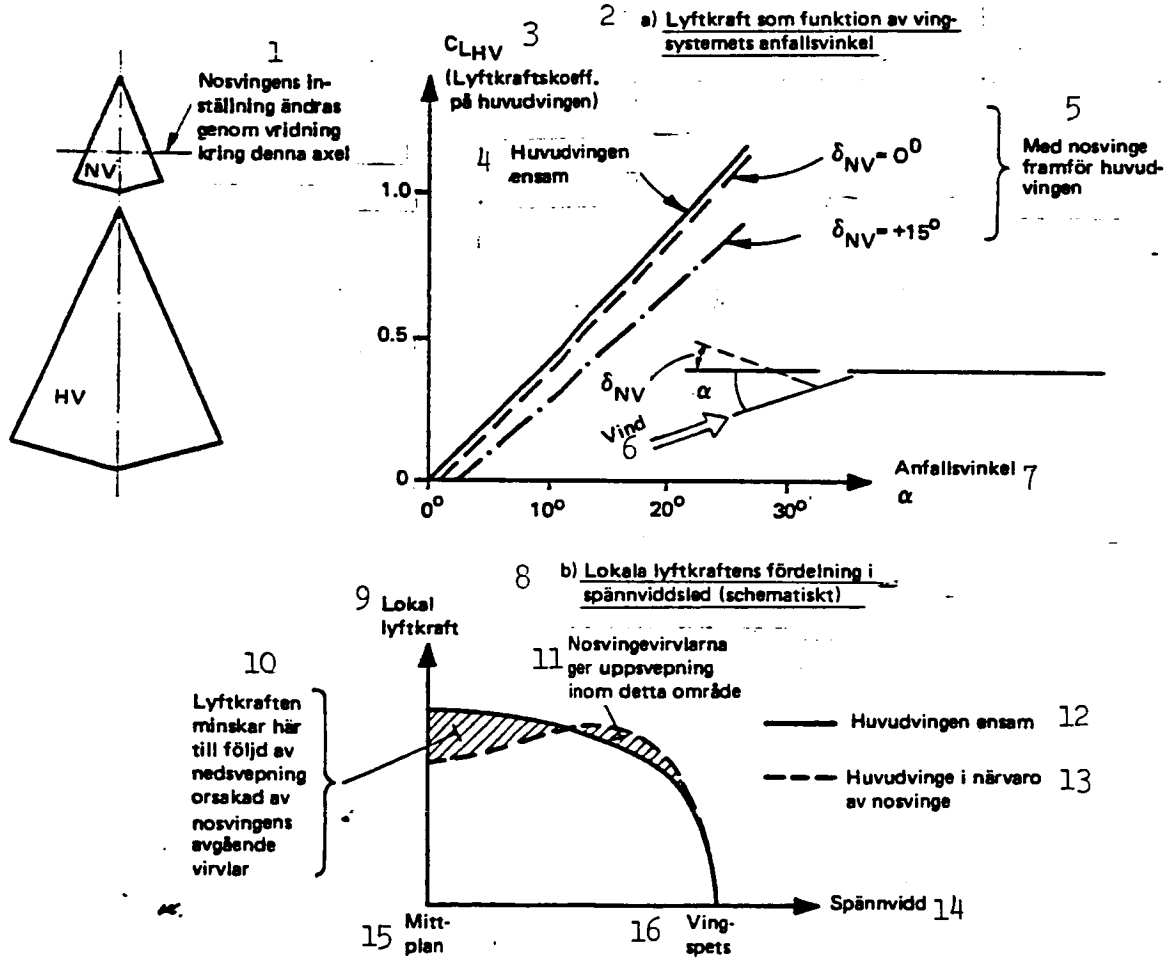

Fig. 22. Effect of the position of the canard on the lift of the wing. Key: see p. 30.

Key to Fig. 22:

1. The position of the canard can be altered by rotation around this axis.
2. a) Lift as a function of the angle of attack of the wing system.
3. C_L of the main wing (Lift Coefficient of the wing)
4. The main wing alone.
5. With the canard in front of the main wing.
6. Wind direction.
7. Angle of attack.
8. b) Distribution of local lift in the direction of the wing span (schematically).
9. Local lift.
10. The lift is reduced heredue to a downward sweeping motion caused by the vortices detached from the canard.
11. The vortices of the canard cause an upward-sweeping motion within this area.
12. The main wing alone.
13. The main wing in the presence of the canard.
14. Wing span.
15. Center.
16. Wing tip.

/23

In what manner do the canard vortices affect the lift of the wing? Since the canard vortices induce a downward-directed speed over the central portions of the wing, especially in the vicinity of its apex, a reduction in lift must develop there. This is confirmed by the fact that the leading edge vortices of the wing according to Fig. 21 c no longer originate from its apex but flow from two points on its leading edge just outside the canard vortices. On the other hand, a lift-inducing low pressure develops below the canard vortices due to locally increased excess speed because the vortices pass just above the upper surface of the wing. However, the net result is that the canard contributes to a reduction in lift of the wing. This is evident from Fig. 22a, which illustrates the lift coefficient of the main wing, $C_{L_{HV}}$, (in reference to the wing surface) as a function of the angle of attack of the wing, i.e., α. This reduction increases when the positional angle of the canard, δ, becomes wider.

The reduction of the lifting power of the wing is, of course, not a desirable effect. In order to investigate whether this could be avoided, experiments were made with an altered wing design, the new shape of which was achieved by cutting away the inefficient apical portion and instead

increasing the wing span so that the surface remained the same as before; cf. Fig. 23. The results of the tests are evident from Fig. 24, illustrating the resulting trimmed lift coefficient, C_L, valid for the combination of wing + canard as a function of the angle of attack of the wing, i.e., α, in comparison with the corresponding graph of the original configuration.

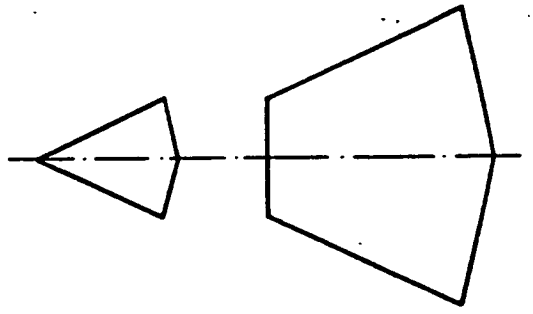

+: o Removing a portion of the wing results in a shorter, thus, a lighter aircraft.
o Satisfactory stability properties at low speed.
o Less wet surface = lower subsonic drag.
o Larger aspect ratio - a lesser portion of the wing surface lies within the downward-sweeping field of the canard.

-: o Unsatisfactory stability properties at trans-sonic speed.
o Less satisfactory distribution of area → increased supersonic drag.
o Lower construction height of the wing root → a heavier wing.

Fig. 23. Delta tandem configuration with the apex of the wing removed.

The trimming means that the angle of adjustment of the canard, δ, can be altered in relation to the angle of attack, α, so that there is always an equilibrium of moments around the position of the point of gravity which provides both configurations with the same stability margin. (This concept is defined under sect. 2.4.) The data necessary for the trimming of the adjustable angle of the canard, δ, can be seen from Fig. 24. The change in the shape (i.e., the removal of a part of the wing) has, as is apparent, had the result desired: an increase by ca. 25% in trimmed lift at a given angle of attack.

This gain in lift was the eseential reason why FPL 37 got its present configuration. Because of its characteristics at high speed, it was not possible to cut off the wing squarely such as illustrated in Fig. 23. Instead a compromise with a reduced leading edge sweep-back angle (45°) was opted

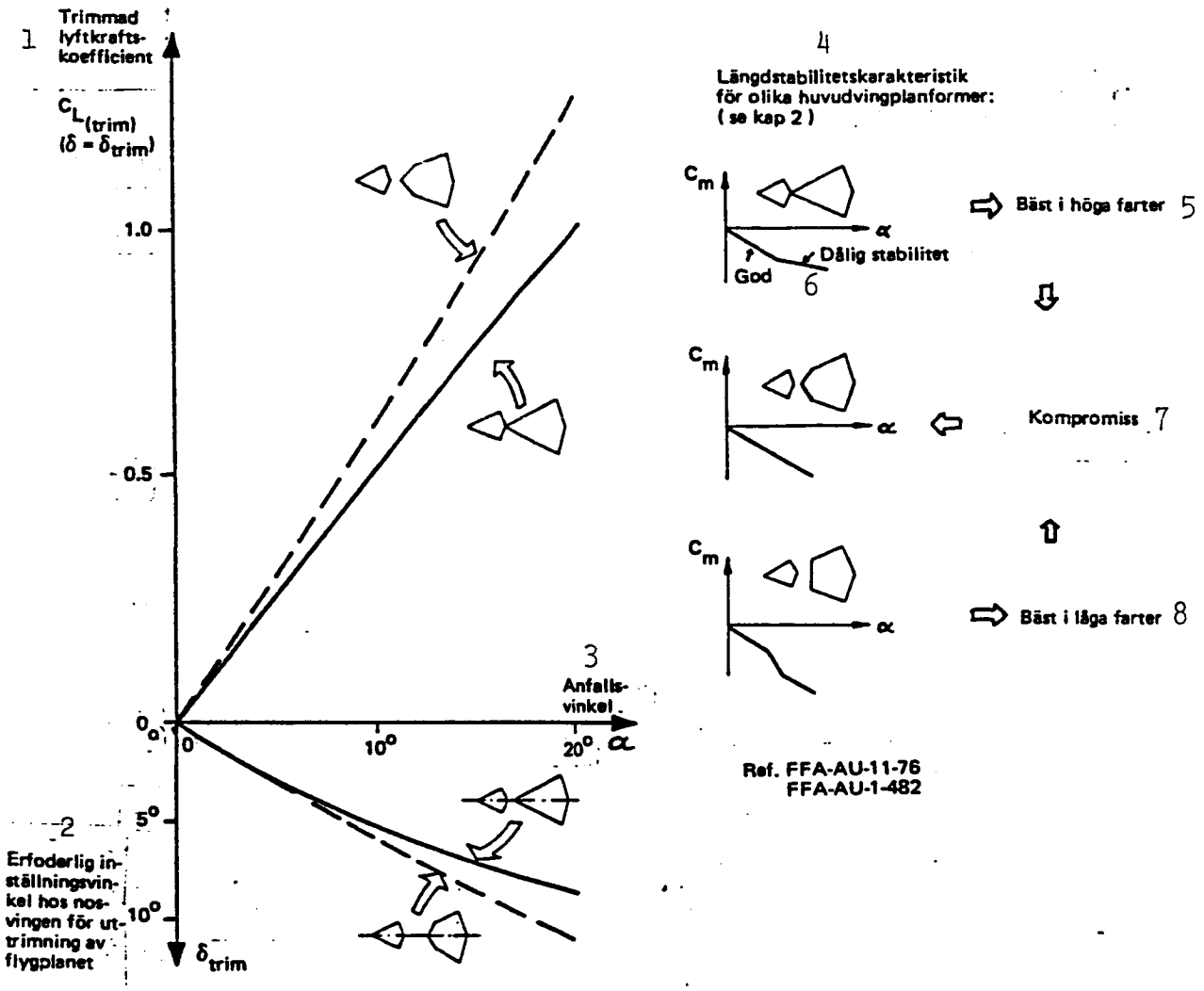

Fig. 24. Effect of a "lopped off" leading edge of the main wing.
Key: 1. Trimmed lift coefficient.
2. Adjustment angle of the canard, necessary for trimming the aircraft.
3. Angle of attack, α.
4. Longitudinal characteristics of different planar shapes of the wing (cf. Chpt. 2)
5. Most satisfactory at high speed.
6. Satisfactory/unsatisfactory stability.
7. Compromise.
8. Most satisfactory at low speed.

for (cf. Fig. 24). This compromise turned out to have the most satisfactory characteristics in respect to the longitudinal stability as well. As mentioned above it is necessary to take the effects of the fuselage bow and the air-intakes into consideration as well when adjusting the force of the wing systems. This fact as well as the limitations on the construction led to that during the final design of FPL 37 a fixed canard with a flap was selected

instead of a mobile wing. In order to make the trailing edge flap as effective as possible, it was executed in the form of a slotted flap. Although in this manner the ideal effect was minimized because the wing system was placed on a relatively wide fuselage and since the trimmable apical surface thus became relatively small there was still a gain on the order of 7 -10% in respect to the pure, trimmed lift.

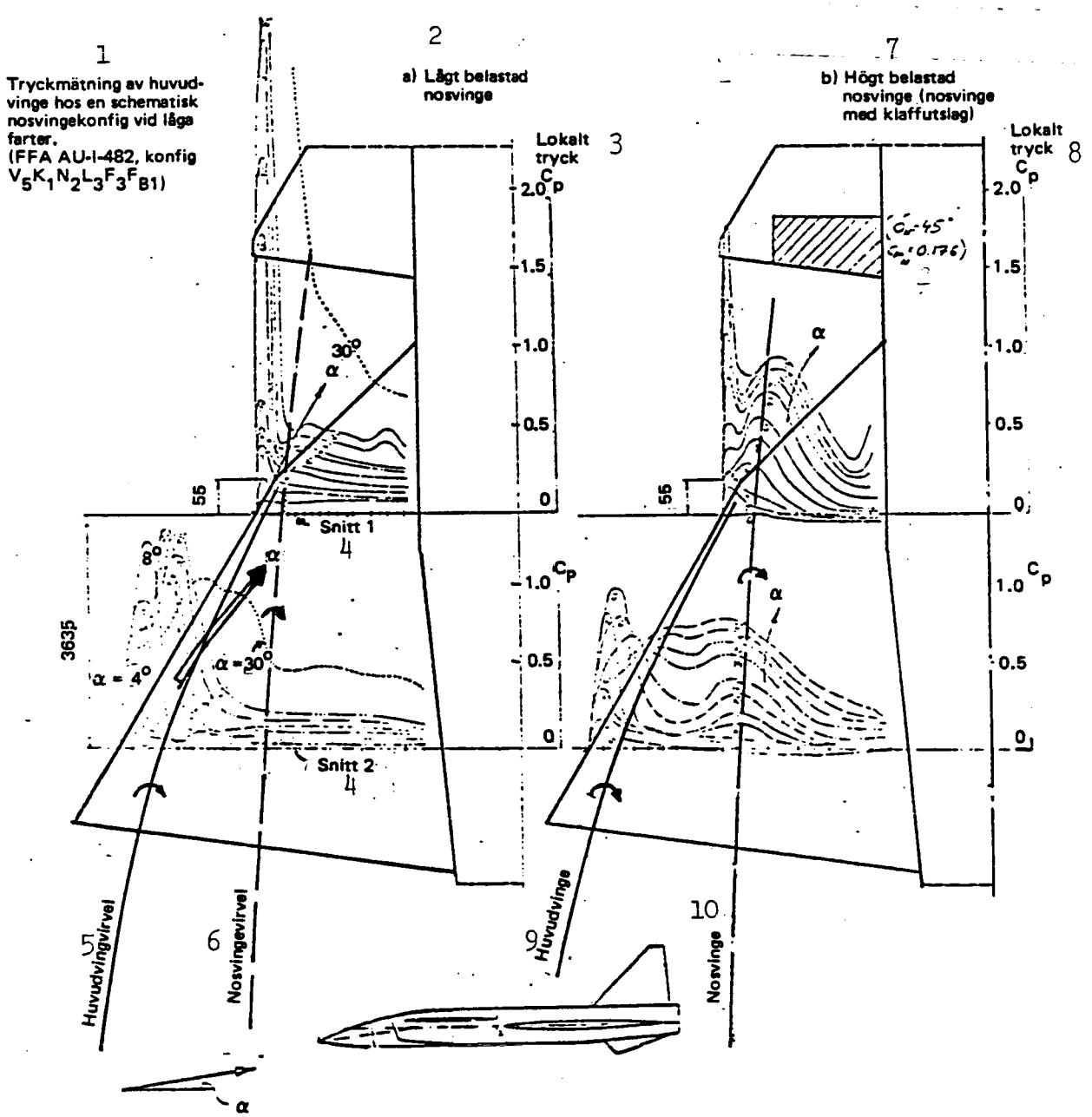

Fig. 25. How the canard affects the distribution of the pressure across the wing.
(Key: see p. 34)

Key to Fig. 25:

1. Measurement of the pressure over the wing in relation to a schematic configuration with a canard at low speed. (FFA AU-1-483, configuration $V_5K_1N_2L_3F_3F_{B1}$).
2. a) Canard with light load.
3. Local pressure
4. Cross section 1 (2).
5. Wing vortex .
6. Canard vortex.
7. Canard with a heavy load (canard with flap deflected).
8. Local pressure.
9. Main wing.
10. Canard.

Figure 25 illustrates what the distribution of the lift looks like at two cross sections through the wing span of the main wing of a schematic 37 configuration. The angle of attack is varied so that it becomes evident how the lift develops when the angle of attack is increased. In case a) the canard has the same adjusted angle as the wing has and is, thus, relatively little loaded, i.e., it produces a weak leading edge vortex in comparison with that of the wing. Case b) shows FPL 37 in a landing configuration where the load on the canard is increased by deflecting its flap. /24 cont.

In case b) there are two distinct peaks illustrating lift; the inner one is caused by the vortex system of the canard. At the same time it is evident that in comparison with case a) the peak of lift close to the leading edge of the wing (i.e., the outer peak) is reduced. /25

From the point of view of lift the advantages of the PFL 37 design can be summarized as follows:

1. Great maximum lift due to the maintenance of a stable flow up to very wide angles of attack (ca. 27°).
2. Due to the trimming of the canard additional lift can be created by means of the extra lift produced by the canard and the additional lift provided by the trailing edge flap and necessary for momental equilibrium (see below). /26

When FPL 37 is landing it is in this manner possible to utilize a lift capacity of the wing system which is almost twice as large as that of FPL 35 (on the condition of similar speed). In practice this advantage can be utilized for a lower landing speed.

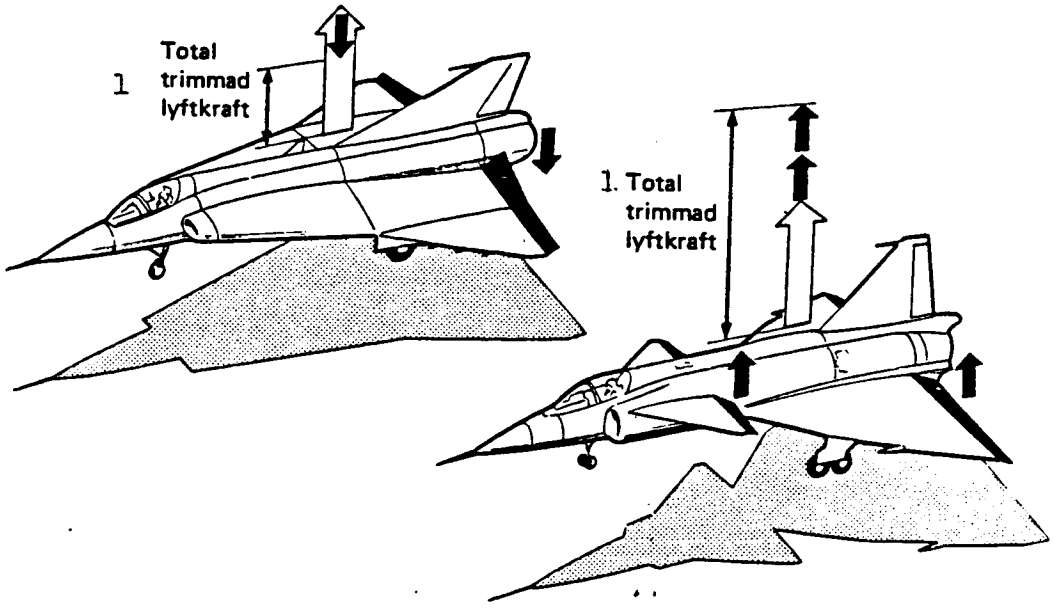

Fig. 26. Comparison between the trimmed lift of FPL 35 and that of FPL 37.
Key: 1. Total trimmed lift.

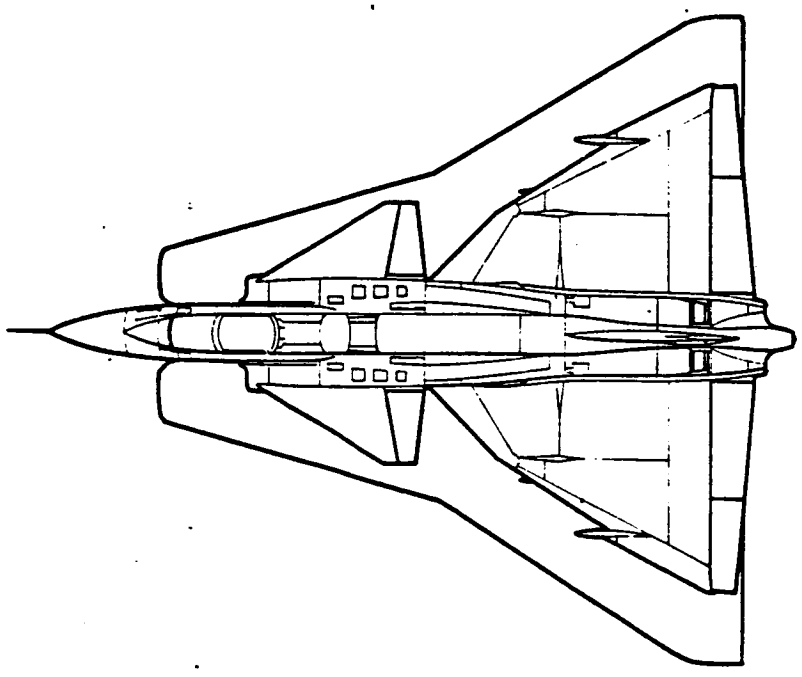

Fig. 27. Wing surface necessary for FPL 35 in order to provide the same lift as that of the 37 configuration during landing.

Figure 27 illustrates the wing surface which would have been necessary for FPL 37 had the wing design of FPL 35 been retained and the demands on the landing performance of FPL 37 had been unaltered.

It is evident from Fig. 25a that the peak of the lift at angles of attack wider than 8 - 9° changes in character, becomes step-like and proceeds inward. A secondarily separated area develops outside the leading edge vortex system of the outside portion of the wing (cf. Fig. 17).

This can be explained so that the vortex over the outer wing is "lifted" by the canard vortex, which according to Fig. 25 is the one most powerful in case b).

2. THE LIFT AND THE PITCHING MOMENT OF THE FPL 37 CONFIGURATION AT LOW SPEED /27

2.1 Introduction

So far we have discussed the aerodynamic principle behind the 37 configuration. We have described how the interference between two delta wings in a tandem configuration can be utilized in order to achieve a substantial lift up to wide angles of attack.

In this section we shall study in detail the characteristics of the aerodynamic forces exerted on FPL 37 during straight-line flight. It is just the interaction between these forces which provide FPL 37 with its special properties. It is therefore worth knowing:

- how the aerodynamic forces vary in relation to the angle of attack; and
- how we are able to affect these aerodynamic forces and the equilibrium between them.

We shall define the concept of longitudinal stability and find out how, in the case of FPL 37, a satisfactory longitudinal stability was achieved up to wide angles of attack. For instance, in what manner is the longitudinal stability affected by externally suspended arms? Many factors affect the longitudinal stability and must be taken into consideration.

In order to be able to follow the reasoning below, we shall recapitulate the definitions of force and moment, coefficients and reference magnitudes. We will only take flying unaffected by an oblique air flow, i.e., pure or symmetric flight, into consideration. Corresponding forces and moments are called symmetrical.

2.2 Definitions of Symmetric Forces and Moments in Respect to FPL 37

/28

Two systems of definition are conventionally applied: a wing-related system and a fuselage related one (Fig. 28).

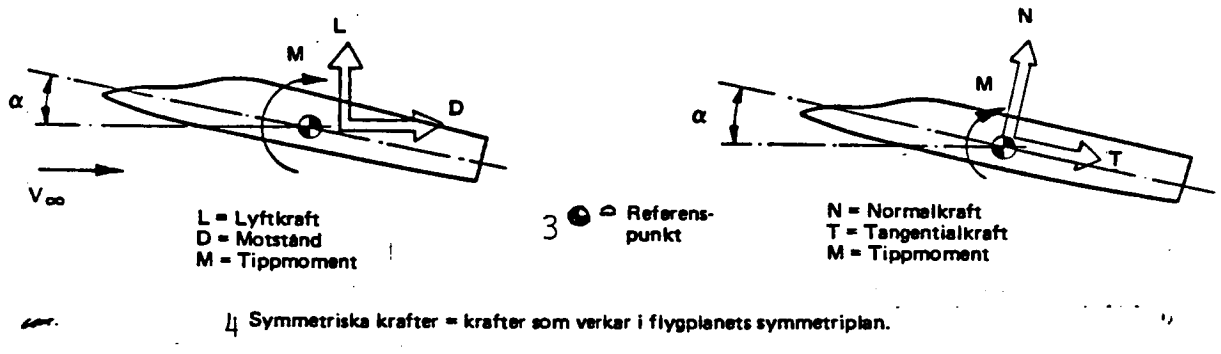

Fig. 28. Definitions of symmetric forces, angles and moments in respect to FPL 37.
Key: 1. Wind-related system (Stability axes).
2. Fuselage-related system (body axes), standard.of FPL 37.
3. Reference point.
L = lift; D = drag; M = pitching moment; N = normal force; T = tangential force; M = Ptiching moment.
4. Symmetric forces = forces acting in the symmetry plane of the aircraft.

The magnitudes are usually expressed in the form of coefficients (i.e., non-dimensional magnitudes). It is then valid that:

the lift coefficient $C_L = \frac{L}{q \cdot S}$ $\longleftrightarrow$ the normal force coeffcient $C_N = \frac{N}{q \cdot S}$,

the drag coefficient $C_D = \frac{D}{q \cdot S}$ $\longleftrightarrow$ the tangential force coefficient $C_T = \frac{T}{q \cdot S}$, and that

the pitching moment coefficient $C_m = \frac{M}{q \cdot S \cdot c}$,

where, as mentioned above, q = the dynamic pressure,
S = the reference surface (usually the wing surface, in respect to FPL 37 = 46 m^2), and
c = the reference chord (in the case of FPL 37 = 7.4 m).

The point around which the moment is estimated is called the reference point and is selected as a suitable rear mean point of gravity, in the case of FPL = STA X_{65_B} = 12350 (according to the system of coordinates valid).

The dependency of the angle of attack on these coefficients is characteristic for the majority of aircrafts and looks, at low speed, in principle as follows:

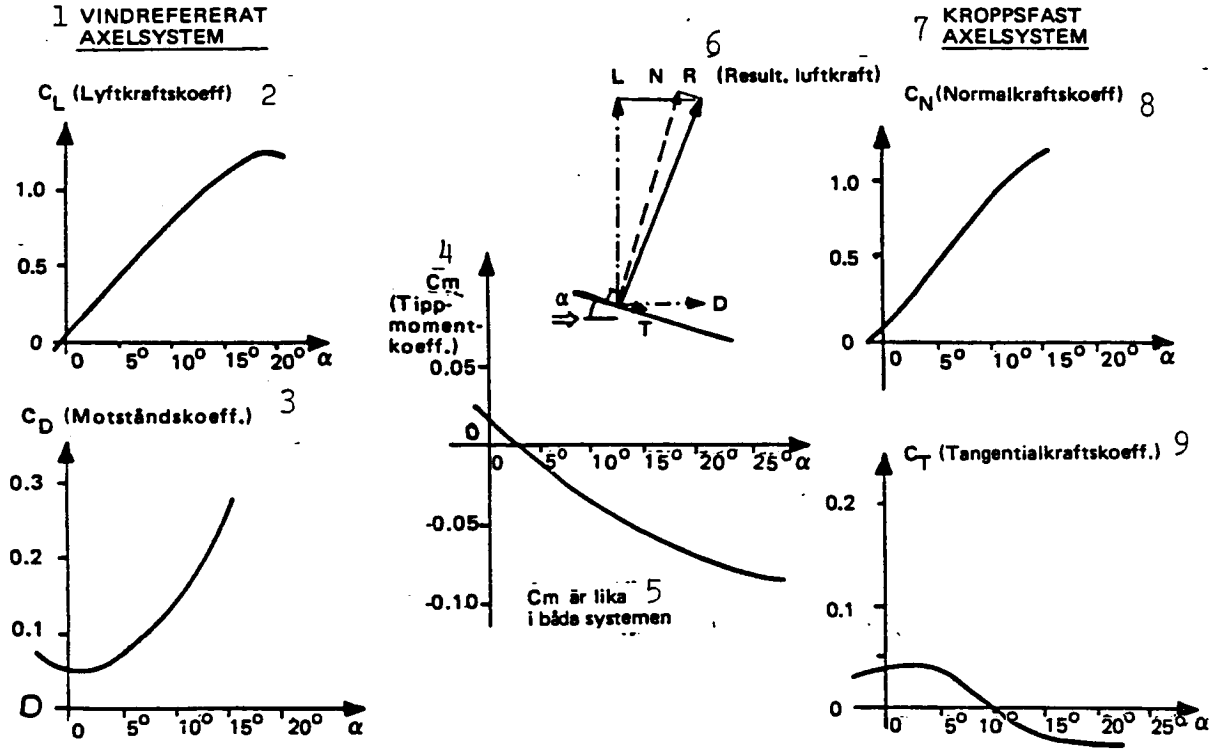

Fig. 29. The dependency of the angle of attach (the characteristics) of symmetric forces and moments of FPL 37.
Key: 1. Wind-related axial system
2. (Lift coefficient)
3. (Drag coefficient)
4. (Pitching moment coefficient.
5. C_m is the same for both systems.
7. Fuselage-related axial system
8. (Normal force coefficient)
9. (Tangential force coefficient)

2.3 Characteristics of Normal Force

The normal force of the fuselage-related system corresponds to the lift of a wind-related system (see Fig. 28). The dependency on the angle of attack in the case of both these forces looks quite similar. For practical reasons normal force and its coefficients are used below for the continued reasoning. (The fuselage-related system is standard in the case of FPL 37.)

Let us contemplate the normal force coefficient (C_N) in detail; as mentioned above, it is mainly dependent on the angle of attack. It is therefore customary to split up the C_N according to the following schematic manner of designation:

$$C_N = \underbrace{C_N\,(\alpha = 0)}_{\text{Contribution independent on the angle of attack}} + \underbrace{C_N\,(\alpha)}_{\text{Contribution dependent on the angle of attack}}$$

At low speed the variation in normal force in relation to the angle of attack (i.e., the characteristics of the normal force) takes the form illustrated in Fig. 30. This figure demonstrates also how various partions of the aircraft (its fuselage, canard or wing) contribute to the normal force (in the diagram expressed by its coefficient, C_N). The zero contribution $C_N = (\alpha = 0)$, is minor and can therefore by ignored for the sake of simplicity.

It is evident that a relatively large amount of the normal force of the /30
canard is lost in the form of an interference load on the main wing. (At narrow angles of attack up to as much as 80% of the load of the canard is lost due to interference). The major portion of the load due to interference can be referred to the apical inner portion of the main wing. At increasing angles of attack the relative size of the interference load diminishes and, finally, the effect of the favorable interaction between the canard and the wing becomes clearly evident. Because of the interaction of the various contributions, a characteristic of normal force results which is fairly linear up to wide angles of attack and has a large maximum value.

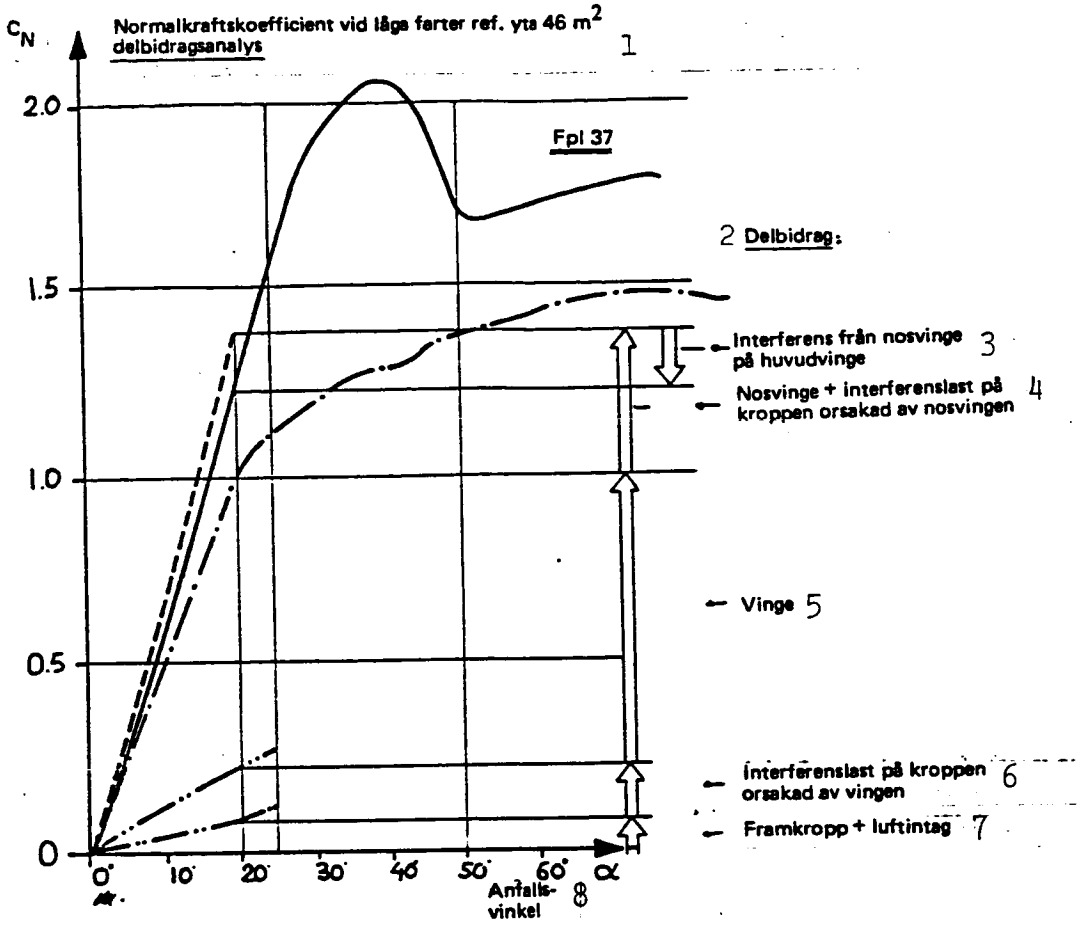

Fig. 30. Characteristics of the normal force of FPL 37 and important partial contributions to the characteristic of this force.
Key: 1. Normal force coefficient at low speed; reference surface 46 m^2. Analysis of partial contrbitions.
2. Partial contributions:
3. Interference of the canard on the main wing.
4. Canard + interference load on the fuselage caused by the canard.
5. The wing.
6. Interference on the fuselage caused by the wing.
7. Bow of the fuselage + air intakes.
8. Angle of attack.

If the elevator is deflected, the normal force is affected as shown by Fig. 31a.

A satisfactory illustration of the variation in normal force in relation to the angle of attack as well as to the elevator angle can be obtained if the graphs of the angles of attack at different elevator deflections are displaced laterally and are made to connect points with a constant angle of attack such as seen in Fig. 31c. There the normal force is represented as a

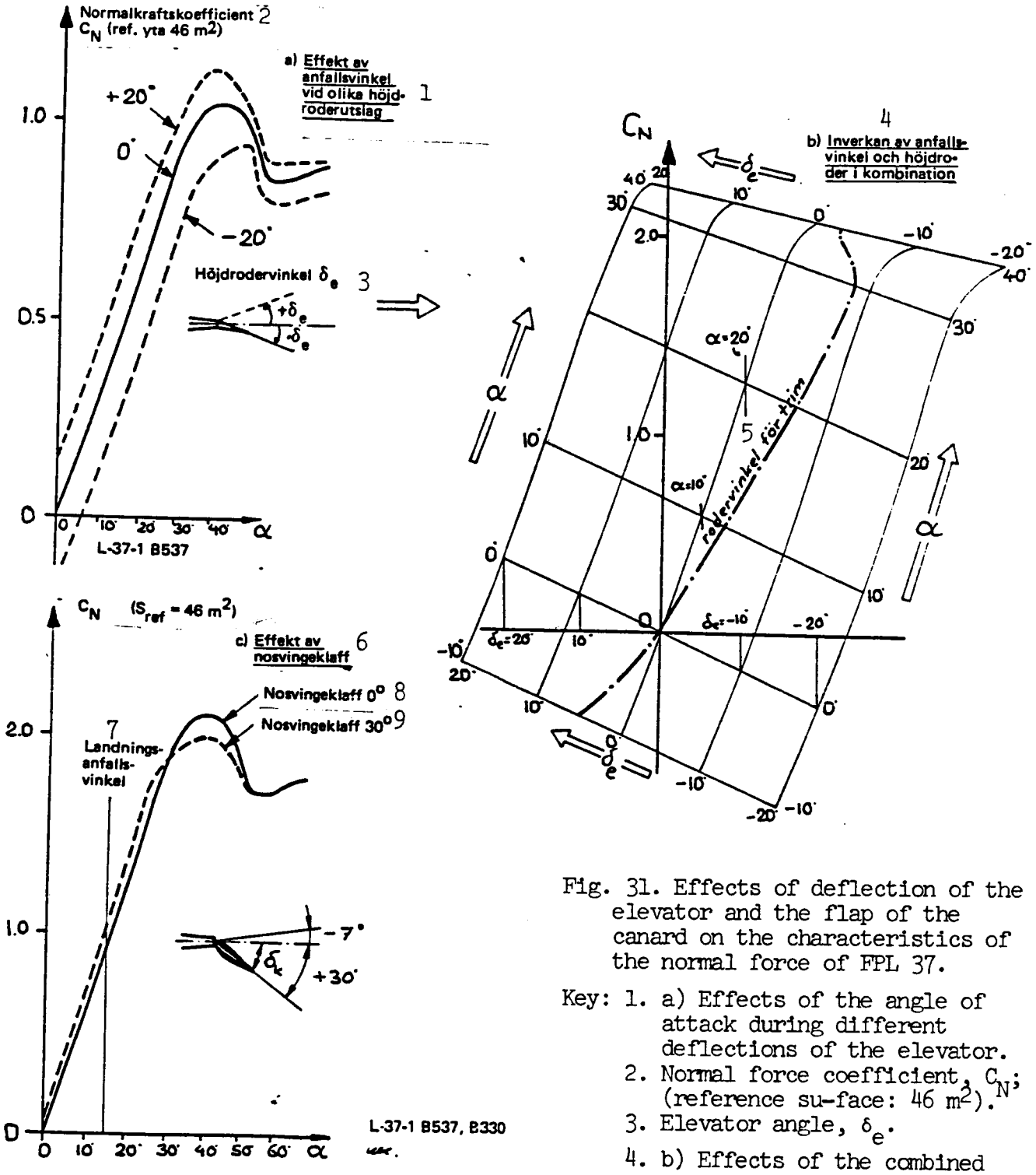

Fig. 31. Effects of deflection of the elevator and the flap of the canard on the characteristics of the normal force of FFL 37.

Key: 1. a) Effects of the angle of attack during different deflections of the elevator.
2. Normal force coefficient, C_N; (reference su-face: 46 m²).
3. Elevator angle, δ_e.
4. b) Effects of the combined angle of attack and that of the elevator.
5. Angle of attack during landing.
6. c) Effect of the flap of the canard.
7. Flap of canard at 0°.
8. Flap of canard at 30°.

"blanket" on top of the angle of attack, α, and the elevator angle, δ_e. When it is known how the elevator angle necessary for trimming (Fig. 31) varies in relation to the angle of attack, the trimmed normal force can be read by means of this "blanket".

The change in the normal force in relation to a deflection of the flap of the canard is evident from Fig. 31c. In the figures the effect of the flap of the canard in comparison with that of the elevator is very limited as a consequence of the fact that a great portion of the contribution from the normal force is lost in the form of interference on the main wing. The principal objective of the flap of the canard is, thus, not to furnish a contribution of its own to the total normal force or lift but instead to balance the deflection of the elevator (i.e., to contribute to the pitching moment) and, thus, give rise to a positive contribution from the elevator to the normal force (see Fig. 32).

Before we proceed to discuss longitudinal stability, it may be appropriate /32
to illustrate how the characteristics of the normal force of FPL 37 hold up in comparison with those of our preceeding types of aircrafts, i.e., FPL 35 and FPL 32:

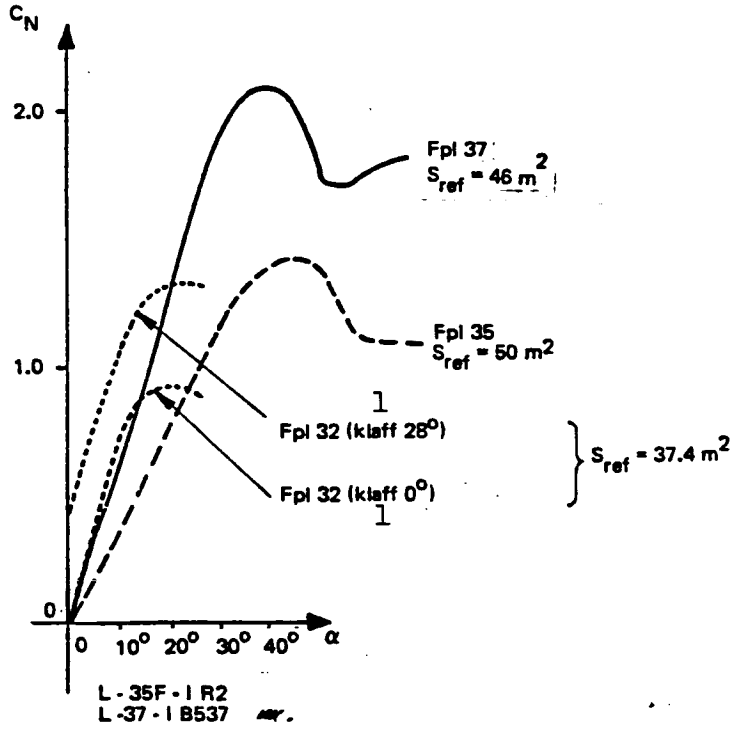

Fig. 32. The characteristic of the normal force of FPL 37 in comparison with that of FPL 35 or FPL 32. Untrimmed aircrafts. Key: 1. Flap.

Conventional aircrafts with swept-back wings must rely on heavy and complicated mobile elevating arrangements (e.g., large trailing edge and leading edge flaps) in order to be able to compete with delta-winged planes in respect to lift. This is all right at low speed but for several reasons it is difficult to utilize such arrangements effectively when maneuvering at high speed. In many countries this is at present one of the most vital current problems of the aerotechnicians of the 1970s.

2.4 Longitudinal Stability, Pitching Moment and Margin of Stability

We have seen how the aerodynamic forces affecting an aircraft can be distinguished into several partial contributions. If we now look at an aircraft from the side (all the forces are supposed to attack within the symmetry plane of the aircraft), it is easy to demonstrate - like in Fig. 33 - how the different partical forces act at different distances from the point of gravity (or the reference point) of the aircraft. Each partial contribution furnishes a (pitching) moment around the reference point. In the case of a slender aircraft as FPL 37 the partical forces are rather well dispersed longitudinally. In respect to the normal force it is - just like before - possible to distinguish the pitching moment and its partial contribution into one part, independent of the angle of attack (a zero contribution) and one part, dependent on the angle of attack.

If using the coefficients, this can be written:

$$C_m = C_m\ (\alpha = 0) + C_m\ (\alpha).$$

The zero contribution is in general minor and is of no importance at /33
low speed.

The portion depending on the angle of attack is, on the other hand, considerable and of essential importance, since it decides directly whether the airplane is longitudinally stable or not.

The most important partial contribution of the aerodynamic forces in the case of an untrimmed FPL 37 is evident from Fig. 33 (by an untrimmed aircraft we mean that any deflection of the elevator plus the deflection of the canard flap will equal zero).

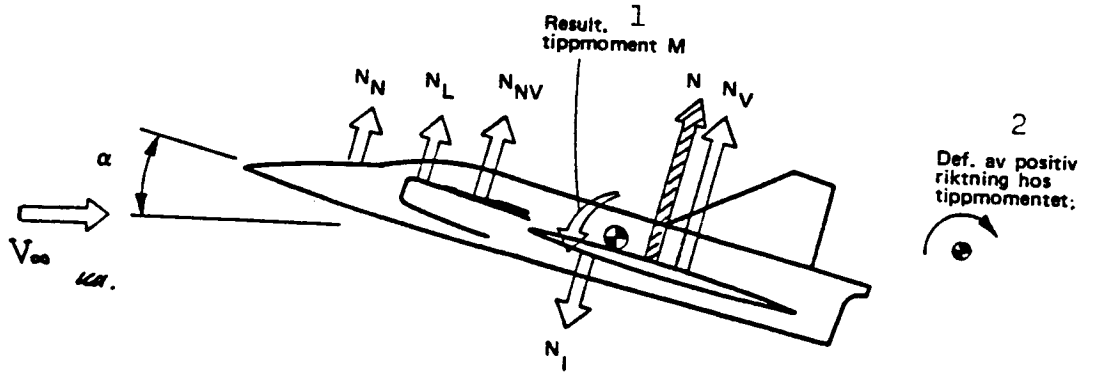

Fig. 33. Partial contributions to the normal force of FPL 37. Attack points and approximate relations between the magnitude of the different contributions.

Key: N_N means the contribution of the bow of the fuselage.
N_L " " " of the air intakes.
N_{NV} " " " of the canard
N_I " " " of the interference load on the wing, caused by the canard.
N_V " " " of the main wing.
1. The resultant pitching moment, M.
2. Definition of a positive direction of the pitching moment.

The resultant force (N in Fig. 33) is equal to the sum of the partial contributions mentioned above and corresponds to the total untrimmed normal force of the aircraft.

At positive angles of attack this will, thus, produce a lowering moment on the bow of the aircraft. Since the normal force increases with increasing angle of attack, the pitching moment will become increasingly negative (the definition of a positive moment is evident from Fig. 33). Thus, the following is valid:

Statically longitudinally stable aircraft:

- The resultant normal force (the portion dependent on the angle of attack lies behind the point of gravity (the reference point).
- An increase in the angle of attacl leads to an increasingly negative (bow-down) moment.

The greater the distance between the point of attack and the ref. point, /34
the more stable is the airplane. The reverse (i.e., N in front of the reference point) produces a "nose-up" moment in relation to an increasing angle of attack, which results in a longitudinally unstable aircraft.

In the case of an ordinary, longitudinally stable aircraft with an ideal, linear characteristic of the pitching moment, the latter depends, consequently, on the angle of attack and is, thus, = 0 only at a single angle of attack.

During the flight it is therefore necessary to restore the equilibrium of the moments, which is one of the conditions for being able to fly straight ahead. This is usually accomplished by deflection of the elevators. It is necessary to balance, - or "trim", - the aircraft and for each angle of attack, a certain deflection is necessary for achieving the correct "trim".

Figure 34 illustrates how a conventional elevator behind the reference point affects the moment of a stable aircraft.

An upward deflection of the elevator (according to the definition = a negative deflection of the elevator) is, thus, necessary for restoring the equilibrium at normal, positive angles of attack. This means that the deflection of the elevator delivers a negative contribution to the lift, the greater the wider the angle of attack is and the greater the more stable the aircraft is. In order to avoid unnecessarily large losses due to trimming the aircraft must, thus, not be too stable.

To achieve an ideal, recti-linear graph of moment, the dependency on the angles of attack must be adjusted so that the final result ends in a momental curve, if possible looking like in Fig. 34.

The gradient of the C_m graph is, thus a direct measure of longitudinal stability. The gradient of the C_m (α) graph is called the "margin of stability" and is usually written as $\partial C_m / \partial \alpha$. Its standard size in the case of FPL 37 (in reference to the mean position of the point of gravity) is, at low speed, on the order of 0.3 m. The magnitude is determined in part by the actual variation of the point of gravity of the aircraft, in

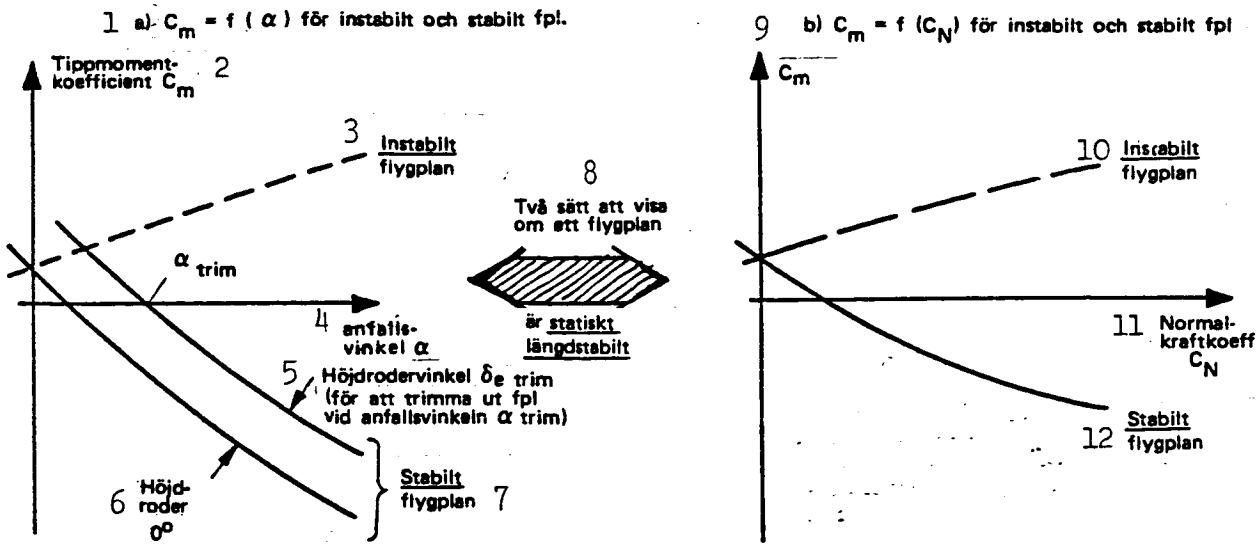

Fig. 34. Key: 1. a) $C_m = f(\alpha)$ for an unstable as well as a stable aircraft.
2. Coefficient of pitching moment, C_m
3. Unstable aircraft.
4. Angle of attack, α.
5. Angle of elevator, $\delta_{e\ trim}$ (for trimming an aircraft at the angle of attack, α_{trim}.
6. Elevator, 0°.
7. Stable aircraft.
8. Two manners of illustrating whether an aircraft is statically stable longitudinally.
9. b) $C_m = f(C_N)$ of an unstable as well as a stable aircraft.
10. Unstable aircraft.
11. Normal force coefficient, C_N.
12. Stable aircraft.

part in respect to what extent the shape of the graph of the moment is affected by different aerodynamic factors (see below).

By means of Fig. 35 it is easy to demonstrate what happens when the distance /35 between the point of attack,belonging to the load and depending on the angle of attack, and the reference point is altered. If the stability margin is reduced, a position will gradually be reached where the gradient = 0 and where, consequently, C_m will not change when α is altered. A neutral stability has been achieved. The reference point (the position of the point of gravity) corresponding to a gradient (i.e., the stability margin) = 0 is called the neutral point (abbreviated as NP). When the neutral point is the same as the reference point, the pitching moment will take the form, shown in Fig. 36.

Neutral (indifferent) stability means, thus, in practice that the aircraft is extremely sensitive for a deflection of the elevator.

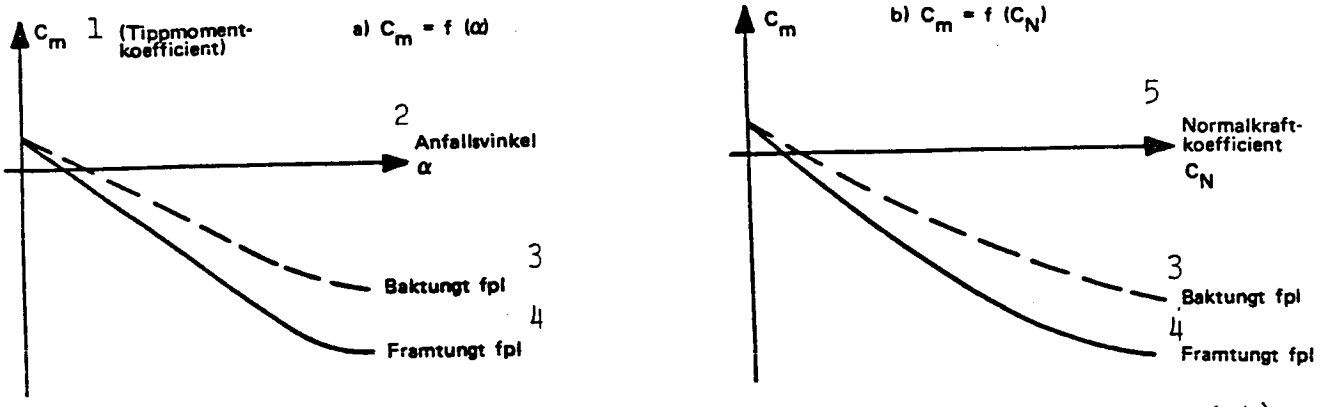

Fig. 35. Effect of the position of the point of gravity (the reference point) on the dependency of the coefficient of pitching moment on the angle of attack.
Key: 1. C_m (coefficient of pitching moment)
2. Angle of attack.
3. Tail-heavy aircarft.
4. Bow-heavy aircraft.
5. Normal force coefficient.

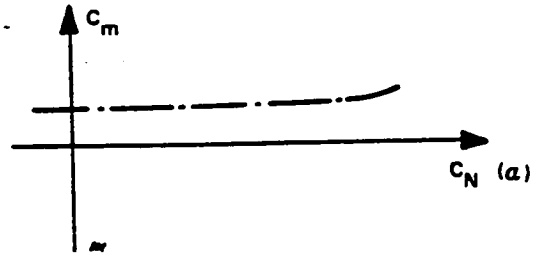

Fig. 36. Pitching moment as a consequence of the normal force of an aircraft with neutral stability.

Unstable graphs of moment can in combination with advanced steering automatics be utilized in order to profit from the lift due to deflection of the elevator. For practical and/or economical reasons FPL 37 does, however, not utilize this instability but is designed as a conventional, stable aircraft. The mean position of its point of gravity, $X_{65} = 12350$, has been selected so that a satisfactory stability can be achieved even during difficult flying conditions together with an external load (the stability margin at low speed will be on the order of 0.3 - 0.5 m, which is a rather representative measure of the distance between the neutral point and the point of gravity in respect to an airplane of that size).

It is usually not difficult to select a position of the point of gravity /36 when designing an aircraft so that the plane will become stable. It is

considerably more difficult to avoid localized instability at certain angles of attack. This is very common in the case of aircrafts with a small aspect ratio. From the point of view of flight characteristics it is important to avoid non-linear graphs of moment. Therefore the problems pertaining to FPL 37 will be discussed in rather great detail. Figure 37 illustrates an example of what a graph of moment can actually look like.

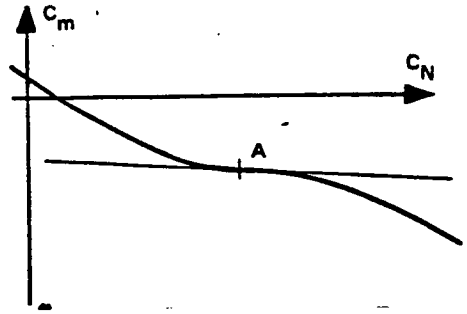

Fig. 37. Graph of the pitching moment with non-linear characteristics.

In case A the local stability margin equals the gradient of the tangent of the curve at that point and this can, therefore, differ considerably from the mean stability margin.

It is an esay task to achieve a linear graph of moment in respect tp a slender aircraft with a large longitudinal scattering of the lift (normal force) portions. In order to touch upon some of the problems, we shall demonstrate how the portions of lift (normal force) vary in relation to the angle of attack in the cases of the bow of a fuselage, typical delta wings with different sweep-back angles of the leading edge, and the interfering load induced on the wing by the canard and typical of FPL 37.

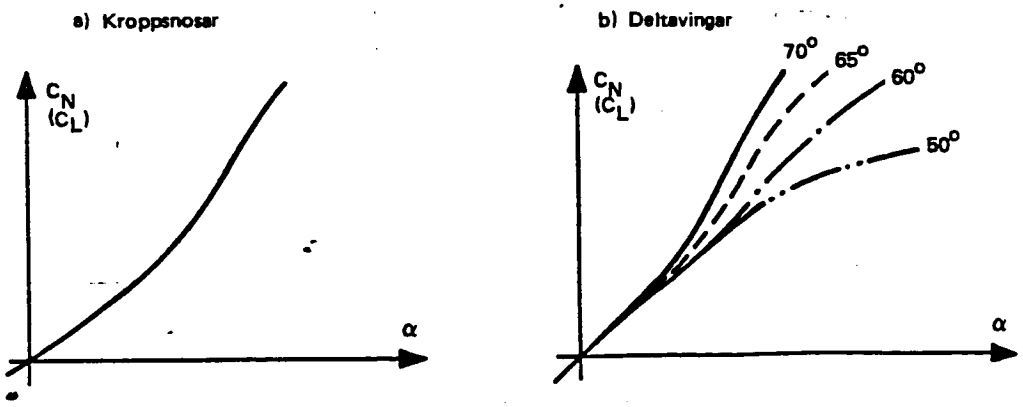

Fig. 37. Examples of how various partial contributions to C_N vary in relation to the angle of attack.
a) Bow of fuselage; b) Delta wings; c) see p. 48.

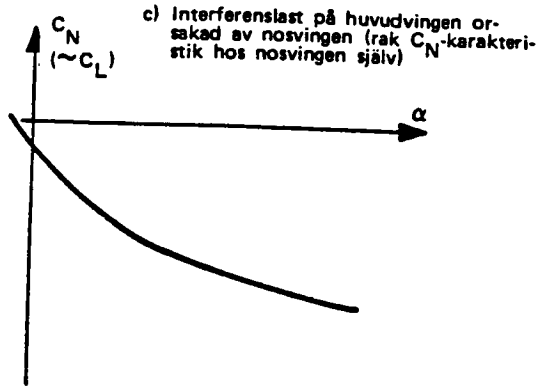

Fig. 38 (cont.). Examples of how various partial contributions to C_N vary in relation to the angle of attack, /37

c) Interference load on the wing caused by the canard (linear C_N characteristic of the canard itself.

In the cases of swept-back or delta wings with large lateral extention, the course of the separation, taking place before the wing actually stalls, plays a major role for the appearance of the graph of pitching moment. In addition to the effect due to the configuration of the wing itself, the course of the detachment is also affected by the area of interfering flow within which the wing is placed (cf. Fig. 19). It is typical for acute swept-back wings and delta wings with leading edge separation that there is a large local load in the direction of the chord close to the tip. Tip separation starts there and off-loading of the trailing portion of the wing follows. The increase in lift becomes damped and the entire lift resultant of the wing will be moved forward. A so-called "pitch-up" occurs: cf. Fig. 39.

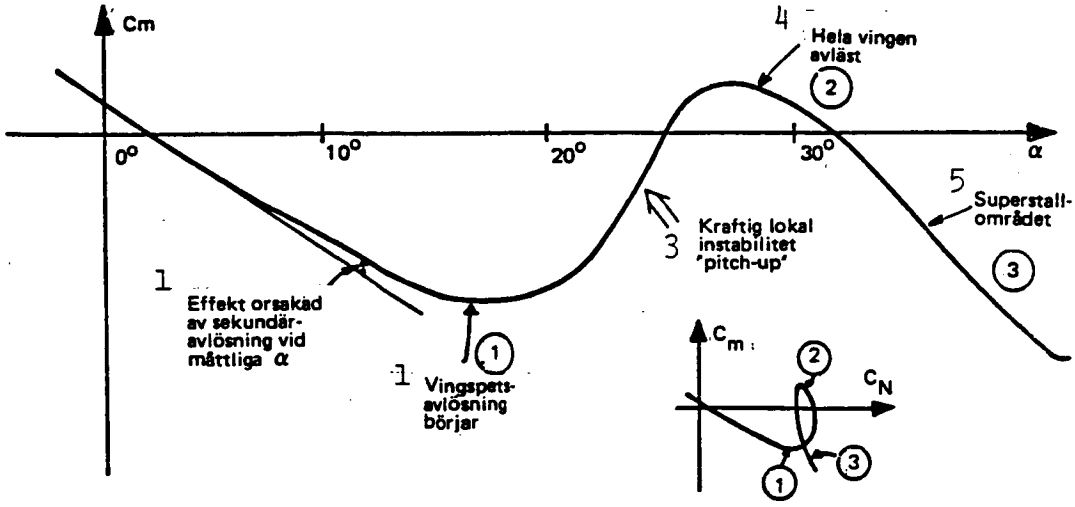

Fig. 39. Characteristics of the pitching moment of a delta wing.
Key: 1. Effect due to secondary separation at moderate α.
2. Separation starts at the wing tip.
3. Strong local instability, "pitch-up".
4. The entire wing is detached.
5. Area of super-stall.

In the worst case the pitch-up can be so severe that it cannot be counteracted by elevator deflection, especially since the trailing edge flap of the wing loses part of its effect when the wing has been detached. In the case of delta wings, small, momentary changes in the type of flow can occur (e.g., sudden locally appearing, secondary separation below the leading edge vortex). This produces graphs og moment with a "kink", in principle similar to that in Fig. 40. /38

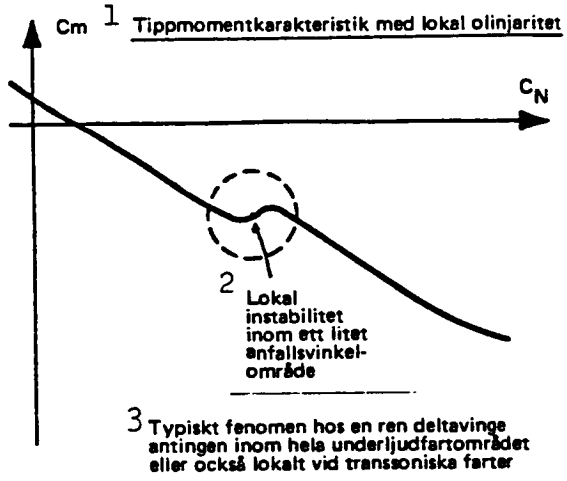

Fig. 40.

Key: 1. Characteristic of pitching moment with local non-linearity (a kink or a "nick").

2. Local instability within a narrow range of angles of attack.

3. A typical phenomenon pertaining to a "typical" delta wing within the entire range of subsonic flight or, locally, during trans-sonic flight.

The air flow around the wing can frequently be affected when, for instance, external equipment is mounted below the aircraft. Deflection of the elevators or ailerons can also disturb the circulation across the wing. In the case of FPL 37 we have succeeded by means of a suitable choise of leading edge sweep-back, planar shape and the mutually relative positions of wing and canard as well as their sizes to achieve a configuration with a practically linear graph of momentum up to ca. 28°. The pitch-up ensuing is attenuated because the canard starts to lose lift at approximately the same time as the pitch-up effect reaches its maximum. Figure 41 gives an idea of the work behind this and also of the sensitivity of FPL 37 to changes in the design. The figure illustrates the effects on the longitudinally stability, exerted by the raised position of the canard and its length as well as the sweep-back of its leading edge in addition to the effects of the planar shape of the wing. (cf. also Fig. 24).

Fig. 41

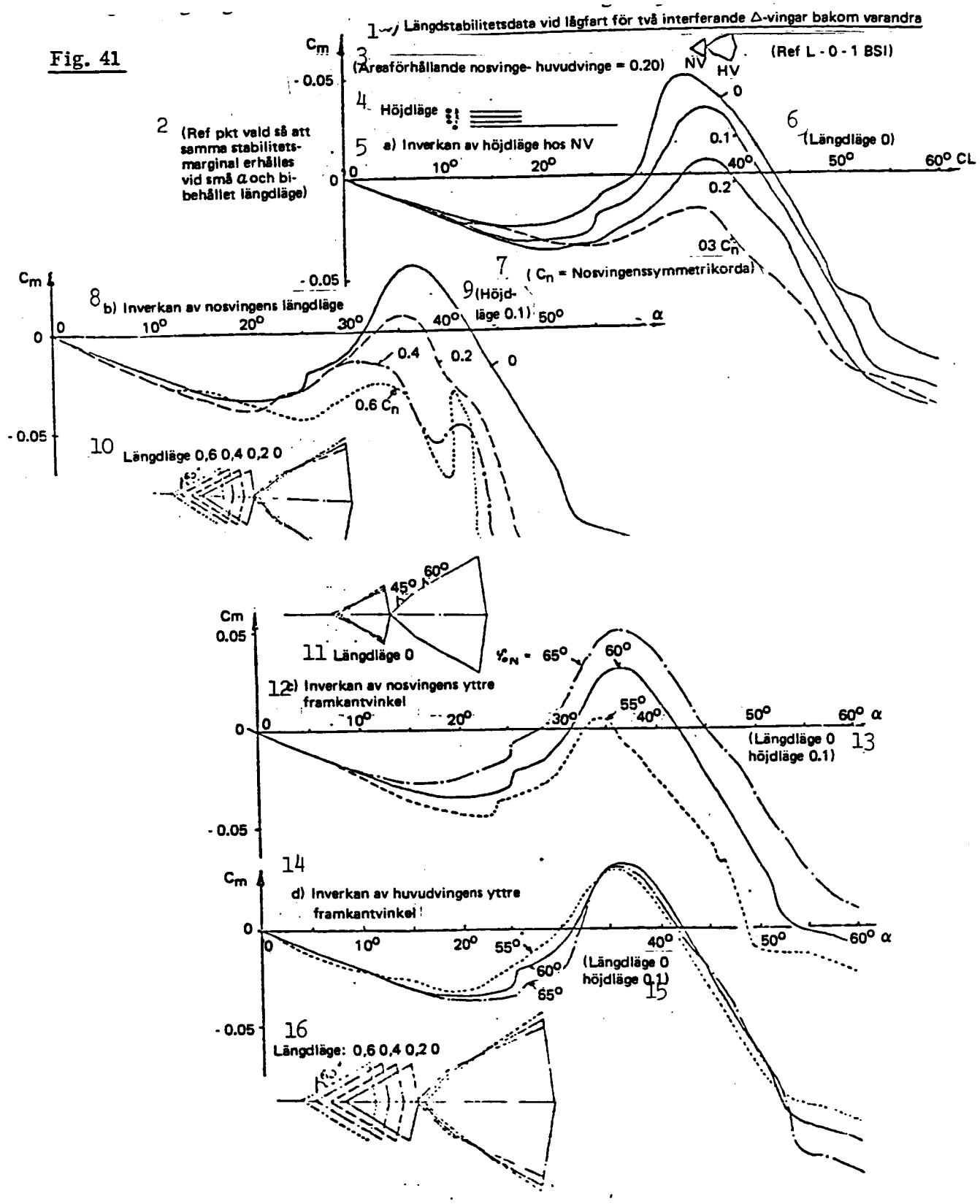

Fig. 41. Key: see p. 52.

Key to Fig. 41:

1. Data on longitudinal stability of two mutually interfering delta-wings in tandem formation at low speed.
2. (Reference point selected so that the same margin of stability is achieved at narrow angles of attack and a constant longitudinal position)
3. (Areal correlation between canard and wing = 0.20)
4. Vertical position
5. a) Effect of the vertical position of the canard (NV)
6. (Longitudinal position 0)
7. (C_N = the symmetry chord of the canard)
8. b) Effect of the longitudinal position of the canard.
9. (Vertical position 0.1)
10. Longitudianl positions 0.6, 0.4, and 0.2.
11. Longitudinal position 0
12. c) Effect of the outer leading edge angle of the canard
13. (Longitudianl position 0, vertical position 0.1)
14. d) Effect of the outer leading edge angle of the main wing
15. (Longitudinal position 0, vertical position 0.1)
16. Longitudinal position 0.6, 0.4 and 0.2.

2.5 Effect of Modification of the Leading Edges of the Wing and the Canard on the Pitching Moment

It is, thus, possible to affect the course of the pitching moment by means of relatively limited modifications of the leading edges of the canard and the main wing. This fact has also been utilized in order to improve the characteristics of FPL 37. Such modifications are illustrated in Fig. 42.

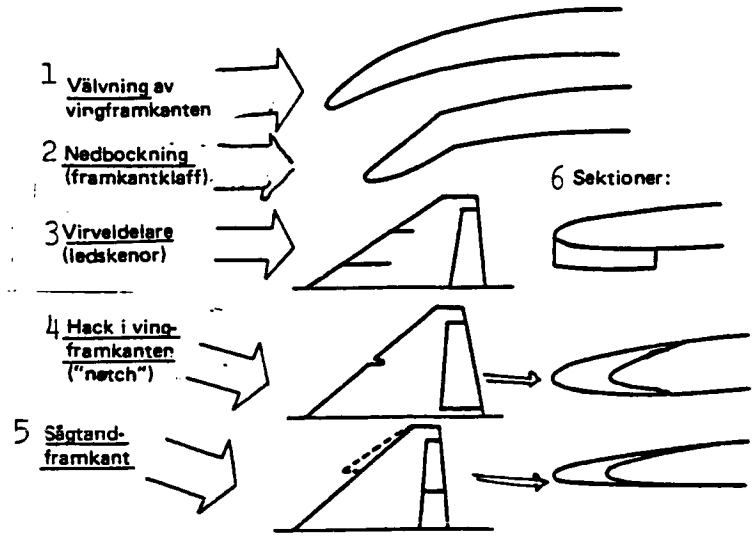

Fig. 42. Various means for eliminating local disturbances of the pitching moment.
Key: 1. Cambering of the leading edge of the wing.
2. Bending down (leading edge flap)
3. Vortex dividers (guide rails
4. Notch in the leading edge.
5. "Sawtooth notch" in the leading edge.
6. Cross sections

All these modifications contribute to smoothing out or straightening the course of the graph of pitching moment. They will be discussed below.

a) Cambering /40

The main objective of cambering is to reduce the drag at wide angles of attack. As a side effect the longitudinal stability as well is affected. In part the limit of the angle of attack is raised at a point where the to leading edge separated flow occurs (Fig. 43):

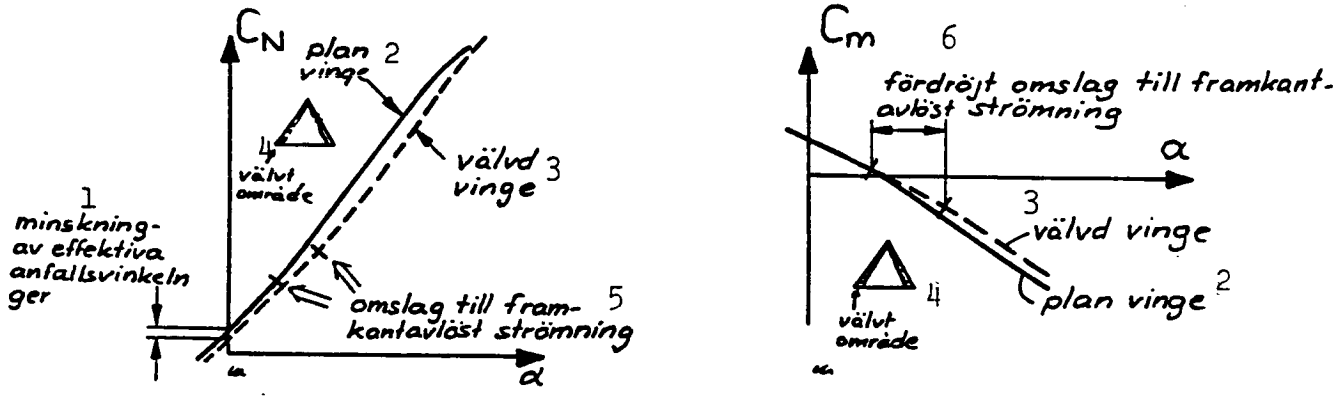

Fig. 43. Effect of a cambered leading edge of the wing on the lift (normal force) and the pitching moment of a delta wing.
Key: 1. Reduction of the effective angle of attack results in ...
2. Flat wing.
3. Cambered wing.
4. Area cambered.
5. Conversion to leading edge separated flow.
6. delayed conversion to leading edge separated flow.

In part the position of the leading edge vortex, too, is affected just like the size of the secondarily separated area (cf. Fig. 17) and its increase in size in relation to an increasing angle of attack. In less fortunate cases of a badly adjusted cambering, abrupt conversions of the circulation can occur.

By allowing the cambering to diminish toward the wing tip, the conversion to leading edge separated flow can be made to start at the tip and proceed inward. In reverse, an increased camber toward the tip can make the starting point proceed rearward in relation to widening angles of attack. It is also

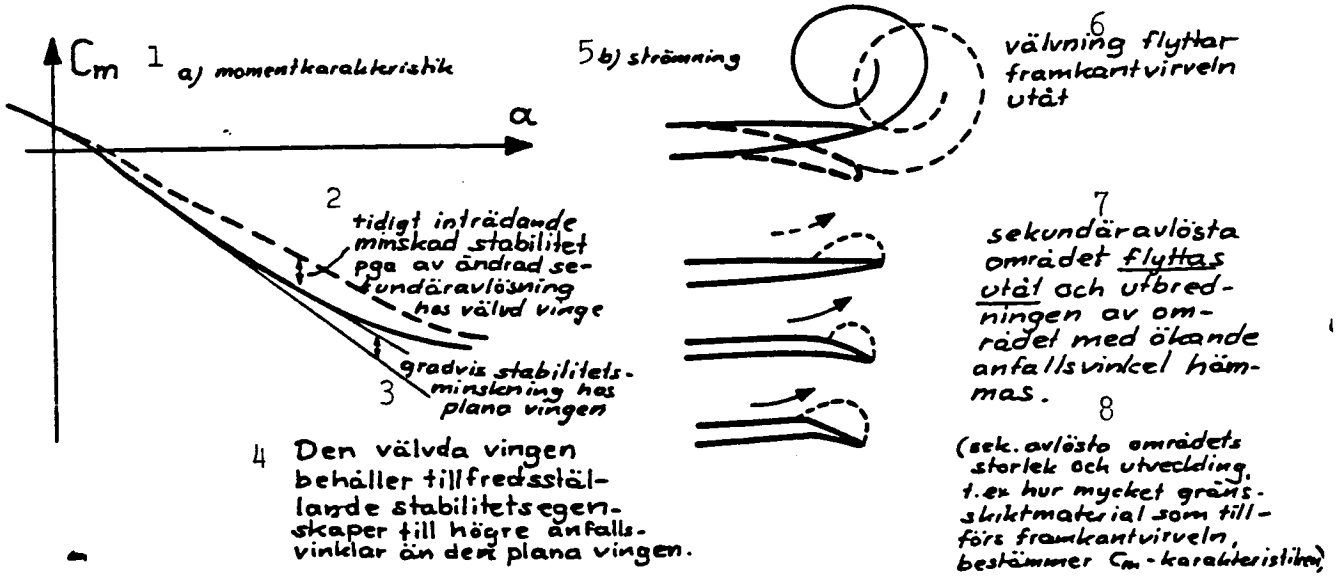

Fig. 44. Effect of leading edge cambering on the circulation around a delta wing.

Key: 1. a) Characteristics of the moment.
2. Reduced stability, occurring early, due to altered secondary separation of a cambered wing.
3. Gradual reduction of the stability of a flat wing.
4. The cambered wing retains more satisfactory characteristics of stability at wide angles of attack than a flat wing does.
5. b) Circulation.
6. The cambering moves the leading edge vortex outward.
7. The area. secondarily separated, is moved outward and the spreading of the area at increasing angles of attack is hampered.
8. (the size and development of the area, secondarily separated, determines the C_m characteristic, e.g., how much border layer material is added to the leading edge vortex.)

to affect the course of the separation at the wing tip within narrow limits.

Cambering, satisfactory from the point of view of drag, is not always satisfactory from the point of view of stability. It is particularly easy to lose stability at wide angles of attack when the area secondarily separated /41
increases in size. In the case of FPL 37, the external portions of the canard and the wing are provided with cambered leading edges. These curvatures compensate in general for each other in relation to longitudinal stability.

b) Partitioning of the Vortex Layer, - "the Sawtooth Notch"

In order to counteract too sudden changes in the size of the areas, secondarily separated, the layer of leading edge vortices and be partitioned and,

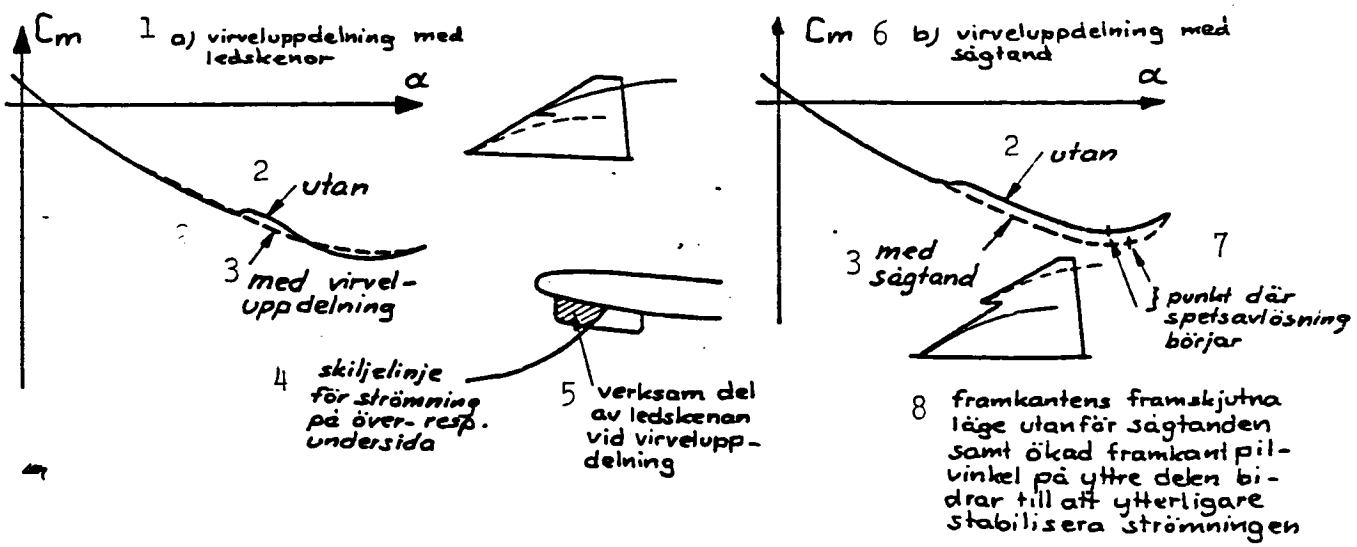

Fig. 45. Effects of vortex dividers and leading edge with a sawtooth notch.
Key: 1. a) Vortex partitioning by means of guide rails.
2. With ...
3. without vortex partitioning.
4. Line separating the air flow on the upper and the lower sides, respectively.
5. Portion of the guid rail effective. for partitioning of the vortices.
6. b) Vortex partitioning by means of sawtooth notch.
7. Point where the separation starts at the tip.
8. The advanced position of the leading edge beoynd the sawtooth and the increased sweep-back of the leading edge outer part contribute to further stabilize the air flow.

thus, a softer transition can be accomplished. In general the total lift can be somewhat altered when more air from the boundary layer is fed into the area, secondarily separated. Vortex dividers in the form of guide rails (fences) are found on the outer portion of the wing of FPL 35. On the prototype of FPL 37 there was also similar fences on the outer portion of its wing. However, a corresponding effect can be achieved by means of the armament girders below the wing or if a jack or "notch" is made in the leading edge of the wing. A notch is used for splitting up the vortices of, among others, the Mirage III. The effect of vortex dividers and sawtooth notches is evident from Fig. 45.

The final fine-adjustment of the graph illustrating the moment of FPL 37 was achieved by introducing a down-curved addition (a slat) to the leading edge of the main wing at its extreme end. In connection with the reconstruction

the antenna pod, previously placed on the lower side of the wing, was moved so that it became "integrated" with the sawtooth. This further improved the efficiency of the leading, sawtoothed edge at the same time as the level of vibration at large load factors and high speed was also improved. Finally, the new construction provided a possibility for introducing still another position of an armament girder (i.e., R 7).

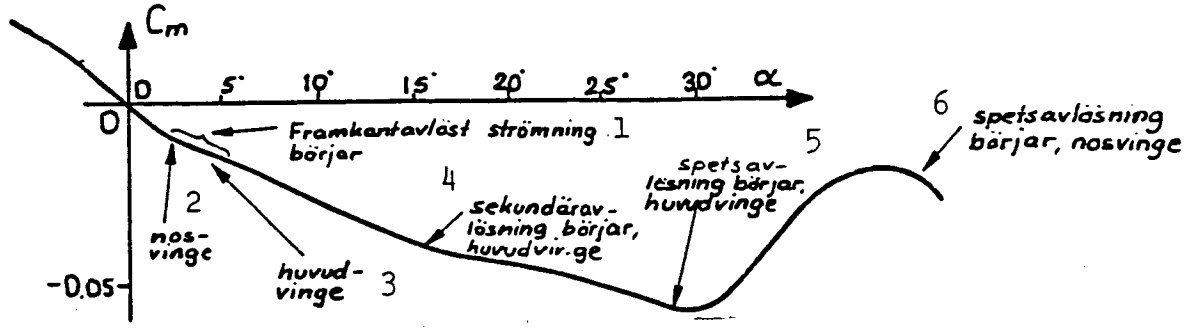

Fig. 46. Effect of the course of the air flow on the characteristics of the pitching moment of the EPL 37 configuration.
Key: 1. Flow separated by the leading edge begins.
2. Canard.
3. Wing.
4. Secondary separation starts; the main wing
5. Tip detachment starts;the main wing.
6. Tip detachment starts; the canard.

/42

The addition of the sawtooth led to that it became possible to increase the sweep-back of the leading edge at the extreme portion of the outer wing from 59.9° to 63°. Thanks to the cambering and the increased sweep-back of the leading edge, an especially stable air flow close to the wing tip was accomplished. The favorable effect, achieved by further advancing the starting point of the vortex at the outer portion of the wing to a position in front of the leading edge of the central wing contributes also to the stability. A "brisk" start of the vortices is obtained without interference from the leading edge of the central portion of the wing. The stabilizing of the circulation across the outer portion of the wing, accomplished thanks to the sawtooth, did also lead to that the disturbances due to external equipment could be reduced.

2.6 Characteristics of the Pitching Moment of FPL 37 in Comparison With that of Other Aircrafts

The conclusive graph illustrating the moment of FPL 37 in comparison with that of FPL 35 and FPL 32 is shown in Fig. 47. The characteristics of the pitching moment of FPL 37 is also compared with that of some foreign aircrafts.

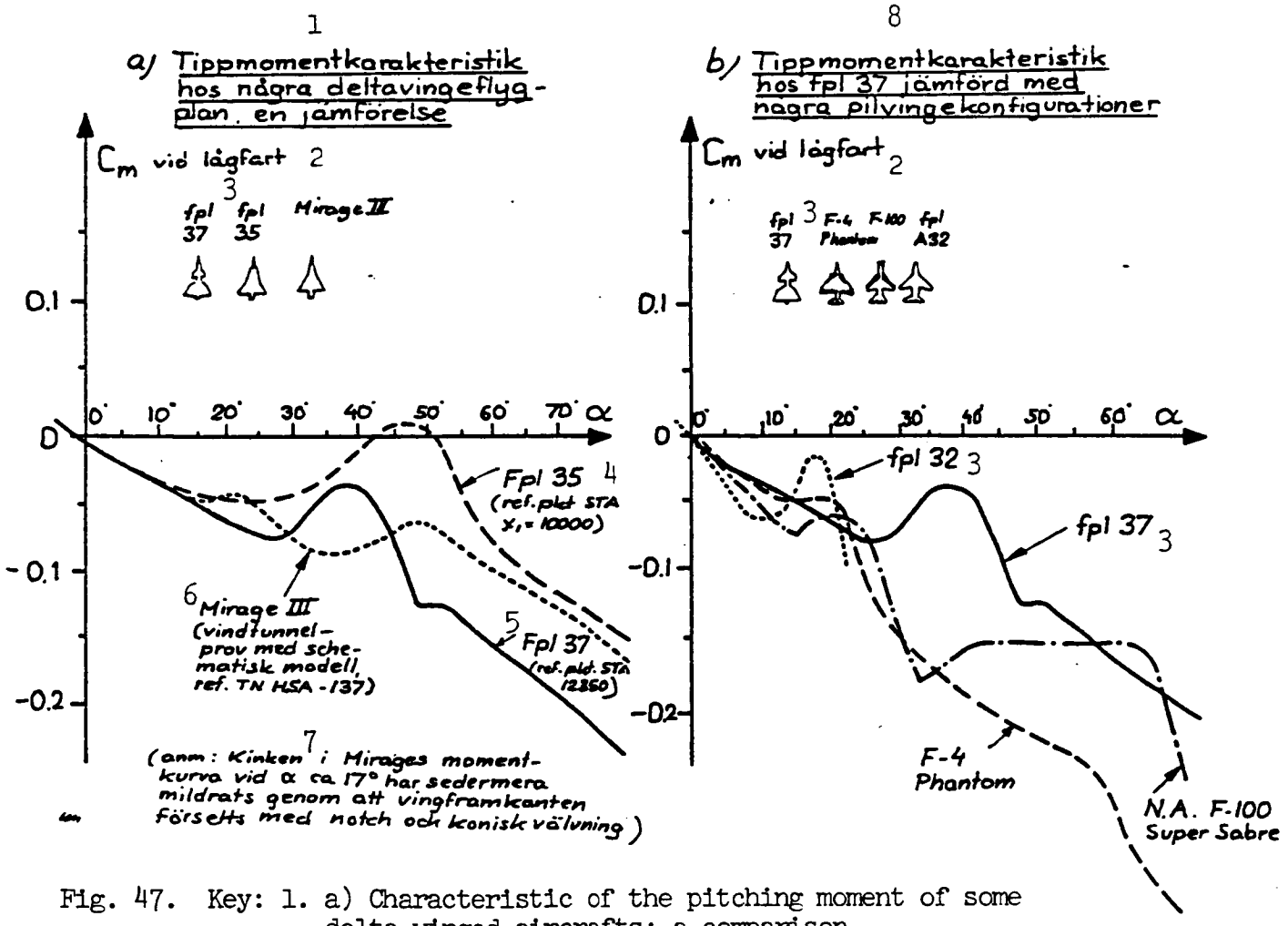

Fig. 47. Key: 1. a) Characteristic of the pitching moment of some delta-winged aircrafts; a comparison.
2. at low speed
3. fpl = aircraft
4. FPL 35 (reference point: STA x_1 = 10000)
5. FPL 37 (reference point: STA = 12850)
6. Mirage III (wind tunnel experiments with a schematic model, reference: TN HSA-137)
7. (note: the kink in the graph of the moment of the Mirage at α ca. 17° has since been alleviated by making a notch in and cambering the leading edge of the wing.)
8. b) Characteristic of the pitching moment of FPL 37 in comparison with some aircrafts with swept-back wings.

It is evident that the graphs of the pitching moments become disturbed /43
at much narrower angles of attack in the case of conventional, swept-back-winged aircrafts. The strong pitch-up of FPL 32 at relatively narrow angles of attack is due to the fact that the stabilizer becomes shaded at the same time as the separation above the wing starts. The efforts made in order to improve the characteristics of the moment of modern aircrafts are evident, e.g., in respect to the F-4, where again there is a V-position of the outer wing and the stabilizer and where the outer portion of the wing is equipped with a sawtooth notch.

2.7 External Aerodynamic Factors Affecting the Longitudinal Stability of the Basic Aircraft at Low Speed

The effect caused by the presence of the ground (ground interference) is an important external factor affecting the characteristics of the longitudinal stability of FPL 37. This condition can cause a considerable change in the otherwise satisfactory basic longitudinal stability of the aircraft and shall therefore be described in detail.

a) Ground Interference

Like in the case of most conventional aircrafts, the ground interference causes an increase in the longitudinal stability of FPL 37, the more pronounced, the closer to the ground the aircraft flies. The effect can be felt already at an altitude, corresponding to a couple of aircraft-lengths only. The increase in stability depends on the fact that the lifting force on the trailing portion of the wing increases. This increase becomes particularly noticeable in respect to shapes which make use of wide angles of attack when landing and have a large wing surface placed far back. The phenomenon is well known by those who have flown FPL 35. The same type of disturbances of the moment occurs there.

The effect of the ground interference on the normal force and the pitching moment is evident from Fig. 48. The wings flaps are also affected - but more about that later on.

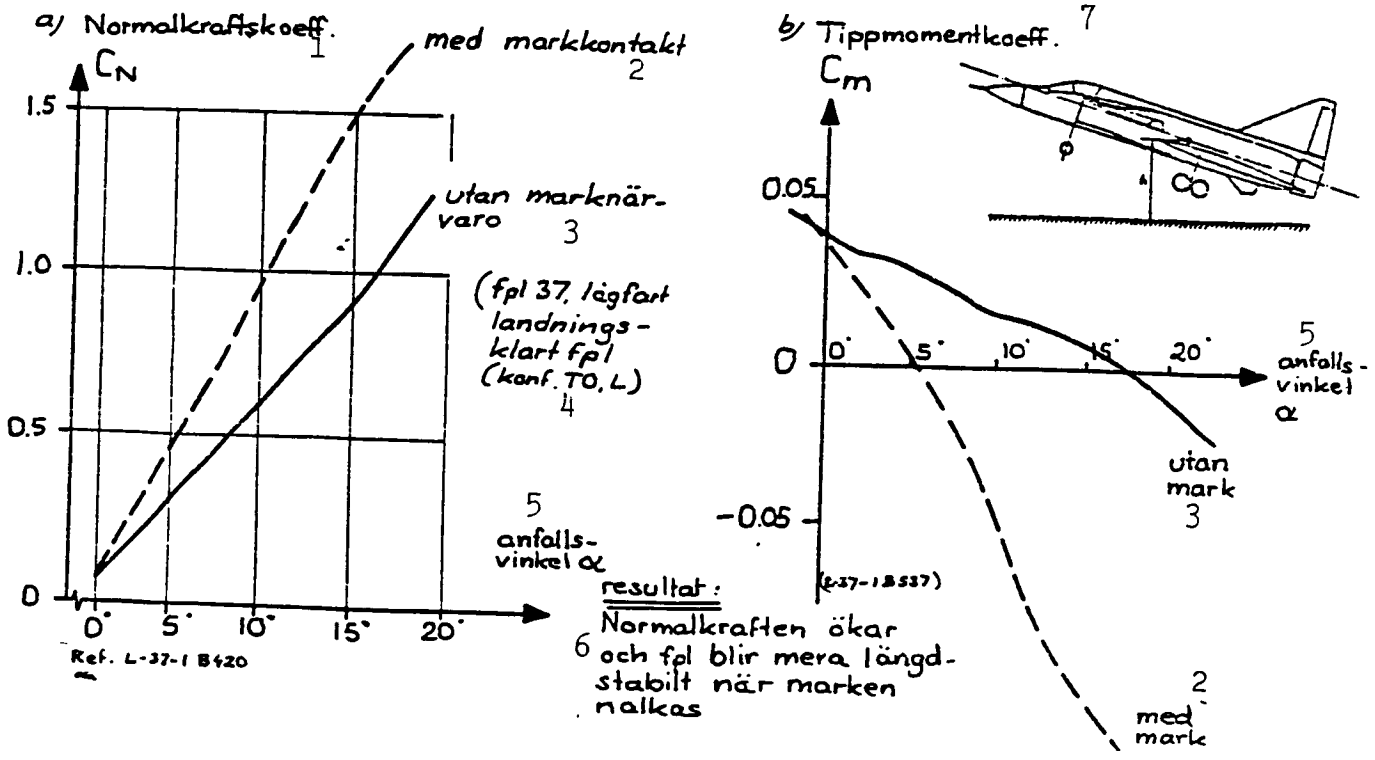

Fig. 48. Effect of ground interference; FPL 37.
Key: 1. Coefficient of normal force.
2. In contact with the ground.
3. Without presence of the ground.
4. (FPL 37, low speed, aircraft ready to land; conf. TO, L)
5. Angle of attack, α.
6. Result: The normal force increases and the aircraft becomes more longitudinally stable when approaching the ground.
7. b) Coefficient of the pitching moment.

Definition:

Below FPL 37 with the landing gear lowered and the flap of the canard deflected at -30° will be designated as "Configuration TO, L" (abbreviated as: TO, L) while an aircraft without any external load shall be called "Configuration Combat" (abbreviated as: CO).

/44

The large increase in lift in the presence of the ground can - when using the vortex-analogy like above - be explained as a reflex phenomenon; cf. Fig. 49.

The reflected vortex imparts a further reduction in the flow speed below the lower surface of the wing with an increase in pressure below the

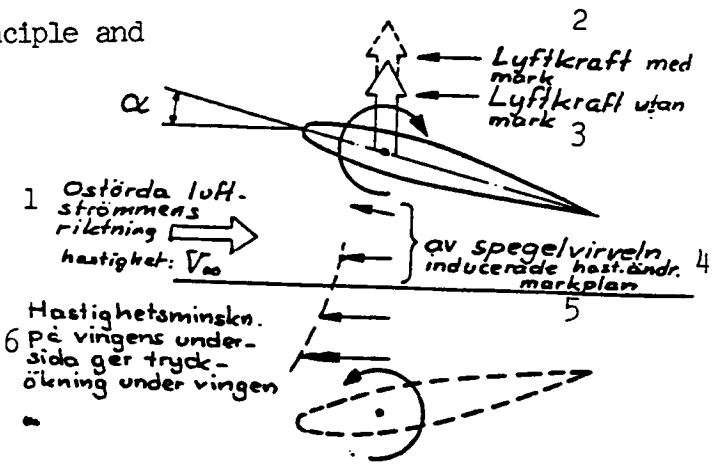

Fig. 49. Ground interference; principle and mirror effect.
Key: 1. Direction of undisturbed air flow, speed V
2. Lift associated with ground effect.
3. Lift without ground effect.
4. Change in speed caused by the reflected vortex.
5. Ground level
6. The reduction in speed below the lower surface of the wing produces increased pressure below the wing.

wing as a consequence. The circulation around the wing becomes more forceful because the difference in velocity of the flow across the upper and the lower surfaces is increased.

The powerful "nose-down" moment depends on the fact that the rear portion of the wing at such angles of attack is closer to the ground and, thus, is most affected by the interference of the ground effect.

b) Air Intake Factor

Considerably more air enters the air intake at low speed than the amount corresponding to the speed of free flow. The amount of air sucked in when compared to that at a speed of free flow is usually expressed as the air intake factor, i.e.:

$$C_A = \frac{\text{air flow through air intake}}{\text{density of the air x speed of free flow x intake area}}$$

With the aircraft at an angle of attack, a reorientation of the air flow occurs at the air intake. The change in direction of the intake impulse results in an upward-directed force on the cross section of the air intake: cf. Fig. 50.

The force resulting from the reorientation is proportional to the air-intake factor and the size of the angle of attack and provides, thus, a destabilizing contribution to the pitching moment, (a "nose-up" moment).

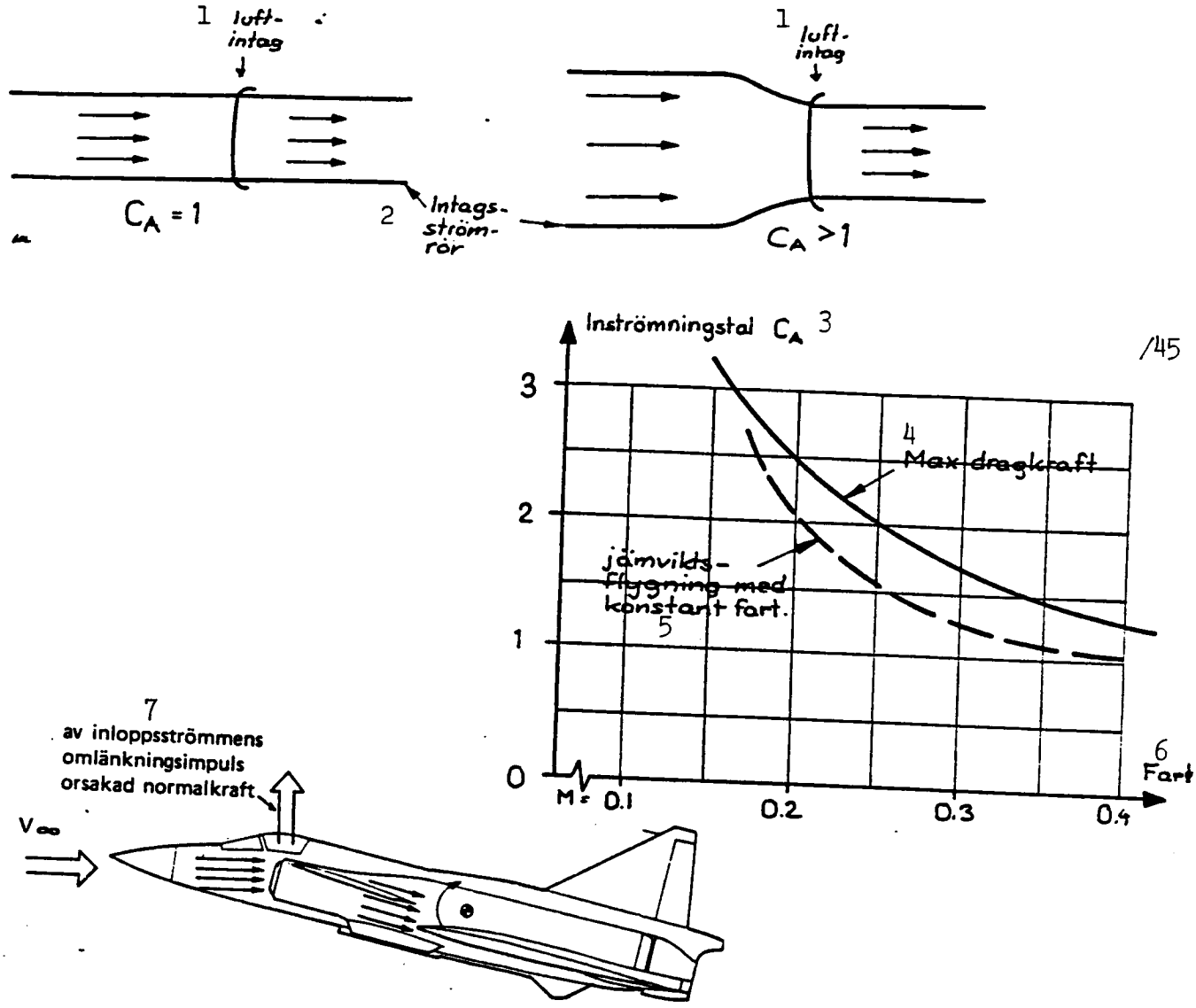

Fig. 50. The air intake factor and its effect on the logitudinal stability.
Key: 1. Air intake.
2. Air intake pipe.
3. Air intake factor, C_A.
4. Maximum traction.
5. Trimmed flight at constant speed.
6. Speed.
7. Normal force caused by the reorientating impluse of the air intake.

Other, lesser disturbances of the moment occur in addition to the effect of the reorienting impulse due to the altered flow conditions across the canard. Thus, e.g., the local angle of attack can change in front of the canard when the shape of the air intake is altered.

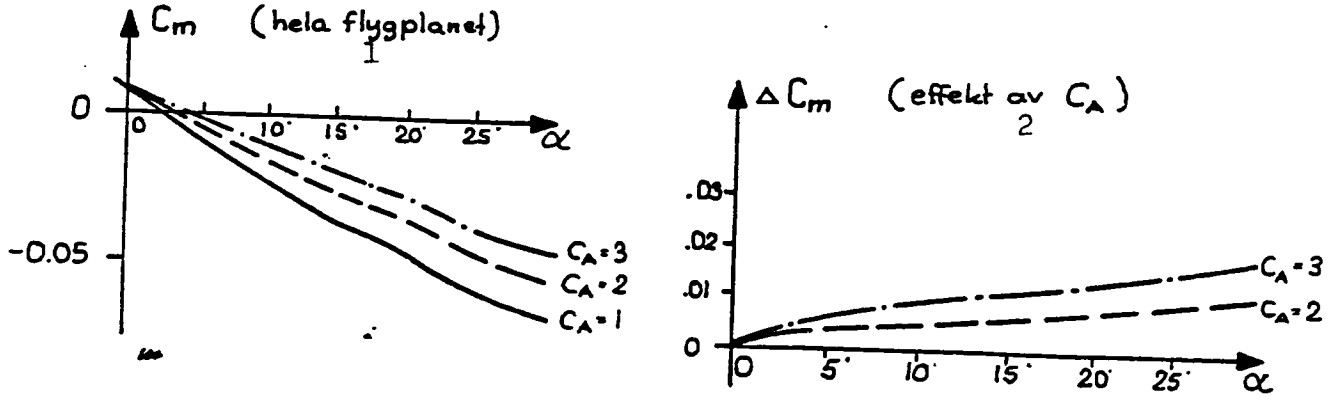

Fig. 51. Key: 1. (the entire aircraft); 2. (effect of C_A).

This effect exists for all aircrafts equipped with air intakes in front of /46
the point of gravity (thus, also for FPL 35) but it is especially noticeable in the case of FPL 37, in part because this plane can fly at such a slow speed (which means a large air intake factor) in combination with wide angles of attack and, in part due to the large amount of air used by the FPL engine (a high-pressure turbofan engine).

This effect should up to a point be taken into consideration in connection with the aerodynamic design of the plane, but since this aircraft shall be able to fly at low speed as well as at high speed, a compromise must usually be made.

2.8 Problems of Longitudinal Stability When Deflecting the Flap of the Canard

Deflection of the flap of the canard contributes - briefly stated - only a zero moment (see below), independent of the angle of attack. When the load on the canard is increased, the part of the pitching moment, which depends on the angle of attack, and, consequently, the longitudinal stability as well become affected. The air flow around the canard is in the case of FPL 37 so stable thanks to the interference of the wing that no major change in stability occurs before the plane reaches angles of attack, wider than 27°. Then the pitch-up when the flap is deflected will be even smoother than in the case of an unloaded airplane without the flaps deflected. Before selecting

the final configuration of the flaps of FPL 37, problems were encountered in the form of local detachment at the flap which caused disturbances of the kind called " a dip" in the graph of the moment: cf. Fig. 52.

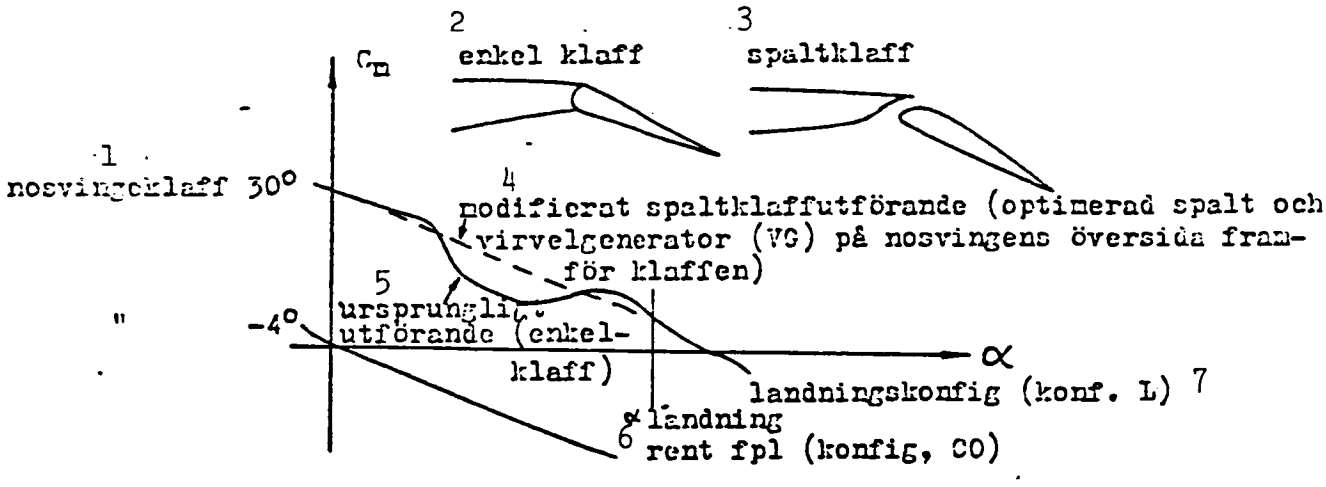

Fig. 52. Effects of a slotted flap on the longitudinal stability of FPL 37.
Key: 1. Flap of canard at 30°.
2. Plain flap.
3. Slotted flap.
4. Modified design of the slotted flap (slot optimized and a vortex generator, VG, on the upper surface of the canard in front of the flap).
5. Original design (plain flap).
6. Landing configuration (Conf. L).
7. Landing, unloaded aircraft (Conf. CO).

The "dip" caused local instability at certain angles of attack. In addition there was a risk for vibrations. For the final shape of FPL 37 the problem was solved by a careful design of the slot on the canard flap and the introduction of a vortex generator (a boundary layer control) on the upper surface in front /47 of the center-bearing of the flap. The vortex generator is shaped like an obliquely positioned triangular fin and functions like a delta wing at wide angles of attack. The turbulent flow takes care of the boundary layer behind the vortex generator. The disorderly flow close to the surface of the wing changes into one more orderly and stable.

This measure illustrates the solution of a typical problem when designing the slot of the flap (it applies to all aircrafts with slotted flaps) in order to avoid interference from the attachments (hinges) of the flaps and other maneuvering organs.

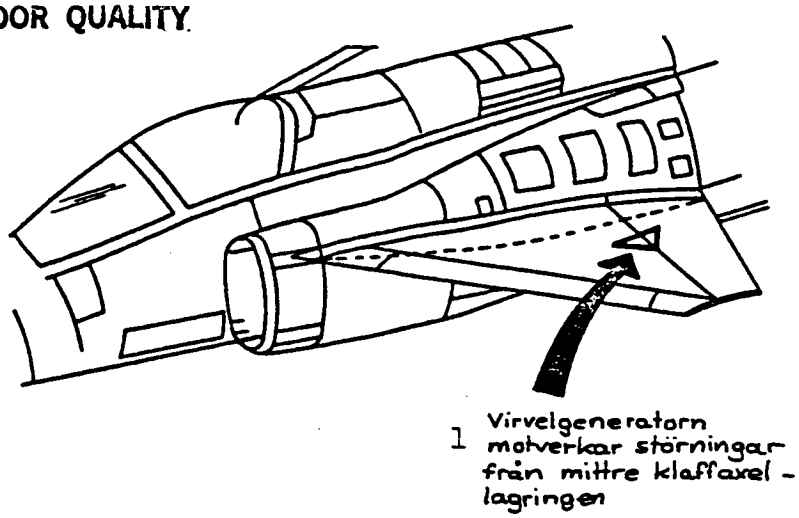

Fig. 53. Placement of a vortex generator on the canard.
Key: 1. The vortex generator counteracts interference from the central-axial bearing of the flap.

2.9 Problems of Longitudinal Stability When Deflecting the Elevator

Just like when deflecting the flap of the canard, a deflection of the elevator will change the zero moment only within the area of normal flight. Like in the case of the flap of the canard, the deflection of a trailing edge-elevator of a delta wing will affect the circulation around the wing tip in special cases due to the fact that the change in load becomes locally of major importance at that point.

At large, positive deflection of the elevator, the pitch-up can become magnified such as illustrated in Fig. 54. In practice this phenomenon is of minor importance since an unfavorable combination of elevator angle an angle of attach cannot be achieved during trimmed flight.

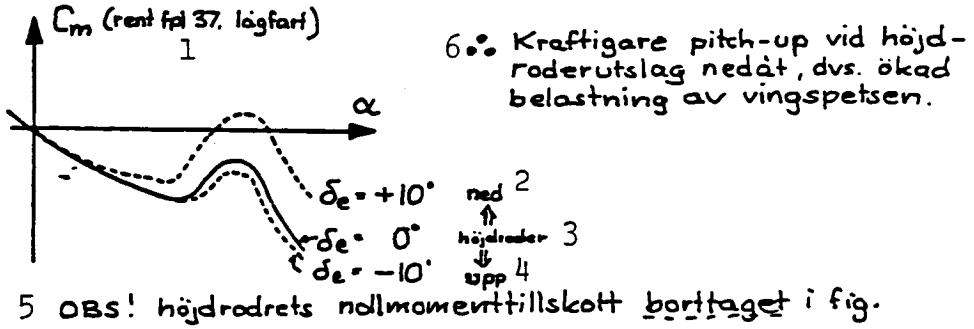

Fig. 54. Effect of the elevator on the characteristics of the pitching moment of FPL 37.
(Key: see p. 65)

Key to Fig. 54:

1. ("clean" aircraft, FPL 37 at low speed)
2. Downward
3. Elevator
4. Upward
5. Note! The contribution of the zero moment of the elevator is not included in the figure.
6. Thus: A more forceful pitch-up occurs at the deflection of the elevator downward; i.e., when the load on the wing tip increases.

A cause contributing to this phenomenon is the sawtooth notch in the leading edge of the outer wing of FPL 37. It contributes to the fact that the graph illustrating the moment at large positive deflections of the elevator will have a smoother course than that in the case of a delta wing with a smooth edge.

2.10 Problems of Longitudinal Stability in Connection With an External Load /48

The FPL 37 is able to carry an external load suspended at 7 points of attachment (3 below the fuselage, 4 below the wings). A more complicated picture of the air flow occurs when the aircraft carries an external load. In part forces and moments are added to the aircraft by the external load, in part it affects the circulation around the aircraft and, thus, the characteristics of the lift and the moments. The large airfoils of the plane in relation to the external equipment carried cause the contribution due to interference to become a major source of disturbances on FPL 37 while, on the other hand, the effects of the aerodynamic forces, directly affecting the external load, are small.

The greatest interference with the longitudinal stability originates from the external load when placed below the root of the wing (at the V7 girder). Due to the fact that, in part, the equipment is placed on the wing in front of and below its leading edge, the fronts of the arms are subjected to a lateral as well as an upward flow, induced by the vortex systems of the canard as well as the main wing. Local detachment and vortices appear therefore relatively quickly in relation to the increased angles of attack of these parts. The disturbances lead to that the stable separation above the main wing, caused by the leading edge, is interfered with

in such a manner that, in part, the development of the leading edge vortex becomes locally obstructed and, in part, low energy air (a boundary layer) is added to the leading edge vortex of the main wing.

The result is that the wing gradually loses its lift in relation to an increase in angle of attack, which means that the stability is lessened. The reduction in stability is further accentuated by the fact that the external load below the wing moves the point of gravity farther rearward.

The 04-missiles, placed below the wing constitute the worst alternative of external load from the point of view of stability. Their aerodynamic effect is evident from Fig. 55.

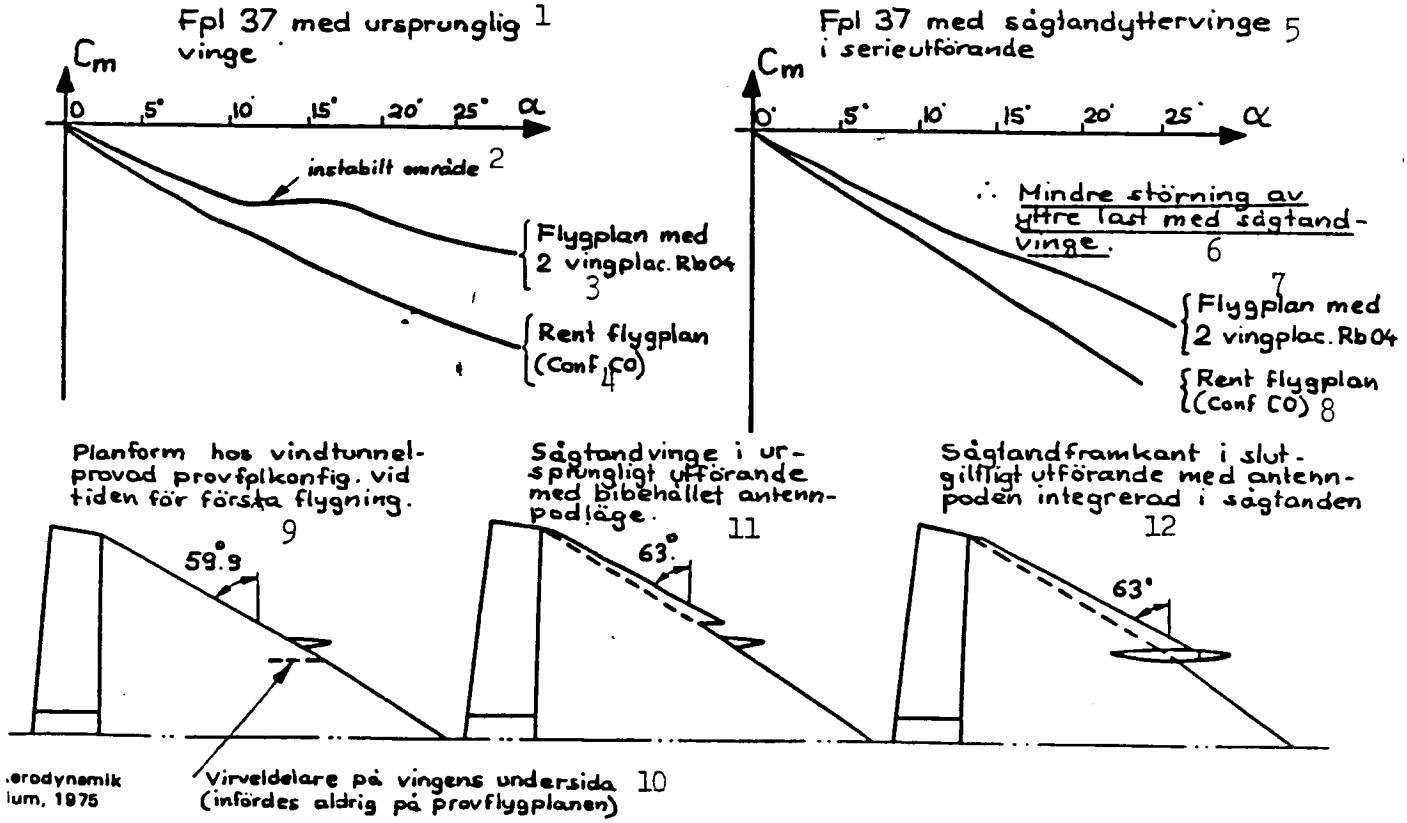

Fig. 55. Effects on the longitudinal stability of 04-missiles, placed below the wing, as well as of an outer wing with a sawtooth edge.
Key: 1. FPL 37 with the initial type of wing.
2. Area of instability.
3. Aircraft with 2 wing-mounted 04-missiles.
4. Aircraft without load (Conf. CO).
5. FPL 37 with serialized wing with a sawtoothed edge.
6. Thus, less disturbance due to the external load when the wing is equipped with a sawtooth. [Key cont. p. 67.]

Key to Fig. 55, cont:

7. Aircraft with 2 wing-mounted 04-missiles.
8. Aircraft without a load (Conf. CO).
9. Design of a wind-tunnel tested configuration of a test plane at the time of the first flight.
10. Vortex divider on the lower side of the wing (was never mounted on the test plane).
11. Initial design of a wing with a sawtoothed edge with the antenna pod in the initial position.
12. Final design of the sawtoothed leading edge where the antenna pod is integrated with the sawtooth.

During the design stage the disturbances caused by a wing-mounted external load constituted a problem which could be solved by introducing a sawtoothed edge on the outer portion of the wing; cf. Fig. 55. Thanks to the leading sawtoothed edge the local stability was considerably improved in respect to both landing angles of attack (12 - 16°) and external load. From the point of view of air-worthiness, even the worst alternative, i.e., two wing-mounted 04-missiles on girder V 7, was no longer a problem. /49

As far as aerodynamics is concerned, wing-mounted 04-missiles exert the greatest effect. Next in order come

wing-mounted bomb carriages;
" " [arak] cases;
" " 05-missiles; and
" " countermeasure units.

The interference of armament, mounted at the outer position (R 7) below the wing, is minor from the point of view of aerodynamics, in part due to the flow-stabilizing effect of the leading edge sawtooth. The arms which come into question for that girder position have a low weight and require less space as far as aerodynamics is concerned.

An external load, mounted on the fuselage, does not affect the longitudinal stability but contributes rather to a favorable position of the point of gravity in relation to the stability.

2.11 Zero Moment, Effect of the Canard Flap

As we have learnt above, the pitching moment can be distinguished into one part, independent of the angle of attack (i.e., the zero moment), and another part, dependent thereon; see Fig. 56.

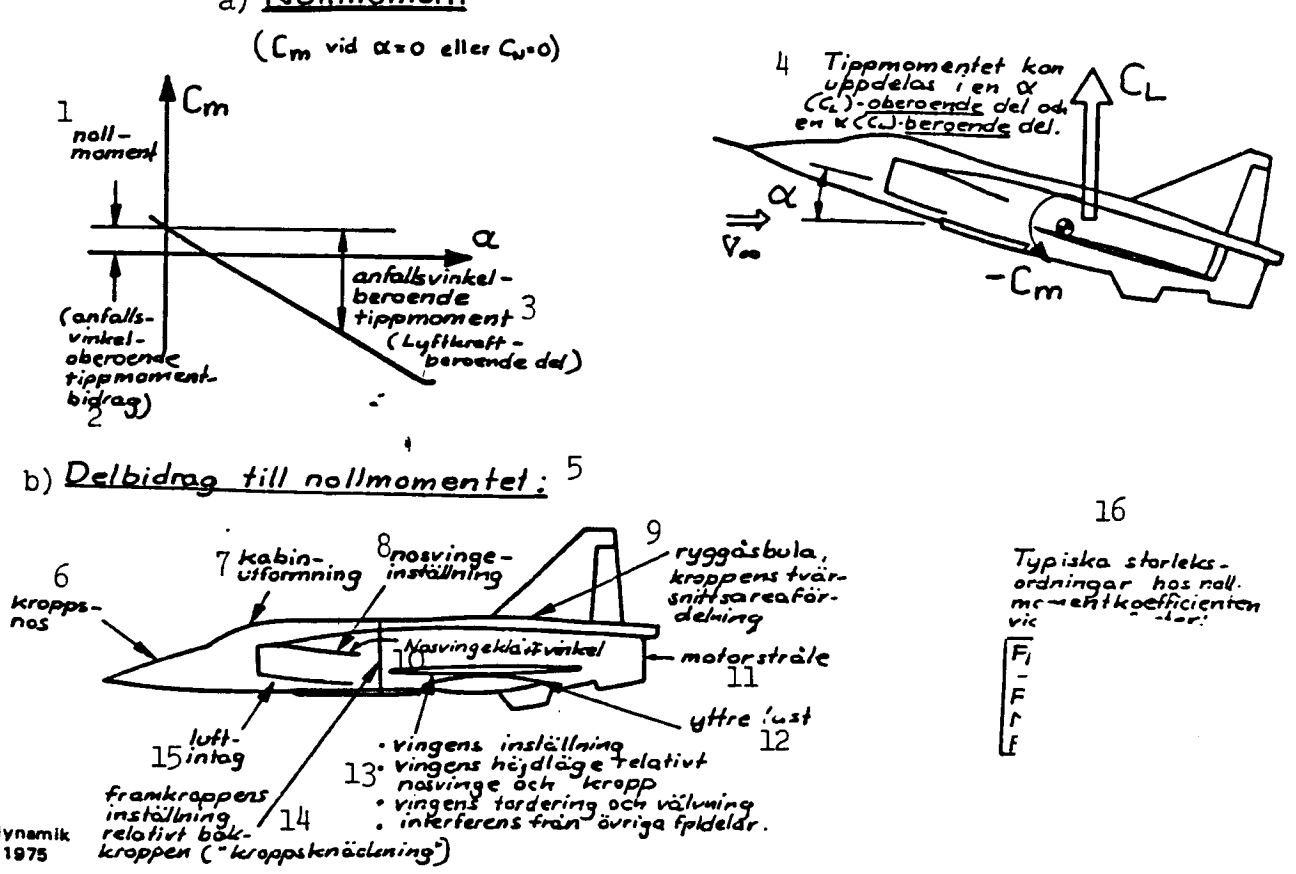

Fig. 56. a) Zero moment (C_m at $\alpha = 0$ or $C_N = 0$).

1. Zero moment.
2. Contribution of pitching moment, independent of the angle of attack.
3. Contribution of the pitching moment, dependent on the angle of attack (part dependent on the lift).
4. The pitching moment can be distinguished into one part, independent of α (C_L) and on dependent on α (C_L).
5. b) Partial contributions to the zero moment:
6. Bow of the fuselage.
7. Design of the cabin.
8. Position of the canard,
9. Bulge on top of the fuselage; the distribution of the cross section of the fuselage.
10. Jet stream.
11. External load.

[Key cont. p. 69]

Key to Fig. 56 cont.

13. o the position of the wing;
    o the relative vertical position of the wing;
    o the canard and the fuselage;
    o the torsion and cambering of the wing; and
    o interference from other parts of the aircraft.
14. The position of the front of the airplan in relation to that of the tail part ("bend in the fuselage")
15. Air intake.
16. Typical magnitudes of the coefficient of the zero moment at low speed:

FPL 37, not loaded	- 0.006
" ", landing configuration	+ 0.036
FPL 35 F	0.000
Mirage III	+ 0.010
F-4, the Phantom	- 0.023

The zero moment depends, among others, on such factors as the camber and /50
the position of the wing, the down-slope of the front of the fuselage, etc. At low speed and an aircraft without load and flaps and elevators not deflected (an untrimmed aircraft), the zero moment is usually small in comparison with the contribution dependent on the angle of attack. It is, thus, of comparatively little interest. On the other hand, at higher speed the zero moment gains in importance if the angel of attack is narrow. When projecting a new aircraft it is, therefore, important to design the fuselage and the wings, etc., so that the zero moment can be favorably utilized, among others, from the point of view of drag.

In the case of aircrafts with mobile flaps, such as that of the canard on FPL 37, a considerable zero moment has - intentionally - been developed also at low speed. The relative magnitudes of the zero moment and the moment dependent on the angle of attack can be seen from Fig. 52. Due to the important pitch-up moment provided by the flap of the canard, additional lift due to the wing flaps, amounting to 7 - 10% of the total lift, can be obtained (like illustrated in Fig. 26) when flying in a balanced condition (during trimmed flight).

In order to utilize the flap of the canard in the most favorable manner, this one has been designed as a slotted flap, due to which wider deflecting

angles can be applied. The difference between an ordinary plain flap and a slotted one is evident from Fig. 57.

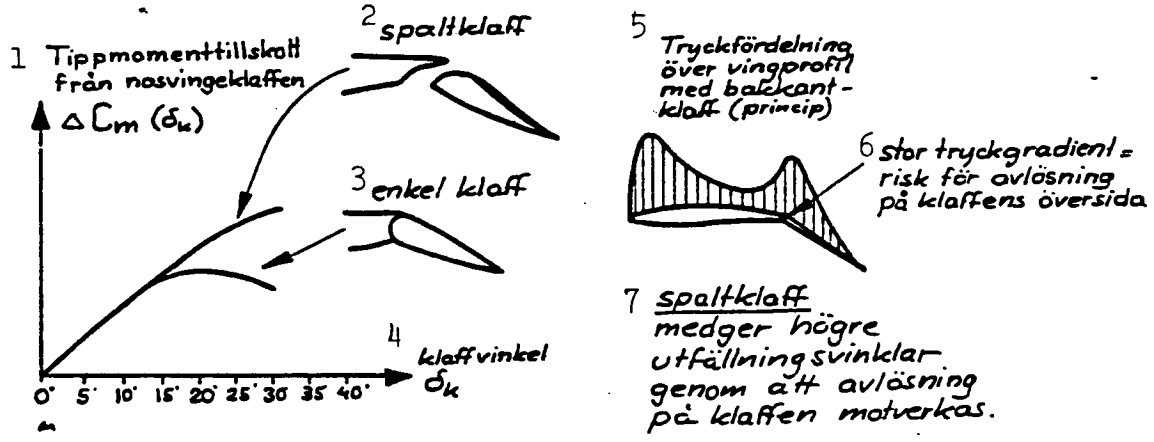

Fig. 57. Comparison between a plain flap of the canard and a slotted flap.
Key: 1. Contribution to the pitching moment by the flap of the canard.
2. Slotted flap.
3. Plain flap.
4. Angle of flap, δ_k .
5. Pressure distribution above the wing profile including it trailing edge flap (principle).
6. Steep pressure gradient = risk for detachment at the upper side of the flap.
7. A slotted flap allows for wider deflecting angles by counteracting separation at the flap.

The air flows from below through the slot of the flap and adds energy to the boundary layer on top, thus, delaying the detachment, which otherwise will occur when an adequately steep pressure gradient is reached. Like evident from the reasoning concerning longitudinal stability, the shape of the slot is of major importance. The fact that a flow on the top side, separated by the leading edge, occurs, makes the design of the flap particularly problematic. During the early stages of the 37-project, there were plans for further increasing the efficiency of the flap by injection of air onto the upper side of the flap; see Fig. 58.

In addition to preventing separation, a reinforcement of the air flow /51
above the upper surface could be achieved by a highly energetic injection of air so that the difference in the speed of the flow and the lift of the canard was increased (due to so-called supercirculation). However, the air

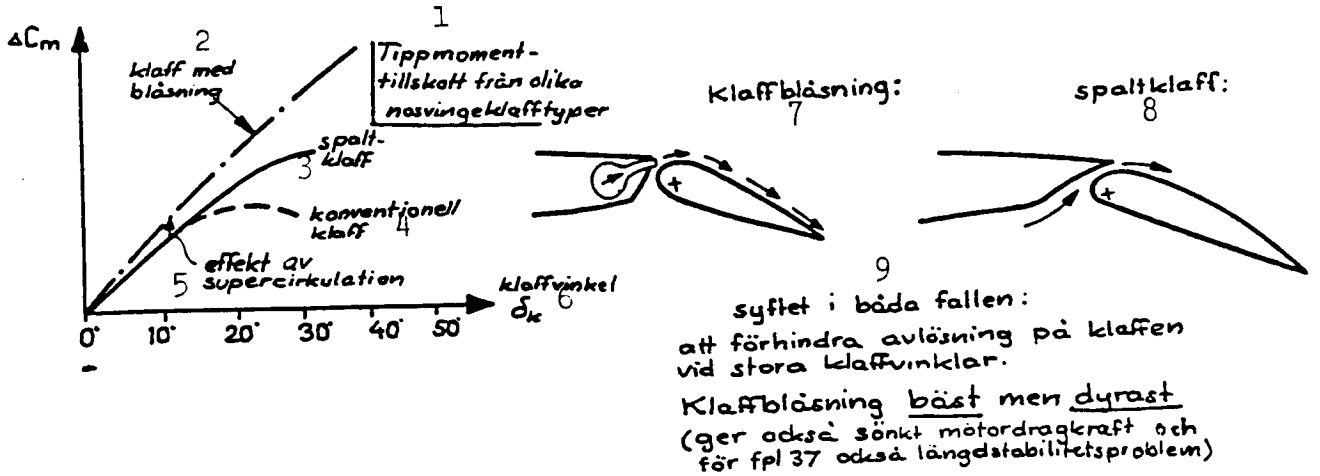

Fig. 58. Effect of blowing an air jet across the flap (air injection over the flap of the canard, initially planned for FPL 37)
Key: 1. Addition to the pitching moment from various types of flaps on the canard.
2. Air jet flap.
3. Slotted flap.
4. Conventional flap.
5. Effect of supercirculation.
6. Flap angle, δ_k.
7. Air jet over flap.
8. Slotted flap.
9. The objective in both cases:
to prevent separation above the flap at wide flap angles.
Air jets above the flap is most satisfactory but also most expensive (it contributes also to reduced traction of the engine and, in the case of FPL, problems in respect to the longitudinal stability).

jet system was both heavy and expensive and offered a lesser margin when a landing maneuver had to be aborted. It was therefore abandoned in favor of a slotted flap.

When landing, the flap of the canard is lowered by 30°. During normal flight, it shall be kept at -4° above the neutral position in order to provide a favorable zero moment at high speed. To compensate for the additional contribution to the zero moment at high speed caused by a heavy, wing-mounted load it is, furthermore, possible to set the flap of the canard at -7°.

2.12 Effects of the Elevator

Trimmed flight means flying in a balanced condition, i.e., so that the .

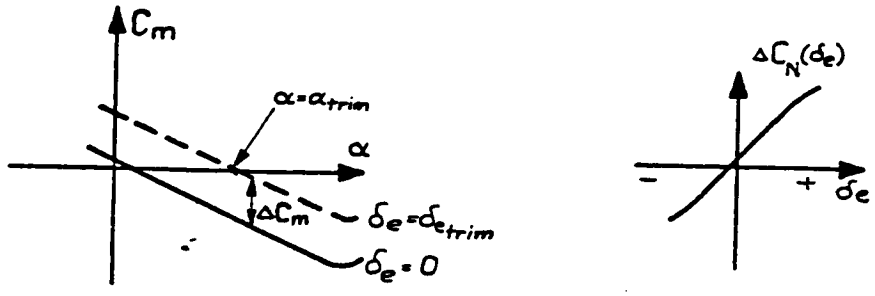

Fig. 59.

sum of all the contributions to the pitching moment will be equal to zero.

In order to achieve this in respect to a conventional aircraft, a tail-mounted steering mechanism with an elevator or, possibly, a mobile stabilizer ("all-flying tail" or stabilizer) is employed.

Thus, a long lever arm is introduced and, consequently, a relatively minor deflection of the rudder is necessary in order to obtain a balancing moment. During normal flight with a stable aircraft a down-ward-directed force is required for balancing the moment of the untrimmed plane. Trimmed lift is lower than the lift acting on an untrimmed plane; a loss of lift due to trimming (loss of normal force) will occur. In the case of delta-winged aircrafts, the necessary trimming force is achieved by means of a trailing edge flap, which in general is designed as a combination of an elevator and an aileron (an "elevon"). The lever arm will be shorter and the loss due to trimming larger than in the case of conventional aircrafts. /52

The neutral point of FPL 35 was moved forward by extending the root of the wing in a forward direction. Thus, a longer lever arm and a lesser loss due to trimming was produced in comparison with what is the case of an ordinary delta-winged aircraft of a type like the Mirage.

As far as FPL 37 is concerned, a longer elevator lever arm was achieved due to the fact that the canard helps moving the neutral point forward. The basic loss due to trimming without deflecting the flap of the canard is, thus, also here less than that of a "pure" delta-winged aircraft. In addition, a zero moment was created by lowering the flap of the canard. When landing, this eliminates completely the loss due to trimming and at somewhat narrower

angle of attack it even provides a trimmed lift which is greater than the one not trimmed.

The deflection of the elevator necessary for trimming at different angles of attack in the case of aircrafts with or without a deflected flap on the canard is illustrated in Fig. 60.

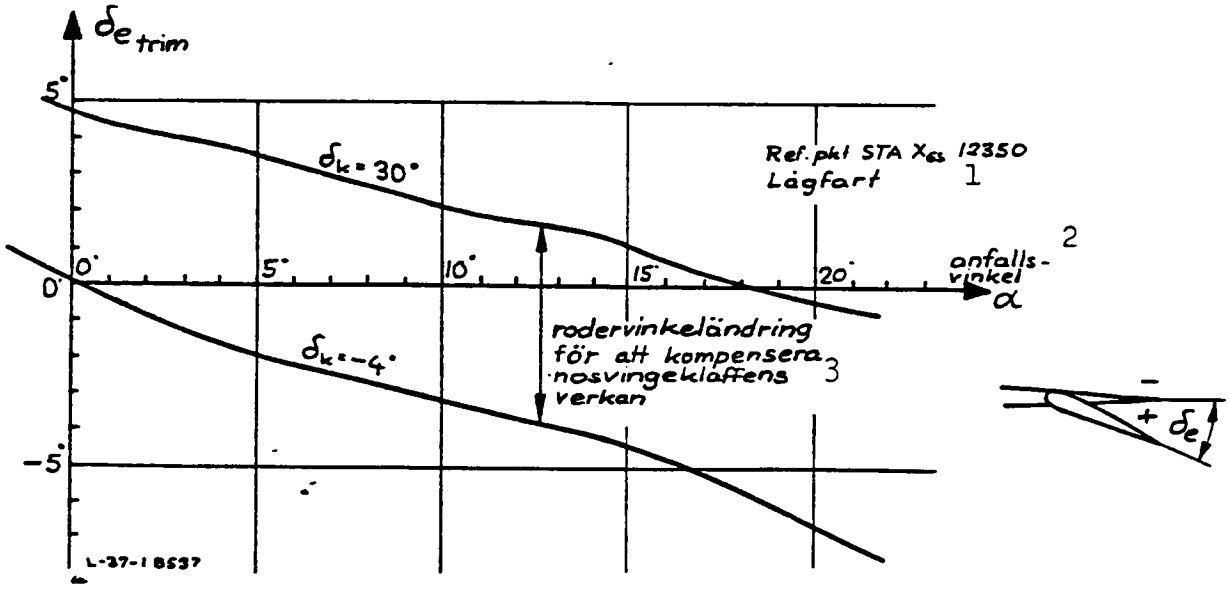

Fig. 60. (Cf. Fig. 52). Angle of elevator for trimming an aircraft in relation to the angle of attack.
Key: 1. Reference point: STA X_{65} 12350; low speed.
2. Angle of attack, α.
3. Alteration of elevator angle in order to sompensate for the effect due to the flap on the canard.

A ca. 5° change in the elevator angle is necessary for trimming against the normal (30°) deflection of the flap of the canard.

The efficiency of the elevator is illustrated in Fig. 61, which shows changes in lift and moment as a consequence of elevator deflection. /53

Just like demonstrated in respect to the normal force, it is possible to represent the dependency on the angle of attack and the elevator angle in the form of a "blanket" within the same diagram by means of which the difference between the change in moment per degree of angle of attack and the change in moment per degree of elevator angle can be directly read (Fig. 62).

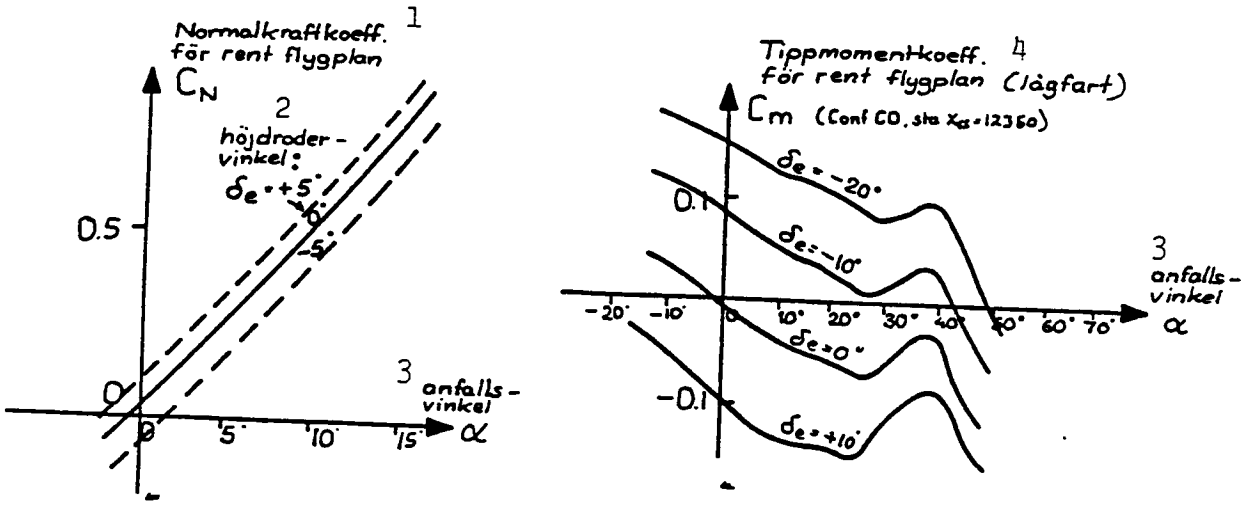

Fig. 61. Key: 1. Coefficient of normal force of an aircraft without external load.
2. Angle of elevator, δ_e = +5°(or -5°)
3. Angle of attack, α.
4. Coefficient of pitching moment of an aircraft without an external load (at low speed).

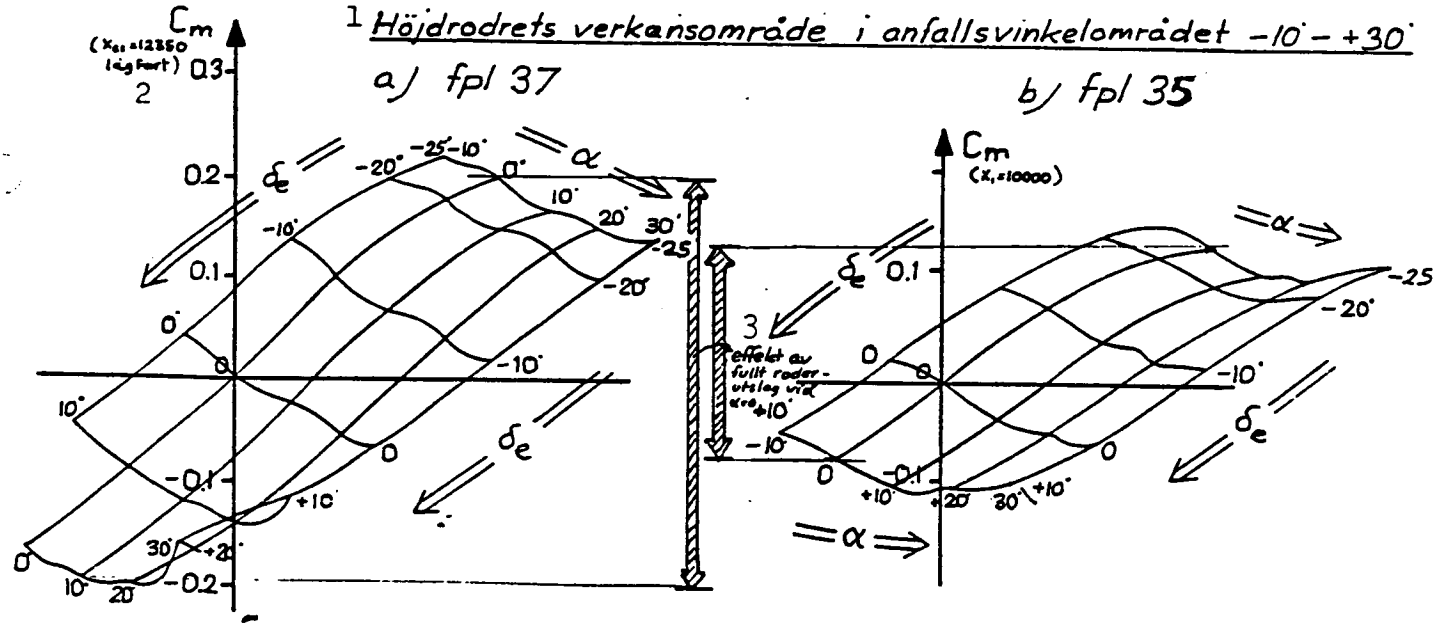

Fig. 62. Variation of pitching moment in relation to the angle of attack and the angle of the elevator.
Key: 1. Effective range of the elevator in relation to the angles of attack ranging from -10° to +30°.
2. x_{65} = 12350, low speed.
3. Effect of complete deflection of the elevator at α_{ro} + 10°.

It is evident that the elevator retains a certain efficiency also at wide angles of attack as well as that the elevator of FPL 37 is relatively more effective than that of FPL 35.

The satisfactory elevator effect of FPL 37 is a consequence of the demand for its capability to fly at low speed. In order to avoid too great /54
sensitivity of the elevator when flying at high speed, the steering mechanism has been designed with a variable gear, which automatically regulates the interaction between the shift lever and the elevator as a function of altitude and mach number.

2.13 Effect of the Elevator in Association with the Ground Interference

Just like the lifting force on the wing is affected by the presence of the ground due to the angle of attack, the lift is also affected by the force exerted by the elevator. The change in elevator effect due to ground interference cannot be ignored in the case of FPL 37. It magnitude is shown in Fig. 63. At an increasing angle of attack, attenuation occurs sooner because of the large increase in lifting power. This means that $C_{L_{max}}$ is attained at a narrower angle of attack and results in that a large portion of the improvement in the elevator effect is lost at ca. 15° angle of attack like illustrated in Fig. 63.

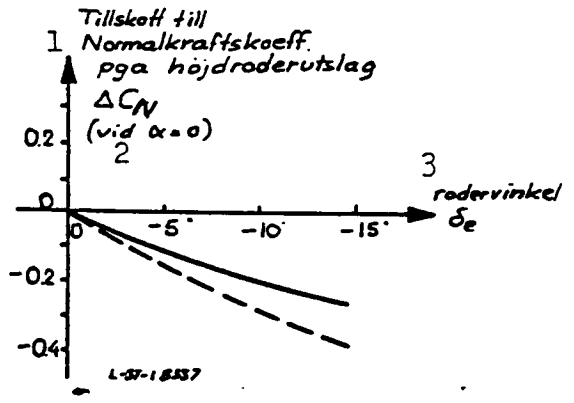

Fig. 63. Key: 1. Addition to the coefficient of normal force due to deflection of the elevator. 2. (at $\alpha = 0$); 3. Elevator angle.

The total effect of the ground interference on the normal force, the pitching moment and the efficiency of the elevator leads to that the angle of attack and the angle of the elevator, necessary for trimming, will change. How large this change will be can be seen from Fig. 64, where it is also possible to make a comparison with FPL 35.

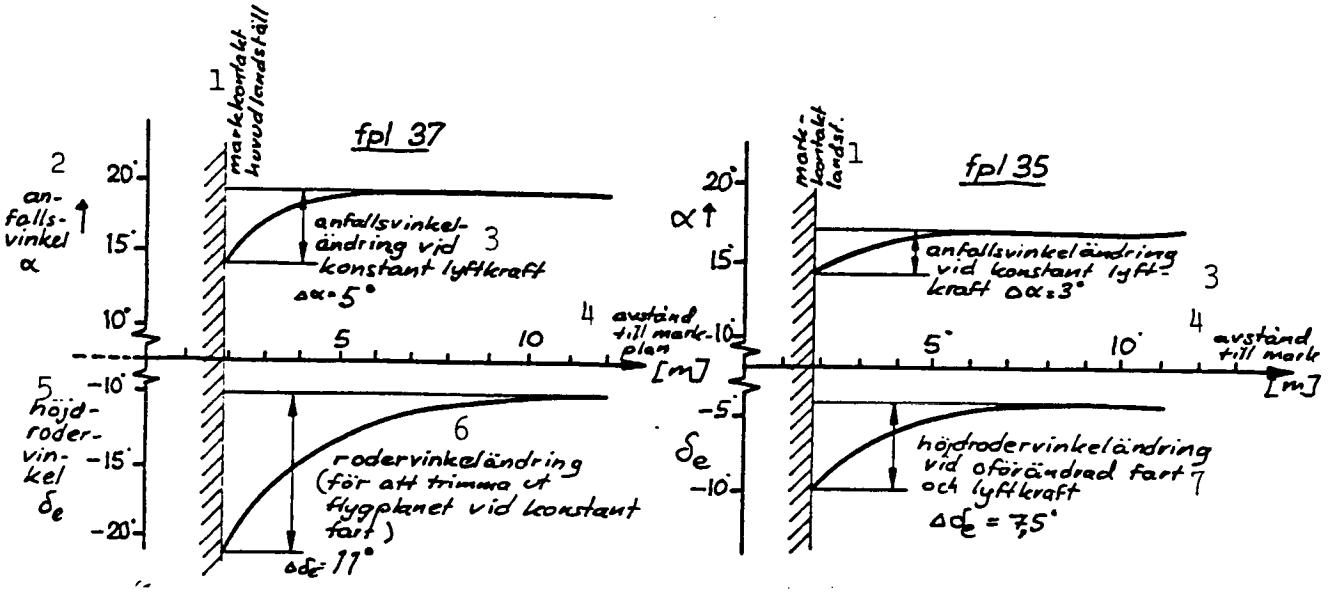

Fig. 64. Effect of the distance to the ground level on the angle of attack and the elevator angle for the purpose of trimming.
Key: 1. Main landing gear in contact with the ground.
2. Angle of attack, α.
3. Angle of attack at constant lift, $\Delta\alpha = 5°$, (or $\Delta\alpha = 3°$).
4. Distance to the ground level.
5. Angle of elevator, δ_e.
6. Change in angle of the elevator (for trimming the aircraft at constant speed).
7. Change in the angle of the elevator at constant speed and lift.

2.14. Pitch Damping, Dynamic Longitudinal Stability /55

A damped or dynamically stable aircraft tries constantly to resume its equilibrium even though the plane is subjected to a sudden disturbance (e.g., an excessive deflection of the rudder or "kytt" [flutter?]) or is made to rotate around some of its axes, e.g., the pitching axis.

From an aerodynamic point of view a measure of pitch damping constitutes the sume of two additional pitching moments, superimposed on the contribution to the pitching moment due to the angle of attack. These additional moments can be defined as follows (Fig. 65):

1. C_{m_q} = egentlig tippdämpning, förklaring se figuren.

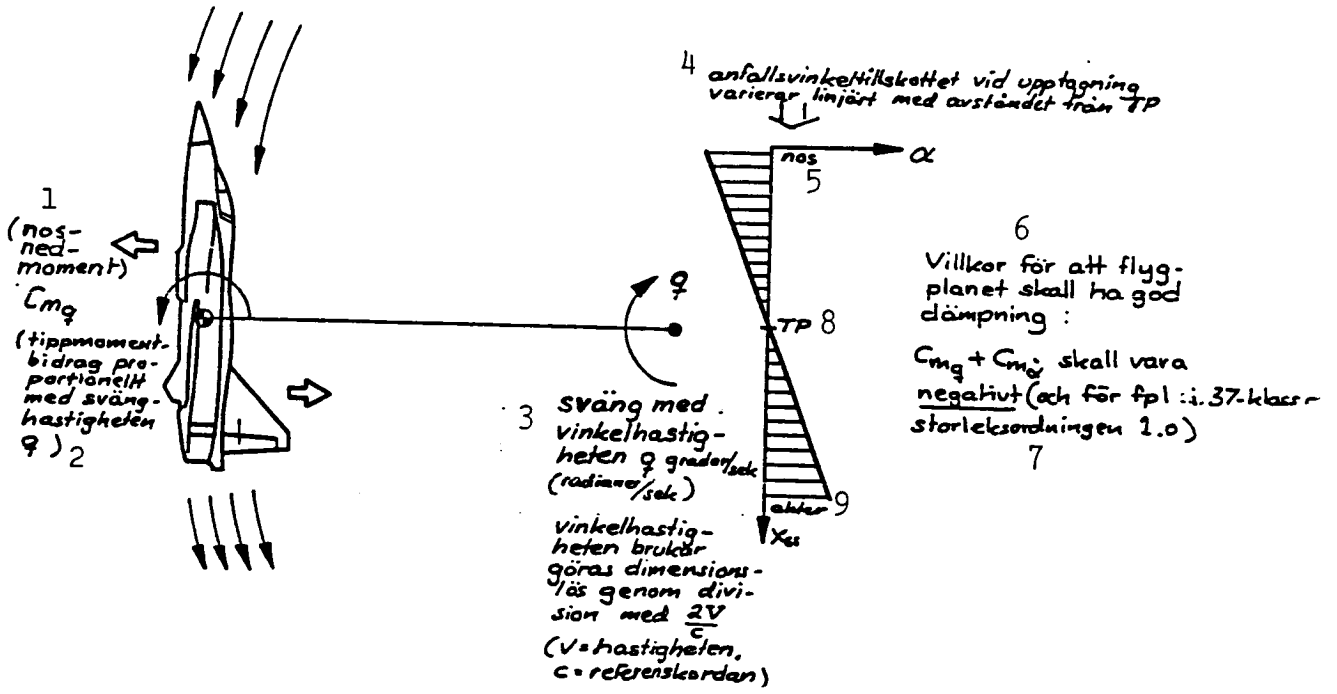

2. $C_{m\dot{\alpha}}$ = tippmomenttillskott på grund av tidsfördröjningseffekter snabbt ändras. Hos fpl 37 kan detta exemplifieras med att systemets interferenslast på huvudvingen inte "hänger med" i gång när anfallsvinkeln snabbt ökas.

Fig. 65. 1. C_{m_q} = actual pitch damping; for an explanation, see the figure.

Key: 1. (pitch-down moment), C_{m_q} .

2. Contribution of the pitching moment in proportion to the speed of rotation.
3. Rotation a the angular speed of q°/sec (i.e., radians/sec.). The angular speed is usually made non-dimensional by division of 2V/c (where V = the speed, c = the reference chord).
4. Contribution of the angle of attack when going upward varies linearily in relation to the distance from the point of gravity (TP).
5. Bow of the aircraft.
6-7. Condition: for satisfactory damping of the aircraft: $C_{m_q} + C_{m_{\dot{\alpha}}}$ must be negative (or, for aircrafts of the 37 class of the magnitude = 1.0).
8. TP = point of gravity.
9. Tail.

2. $C_{m_{\dot{\alpha}}}$ = Contribution from the pitching moment due to effects of time delay when the angle of attach is rapidly changing. In the case of FPL 37, this can be examplified by that the interference load of the vortex system of the canard does not instantly "catch up" when the angle of attach is rapidly changed.

Both these contributions are negative as far as FPL 37 is concerned (pull-out and an increase in the angle of attack both contribute to a pitch-down moment). Thanks to the fact that the canard and the wing are widely separated lontitudinally the attenuation is more satisfactory than in the case of a delta-winged aircraft. The former contribution (C_{m_q}) dominates over the latter ($C_{m_{\dot{\alpha}}}$); (for FPL 37 the $C_{m_q} = -1.25$ at low speed, while $C_{m_{\dot{\alpha}}} = -0.45$.)

The variation in pitch damping in relation to the angle of attack at low speed is evident from Fig. 66. The C_{m_q} diminishes considerably in connection with the collapse of the flow at high angles of attack. The $C_{m_{\dot{\alpha}}}$ contribution can usually be ignored at wide angles of attack (more than 40°).

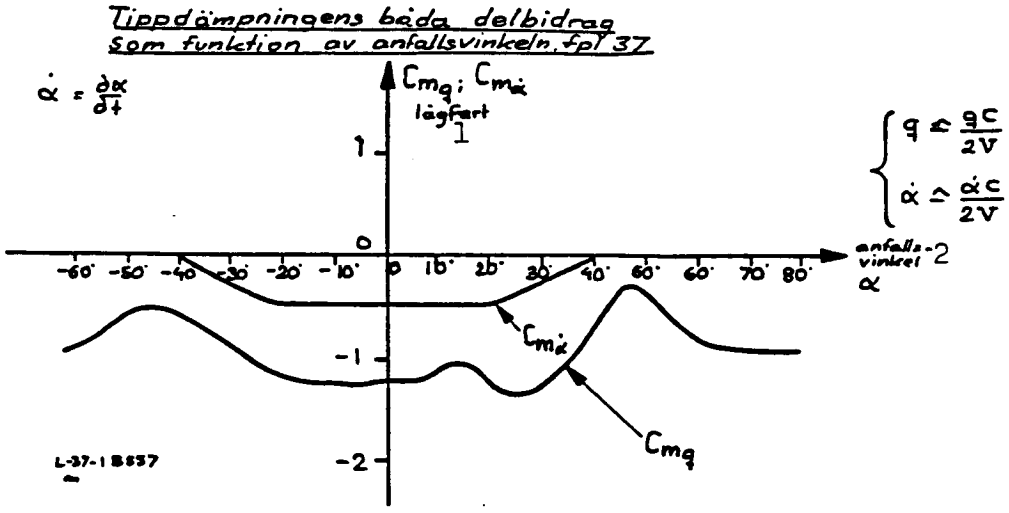

Fig. 66. Joint partial contributions to the pitch damping as a function of the angle of attack; FPL 37.
Key: 1. Low speed. 2. Angle of attack, α.

In the case of a conventional aircraft with a stabilizer, the latter is responsible for a major portion of the damping. For comparison, the aerodynamic damping at low speed of FPLs 37, 35 and 32 as well as that of two foreign aircrafts is shown below. All display adequate damping characteristics.

FPL	$C_{m_q} = C_{m_\cdot}$	S_{ref}	c_{ref}
37	-1.7	46 m^2	7.4 m
35	-1.1	50 m^2	5.319 m
32	-2.08	37.4 m^2	3.14 m
F-4, the Phantom	-3.3	49.2 m^2	4.88 m
the Mirage	-1.4	34 m^2	5.27 m

Note: q and $\dot{\alpha}$ are standardized in the table via the equations:

$$\bar{q} = \frac{qc}{2V} \quad \text{and} \quad \bar{\dot{\alpha}} = \frac{\dot{\alpha}c}{2V}$$

The attenuation is slighty affected by the ground interference and external loads. However, in practice this can be ignored.

3. DRAG AT LOW SPEED

3.1 Drag on an Untrimmed Aircraft

It is customary when comparing performance, etc., to make use of the wind-related system, i.e., we speak of drag and lift instead of tangential and normal forces, respectively. In general, the drag on an aircraft can be distinguished into one part, independent of the angle of attack (i.e., the minimum or zero drag), and another part, dependent on the lift (angle of attack), i.e., the so-called induced drag. This is valid for wind-related systems. We demonstrated already in Fig. 29 how the induced drag depends on and angle of attack (or the lifting force). The distinction into zero drag and induced drag is explained in Fig. 67.

/57

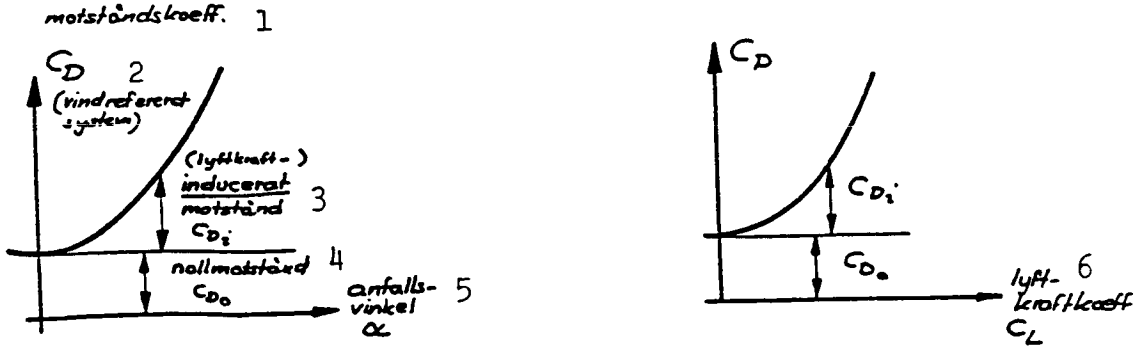

Fig. 67. (Key see p. 80).

Key to Fig. 67:

1. Drag coefficient.
2. (wind-related system)
3. Drag induced (by lift).
4. Zero drag.
5. Angle of attack, α.
6. Lift coefficient.

The induced drag has two typical characteristics:

1. It increases considerably more in relation to tha angle of attack than what lift does. The dependency is approximately quadrangular at normal angles of attack. This can be written:

$$C_{D_i} = k \cdot C_L^2 \quad \text{or} \quad C_{D_i} = k \cdot \ ^2.$$

This is a simplification of the more complete expression of induced drag which is:

$$C_{D_i} = k_1 \cdot C_L^2 + k_2 C_L + k_3$$

where k_1 $\dfrac{1}{\cdot \text{ (the aspect ratio)} \cdot \text{(the elliptic factor, e)}}$: (elliptic factor e = 1 corresponding to elliptic distribution of the load.

2. The induced drag grows larger, the smaller the aspect ratio of the aircraft is; see. Fig. 68. Sharp-edged and thin wings are also unfavorable.

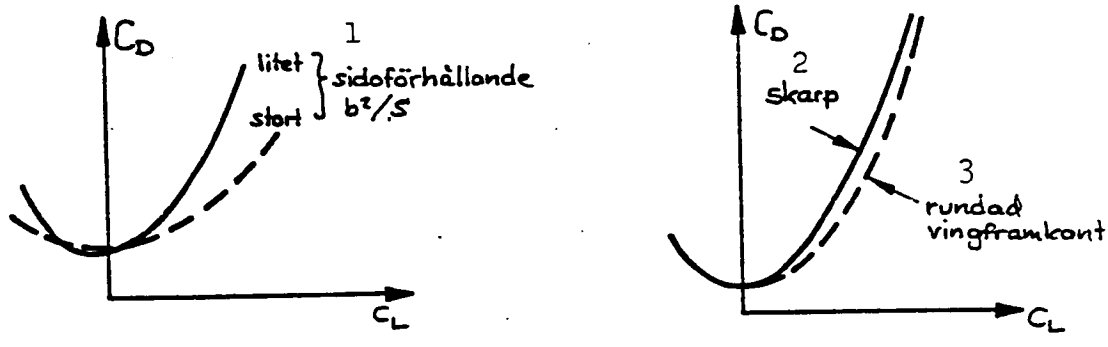

Fig. 68. Key: 1. Major (minor) aspect ratio, b^2/S
2. Sharp ...
3 rounded leading edge.

High-level induced drag is typical of modern supersonic aircrafts. A useful side effect appears in that it is possible to quickly retard the plane in certain situations by increasing the angle of attack. This property can be utilized in tactical situations and in connection with the landing in order to abbreviate the distance rolled (i.e., AD-braking). The performance when turning and in respect to durability are, however, strongly dependent on the magnitude of the induced drag. Therefore great efforts are made when designing an aircraft in order to keep the induced drag at a minimum. This applies also to FPL 37.

A basic principle is that the distribution of load must be elliptic in order to produced the least possible drag. This is in principle demonstrated in Fig. 69.

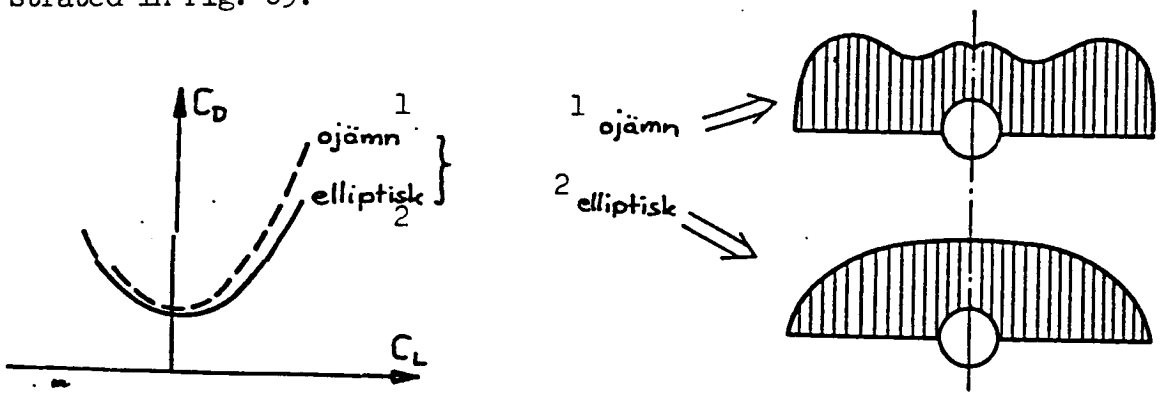

/58

Fig. 69. The Effect of the distribution of load on the drag.
Key: 1. Uneven.
2. Elliptic.

A trapezoidal wing with a large aspect ratio has a load distribution which is rather similar to that of an ideal load distribution. However, the mutual interference between two airfoils placed in a tandem formation makes it more difficult to achieve an ideal distribution. We can apply, e.g., torsion of the wing, local changes in planar shape or cambering (bending down) of the leading edge as methods for affecting the appearance of the load distribution at a given angle of attack.

3.2 Drag During Trimmed Flight

So far we have studied a case where all deflections of the elevators and

the flaps equal zero. A correlation between the elevator angle and the drag can be obtained in a manner similar to that used for the angle of attack while using the formula

$$\Delta C_D \text{ (elevator)} = k \cdot \delta_e^2$$

where δ_e = the deflection of the elevator in degrees or some other angular measure and C_D (elevator) = the contribution of drag due to the deflection of the elevator.

At narrow angles of attack the additional drag is practically equal to zero. At wider angles of attack the elevator tends to "flow along". The least amount of elevator drag occurs during small deflections upward (i.e., a weakly negative δ_e).

Since the angle of attack when flying is in a balanced condition (= trimmed flight) increases approximately in proportion to the angle of the elevator (if the zero moment = 0), the drag due to trimming can be illustrated as in Fig. 70:

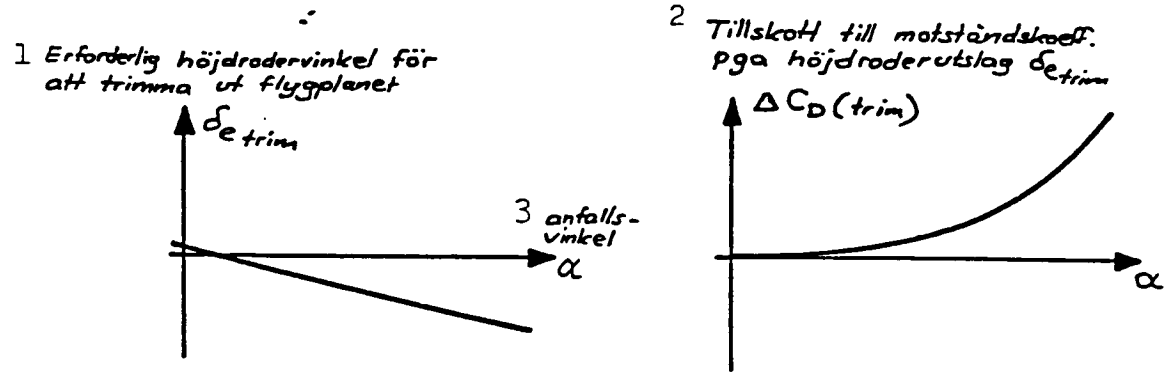

Fig. 70. Key: 1. Elevator angle necessary for balancing the aircraft.
2. Contribution to the coefficient of drag due to the deflection of the elevator, $\delta_{e_{trim}}$.

In the case of aircrafts with a large, positive zero moment the minimum /59
of the drag due to trimming is displaced toward wider angles of attack. FPL 37 shows at 30° deflection of the canard flap the least amount of drag due to trimming by the elevator when the angle of attack is about 15°. There is instead a corresponding addition to the drag caused by the flap of the canard.

Trimming while utilizing <u>two</u> surfaces instead of a single one can be applied in order to reduce the total drag; see Fig. 71 below.

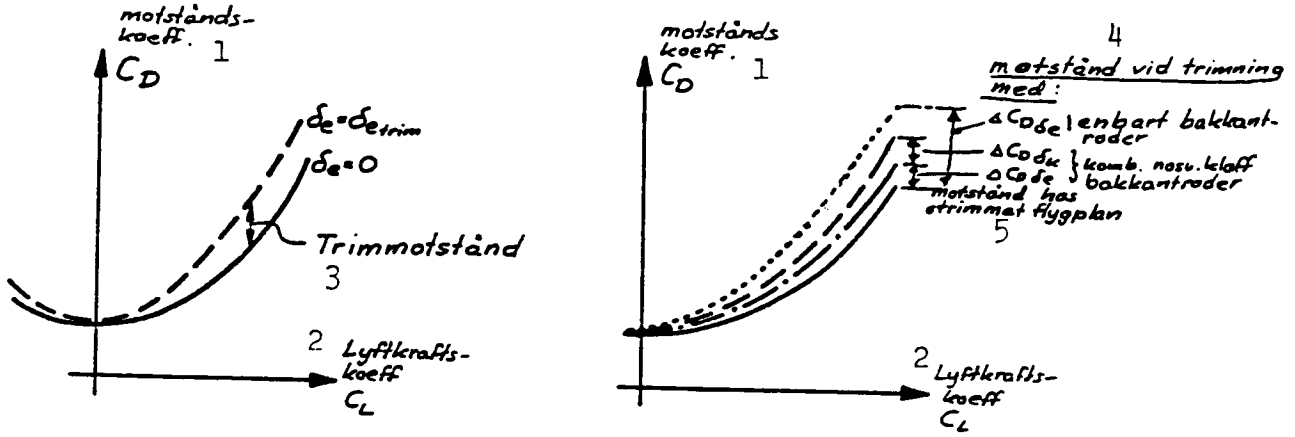

Fig. 71. Key: 1. Drag coefficient.
2. Lift coefficient.
3. Trimmed drag.
4. Drag during trimming by means of: $\Delta C_{D_{\delta e}}$, only the elevator on the trailing edge
$\Delta C_{D_{\delta k}}$, $\Delta C_{D_{\delta e}}$ } combination of canard flap and trailing edge elevator
5. Drag of an untrimmed aircraft.

This method can also be used when landing FPL 37.

3.3 Induction of Induced Drag by Cambering

The induced drag can be reduced by cambering or bending down the leading edge of the aircraft. The principle is evident from Fig. 72.

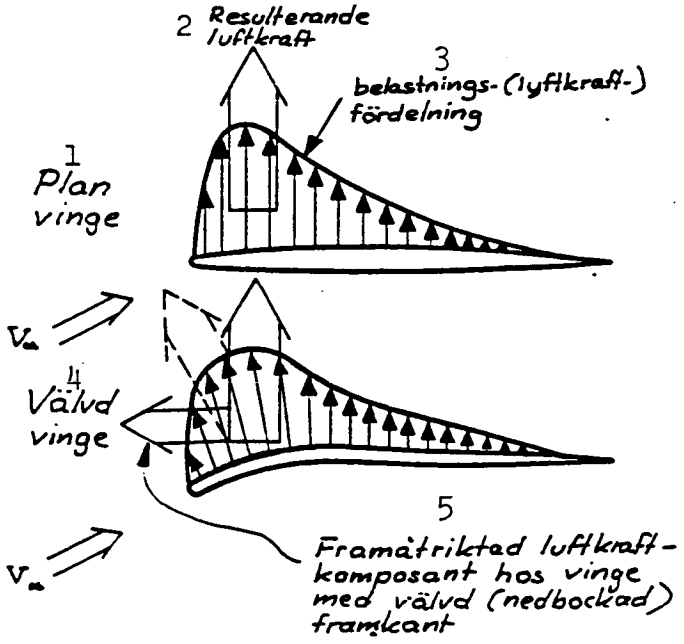

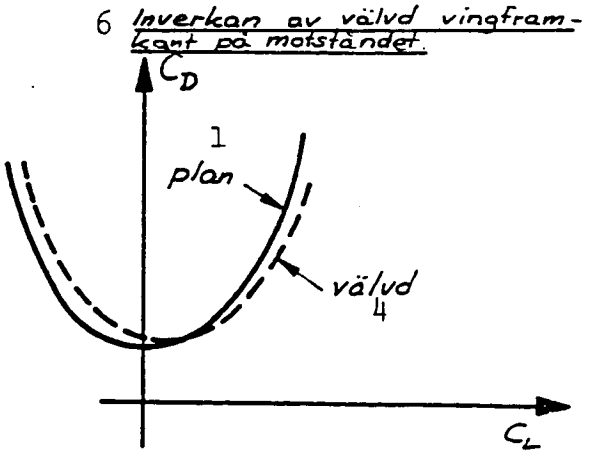

Fig. 72. Key: see p. 84.

Key to Fig. 72:

1. Flat wing.
2. Resulting lift.
3. Distribution of load (lift).
4. Cambered wing.
5. Forward-directed lift component of wing with a cambered leading edge.
6. Effect on the drag of a cambered leading edge.

The same characteristic is utilized as that which makes a rounded leading edge more favorable than a sharp one, i.e., the possibility for utilizing the lower pressure on the upper surface of the wing in order to reduce drag.

Due to the camber the high rate of suction power on the upper surface near the leading edge, caused by the air flow around it, will act upon a surface sloping forward against the direction of the air flow. The result is a forward-directed component of the lift. /60

The cambering principle is applied for the leading edge of the canard and the outer portion of the sawtoothed leading edge of the wing. Due to the fact that, in general, the elevator angle for trimming the plane during straight-line flight (in order to achieve the most favorable extension) amounts to a few degrees below zero (elevator deflected upward), the camber is reduced toward the wing tip close to the trailing edge elevator.

Induced drag does not come entirely without cost. The total drag at a given angle of attack becomes somewhat lower.

Another disadvantage is that the cambering of the leading edge causes a minor increase of the zero drag, which is, however, more than compensated for by the gain in drag at wider angles of attack such as used during landing and when maneuvering with heavy load factors. In the case of FPL 37 advantages from the point of view of longitudinal stability were also gained as a side effect of the increased drag.

3.4 Drag and Tractive Force - Flying in the "Second Regime"

The relation between traction and drag in the case of an aircraft of a type like FPL 37 is illustrated in Fig. 73.

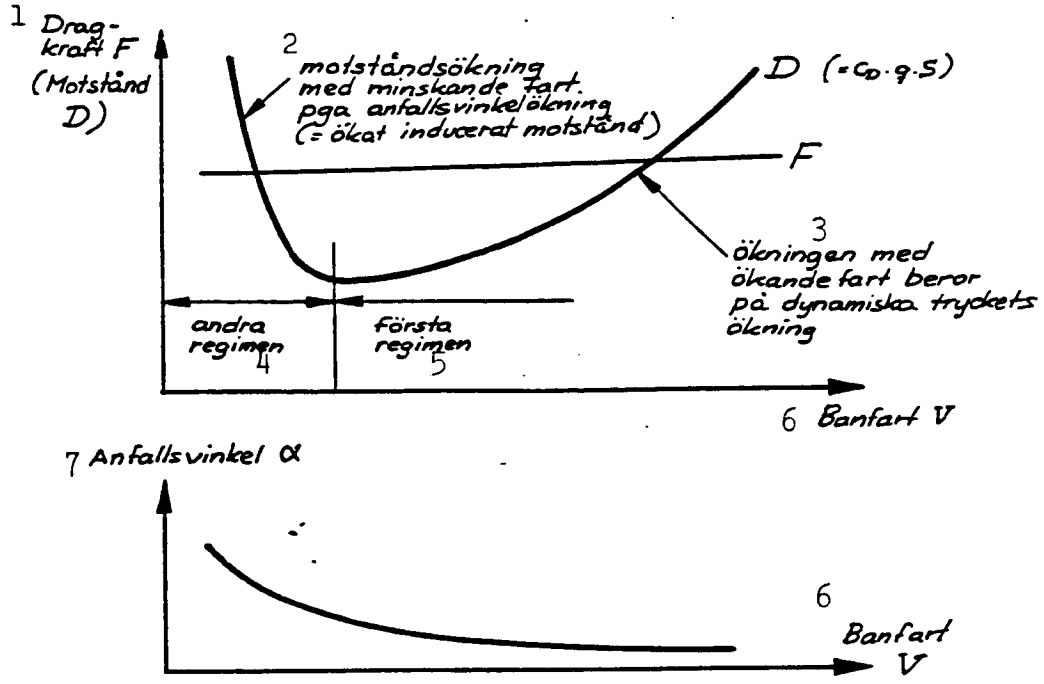

Fig. 73. Drag and traction in the first and second regimes.
Key: 1. Traction, F (drag, D).
2. Increased drag in relation to reduced speed due to increased angle of attack (increased induced drag).
3. The increase in relation to increased speed depends on the increase in dynamic pressure.
4. Second regime.
5. First regime.
6. Trajectory velocity, V.
7. Angle of attack, α.

It has been demonstrated that in the case of an aircraft with a high level of induced drag it is feasible to get down to such a low speed that the induced drag begins to grow in relation to the decreasing speed. Such aviation in the second regime proved to be a problem in connection with the work when planning for FPL 37, where the stringent demands on low flying speed were adament.

The risk for unintentionally slowing down too much increased. An instability developed which resulted in that tampering with the speed in connection with a change in trimming led to further interference with the speed. In order to counteract this kind of speed instability in the second regime, automatic speed control (AFK) was introduced for FPL 37. Due to this flying becomes considerably easier at the low speed which the shape and the high rate of traction permit. /61

4. THE AIRCRAFT IN RELATION TO AN OBLIQUE AIR FLOW, ASYMMETRIC FORCES AND MOMENTS: YAW RESISTANCE AND RUDDER EFFECT

4.1 General - Definition of Asymmetric Forces and Moments

So far only symmetric flight conditions have been studied, i.e., flying without encountering an obliquely directed air flow (straight-line flying). Now we shall consider the forces and moments which affect an airplane in the case of an obliquely approaching air flow (flying in an oblique air flow and banking). The efficiency of the tail fin in the case of an oblique air flow and the resistance to yawing will be treated in addition to the forces acting upon the wings when in an oblique air flow as well as the effect on the side rudder and the ailerons.

We shall start by defining the forces amd moments present due to an oblique air flow.

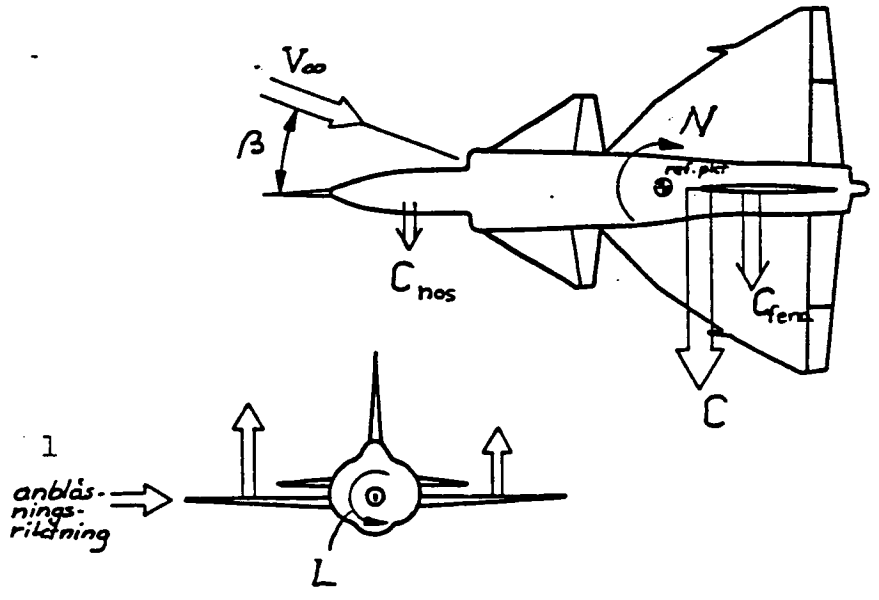

β = angle of oblique air flow
C = component force
L = rolling moment
N = yawing moment
C_{nos} = component force affecting the bow
C_{fena} = component force affecting the tail fin
V = speed of free flow
Key: 1. direction of air flow

Fig. 74.

When encountering an oblique air flow (at lateral angle β) component forces act on the bow and the tail fin in the same manner as on the bow and the wing when flying at an angle of attack. The component forces create a yawing moment (N) around the point of gravity. In addition the disturbance

of the lift above the wing becomes asymmetrical at the combined angles of attack and an obliquely approaching air flow. Usually the lift of the windward wing tends to increase due to an increased oblique air flow while the leeward wing loses about equally much lift. The normal force (or lift) does not change substantially; on the other hand a considerable rolling moment (L) of the aircraft develops. Non-dimensional coefficients can be used in the same manner as in the case of symmetric forces and moments: /62

$$C_C = \frac{C}{qS} = \text{coefficient of component force,}$$

$$C_n = \frac{N}{qSb} = \text{coefficient of the yawing moment,}$$

$$C_l = \frac{L}{qSb} = \text{coefficient of the rolling moment,}$$

where q = dynamic pressure, S = reference surface (wing surface) and b = the wing span.

As far as FPL 37 is concerned we use b = 10.0 m and S = 46.0 m^2. The fuselage-related as well as the wind-related systems can be used in the same manner as in the case of symmetric force coefficients. Below we will primarily consider derivatives and coefficients of the fuselage-related system. The variation in relation to an oblique air flow at an angle of β is illustrated in Fig. 75.

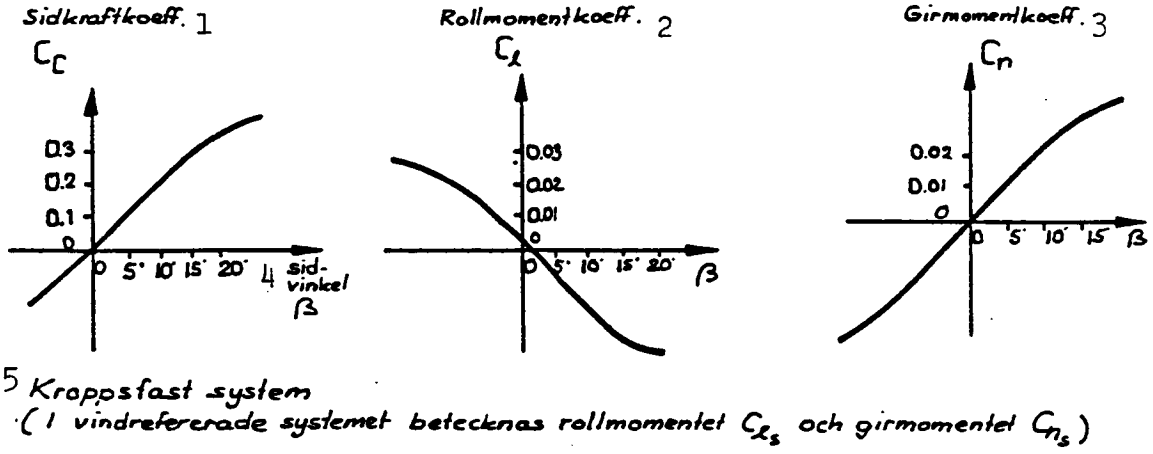

Fig. 75. Key: 1. Coefficient of component force.
2. Coefficient of rolling moment.
3. Coefficient of yawing moment.
4. Lateral angle, β.
5. Fuselage-related system (in wind-related systems the rolling moment is written C_{L_S} and the yawing moment C_{nS})

It is evident from Fig. 75 that all the three coefficients are approximately linearily dependent on the angle β (up to 10°) of the oblique air flow. The gradients of the graphs are therefore often used as a measure of the sensitivity of the side force, the rolling and the yawing moments in relation to an oblique air flow.

The gradients are called: the component force derivative, C_{C_β} ,
the rolling moment derivative, C_{l_β} , and
the yawing moment derivative, C_{n_β} .

($CC_\beta = 1$ corresponds to the case where the component force coefficient increases by 1 in relation to an increase of 1 radians of oblique air flow).

These magnitudes will be used for the following reasoning.

4.2 Component Force, Efficiency of the Tail Fin Depending on the Interference between Fuselage and Wing

a) General

As a rule an aircraft shall be able to tolerate an oblique air flow from various angles during maneuvering as well as sudden side gusts when landing. It must therefore have resistance to yawing (have yaw stability), i.e., it must be able to counteract the tendency to veer sideward when the air flows in from the side (i.e., it should have "wind vane stability"). At an oblique air flow a side force develops on the fuselage, the result of which attacks close to the bow far ahead of the point of gravity and, consequently, produces a powerful, destabilizing yawing moment. /63

In order to counteract this phenomenon, all aircrafts are provided with one or more tail fins (vertical airfoils placed behind the point of gravity) which deliver an adequate contribution to the yawing moment in order to compensate for the destabilizing effect on the bow.

When designing modern aircrafts, great efforts are spent on making the tail fin as effective as possible (i.e., able to provide adequate yaw resistance across the entire range of angles of attack and oblique air flows at all speeds occurring) by using a tail fin surface as small as possible and of minimum weight.

In respect to FPL 37 the dimensioning of the tail fin presented additional problems because, in addition to the interference of the fuselage on the tail fin, there is a very complicated interaction between the wing, the canard and the tail fin. In order to explain this, we will below report on the most important contributions to the component forces affecting the tail fin. These are decisive for the efficiency of the tail fin and, thus, the yaw resistance.

It is of interest to avoid unnecessarily long fuselages for modern aircrafts. Therefore the distance between the tail fin and the point of gravity must be limited. Since the volume of the tail cannot be reduced this means a larger tail fin; compare, e.g., the abnormally large tail fin of the MRCA. The contribution of the component force acting on the tail fin dominates, thus, in comparison with other contributions, among which that of the fuselage bow is, in general, the next largest. In addition to these contributions, there are also others which, however, can be ignored at narrow angles of attack.

The component force acting on the tail fin in the case of an oblique air flow corresponds to the lift acting on a wing at angles of attack. If we ignore special, interfering effects, the side force affecting the tail fin will therefore depend on the aspect ratio, the trapezoidal ratio and the sweep-back angle in addition to the side force acting on the tail fin. Due to the mirror effect, active on the wing surface, the effective aspect ratio is increased and the interfering load of the tail fin, acting on fuselage, is likewise increased.

The picture of the circulation around the tail fin is, however, not as simple as that around the wing, which mainly encounters angles of attack varying in the direction of the span in a simple manner or even considered constant over large portions of the wing span.

In the case of an airflow consisting of direct angles of attack and an oblique airflow considerable effects of interference from the wing (in respect to FPL from the canard as well) and the bow of the fuselage develop, especially at large angles of attack. These contributions are particularly important for modern, slender aircrafts and, perhaps especially, for delta-

winged aircrafts. Therefore we shall treat these interfering effects in detail.

b) Wing/Tail Fin Interference Due to an Oblique Air Flow; Principle.

The principle governing the development of a component force due to wing/tail fin interference is evident from Fig. 76.

/64

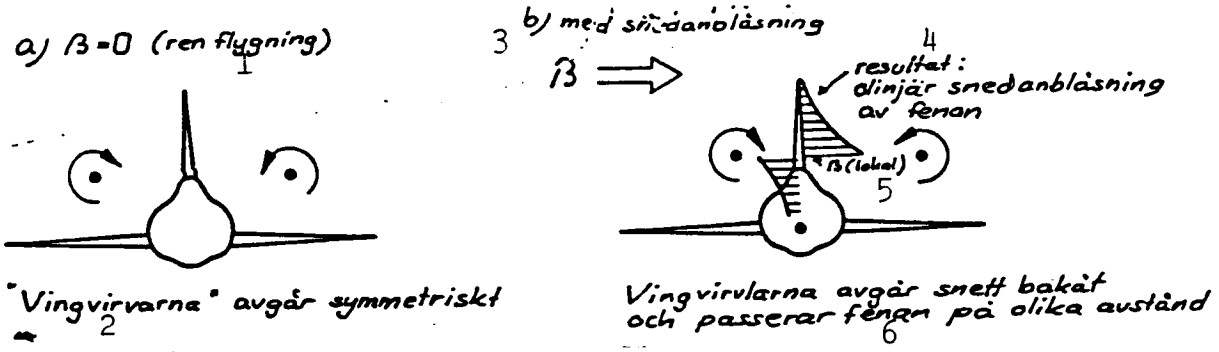

Fig. 76. Key: 1. β = 0 (straight-line flying)
2. The "wing vortices" are symmetrically detached.
3. In an oblique airflow
4. Result: non-linear oblique air flow affecting the tail fin.
5. β (local).

The illustration of the flow above the wing has been coarsely simplified (in conformity with the previous reasoning) into one single pair of separating vortices.

Due to the oblique air flow the vortex above the windward wing passes close to the tail fin, while the distance between the tail fin and the leeward vortex increases. The distribution of the transverse flow caused by the windward vortex will not be completely neutralized by that of the leeward one like in the case of symmetric flow. The result is a distribution of side-sweep, induced by the vortices and superimposed on the basic,oblique flow. This effect is accentuated when the force of the vortices increases in relation to increasing angles of attack.

The additional side sweep causes a force, the resulting size of which depends on at what vertical level the wing vortices pass the rear of the fuselage and the tail fin as well as on the potency of the side-sweep. The effect of the vortex passage in an oblique air flow is evident from Fig. 77.

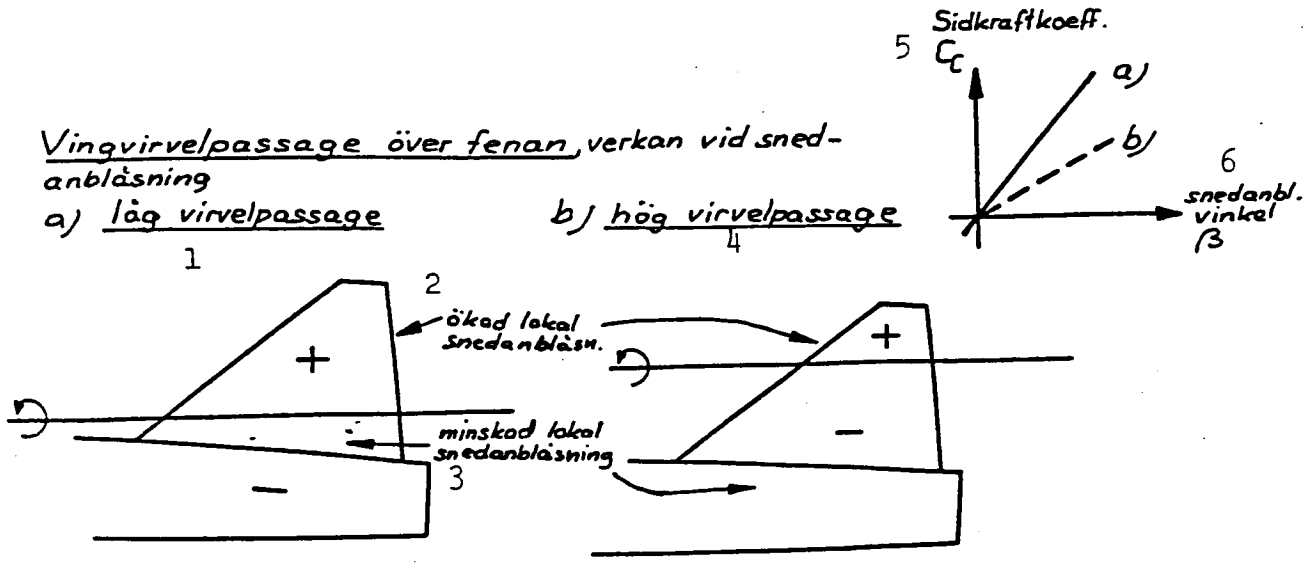

Fig. 77. Passage of the wing vortices past the tail fin; effect at an oblique air flow.
Key: 1. Low level passage.
2. Locally increased oblique air flow.
3. Locally decreased oblique air flow.
4. High-level vortex passage.
5. Coefficient of component force.
6. Angle of oblique air flow.

A low-level passage of the vortex causes the contribution of the increased side-sweep to dominate above the line of vortices. The componant effect resulting on the tail fin increases and, thus, the efficiency of the tail fin as well. At a more elevated passage of the vortices, the condition is the opposite: the efficiency of the tail fin is diminished. This is a well known /65
phenomenon and is the reason why aircrafts with the wings in a raised position are constructed with larger tail fins than corresponding planes with the wings at a lower position (Fig. 78). (What is stated here is also analogically valid if instead of a single vortex a layer of vortices is assumed.)

Fig. 78.

If we use a conventional aircraft with the wings at a median position for comparison and assume that the surface of its tail fin equals 1, a higher-

level position of the wings means that the tail fin surface must be increased by 1.3 - 1.4 in order to obtain the same resistance to yawing. In reverse, a 0.9 - 0.8 tail-fin surface will be adequate for a plane with the wings at a low-level position.

Consequently, the placement of the main wing on FPL 37 helps to keep the size of the tail fin down. The fact that FPL 37 still has a relatively large tail fin depends, among others, on the condition that it must be efficient throughout the entire range of attack and speed both when flying as a plane without an external load and a plane with a bulky external load, placed far forward.

c) Interference between the Bow of the Fuselage and the Tail Fin; Principle

The reasoning concerning the interference between the vortices and the tail fin can also be applied, e.g., to the interference between the fuselage and the tail fin and that between the air intake and the tail fin. Since the starting point of the fuselage vortices lies further away from the tail fin, the effects of straight and oblique air flows will become more obvious. Under unfavorable circumstances, the windward vortex can come to pass on the leeward side of the tail fin with drastic changes in component force as a consequence. One way to impede this phenomenon is, - like in the case of FPL 37, - to have wide air intakes, which can "take care" of the vortices generated by the bow of the fuselage so that the vortex system resulting will be moved farther away from the tail fin.

4.3 Component Force and Variation in Yawing Moment in Relation to the Angle of an Oblique Air Flow

The contributions of the component force and their addition to the yawing moment are evident from Fig. 79.

To a certain extent the relationship between the contributions concerned /66
depends on the design of the aircraft. In respect to FPL 37, the angles of attack play a major role. The effect of the tail fin at large angles of an oblique air flow will be discussed farther below.

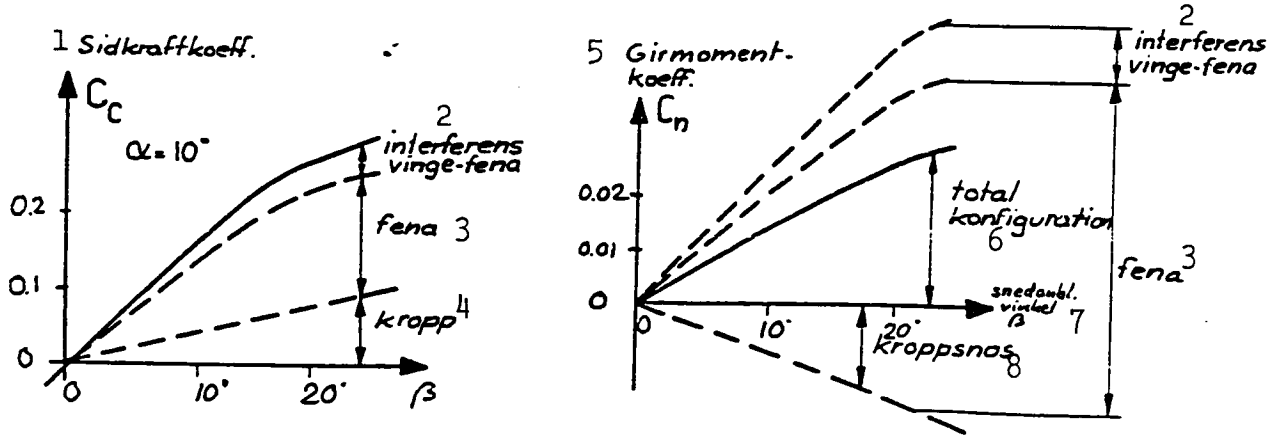

< Karling

Fig. 79. Key: 1. Coefficient of the component force.
2. Interference wing/tail fin.
3. Tail fin.
4. Fuselage.
5. Coefficient of the yawing moment.
6. Total configuration.
7. Angle, β, of oblique air flow.
8. Bow of the fuselage.

4.4 Component Force and Variation in the Yawing Moment in Relation to the Angle of Attack; Wing/Tail Fin Interference. /66

Effect

The interference between the wing and the tail fin described above has largely the following effect (Fig. 80):

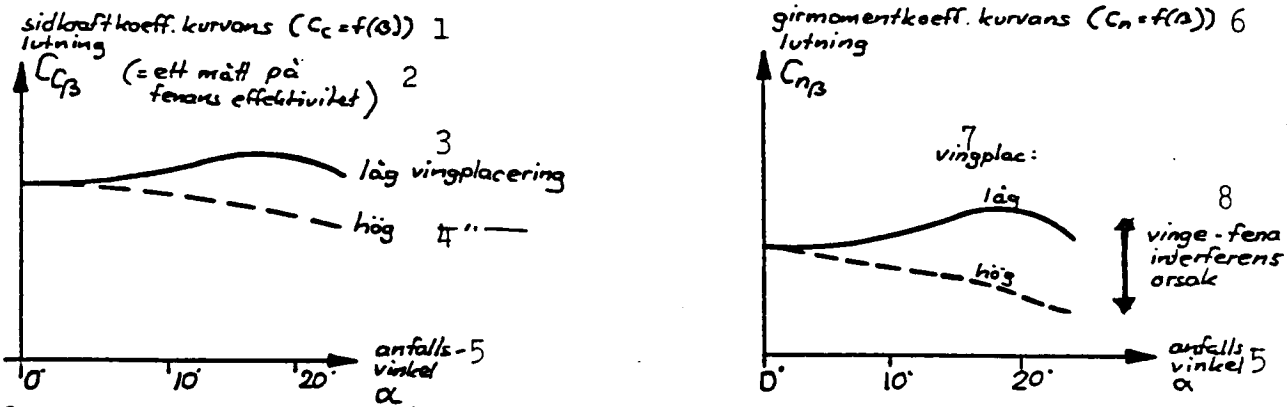

9. Feneffektiviteten sjunker med ökande anfallsvinkel hos flygplan med hög vingplacering

Fig. 80. Key: 1. slope of component force graph; 2. (a measure of the efficiency of the tail fin; 3. wings at a low level; 4. wings at a high level; 5. angle of attack; 6. slope of yawing moment coefficient graph; 7. wing-position: high (low); 8. cause of interference between wing and tail fin.

C-2

The dependency on the angles of attack is intimately related to the passage of the fuselage-generated and the wing-generated vortices around the tail fin. It is also related to the height of the tail fin and its position longitudinally in relation to the wing. The figure above (Fig. 80) is approximately valid for a design like that of FPL 37. It is evident that the interfering effects are strongest in relation to the yawing moment since the contributions from the bow of the fuselage and the tail fin counteract each other.

4.5 Effect of Tail Fin at Wide Angles of Attack

The interference between the bow of the fuselage and the wing affects the efficiency of the tail fin at wide angles of attack. In addition, at wide angles of attack, the contribution from the tail fin itself is also affected by "shading" and because of the fact that its effective sweep-back increases. The shadow-effect leads at positive angles of attack to a decreased effect of the tail fin, while the contribution from the fuselage becomes more dominant. During the separation of the wing (flow collapse) the shading effect increases. The large and sudden changes in the yaw resistance often met with at this kind of angles of attack depend on a combination of increased shading and the fact that the vortex on the windward side changes position.

4.6 Effects of Tail Fin at Wide Angles of An Oblique Air Flow - Measures Toward Increasing the β Maximum of the Tail Fin

The effect of the tail fin at large angles of an oblique air flow can be compared with the dependency of the wing on the lift at large angles of attack. The contributions of the wing and the fuselage can be compared with those of the bow of the fuselage and that of the tail fin according to Fig. 81.

The balance between the load on the bow of the fuselage and that on the tail is, however, more delicate than the corresponding equilibrium between the bow of the fuselage and the wings. By constructing tail fins with a large sweep-back, the separation at the leading edge can be utilized also in /67

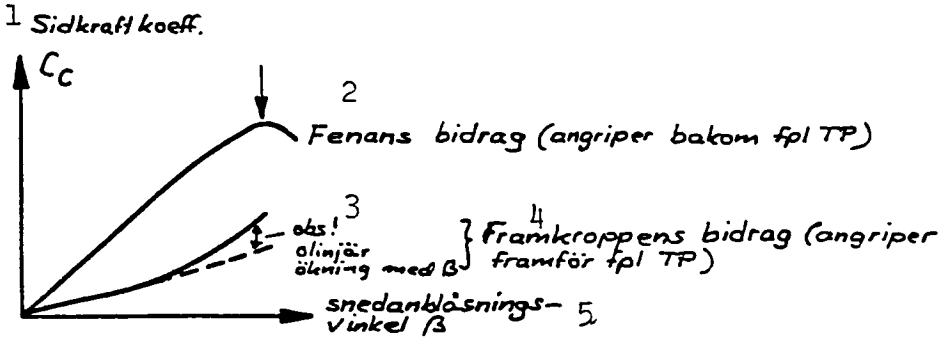

Fig. 81. Key: 1. Coefficient of component force.
2. Contribution of the tail fin (attacks behind the point of gravity of the aircraft).
3. Note! Non-linear increase in relation to β.
4. Contribution of the frontal portion of the fuselage (attacks in front of the point of gravity).
5. Angle, β, of oblique air flow.

in this case; it delays the saturation tendency of the tail fin force at a wide β and "matches", thus, more satisfactorily the contribution from the bow of the fuselage (cf. especially FPL 35 with a ca. 70° sweep-back). Special measures had to be taken in respect to FPL 37 with a 50° sweep-back of its tail fin (designed in order to increase the relative position in height in relation to the vortices generated by the canard and the fuselage) in order to maintain the satisfactory efficiency of the tail fin. A stable flow, separated by the leading edge, does not exist within such a large angular area of oblique flow as, e.g., in the case of the canard and the wing of FPL 37.

A large contribution from the tail fin itself at large angles can also be achieved by aiming at a relatively low aspect ratio (especially ratios around 1 produce large lift maximums). However, this rarely allows a favorable utilization of the fuselage/tail fin or the wing/tail fin interferences. Therefore much testing and compromizing hide behind the choice of the tail fin design of modern fighter aircrafts.

There are several ways of improving the effect of tail fins of the type used for FPL 37, especially at wide angles of β.

Examples are: the introduction of vortex dividers or providing the tail fin with a forward prolongation at its base (a so-called dorsal fin).

Figure 82 illustrates some different measures used for improving the component forces and their effects.

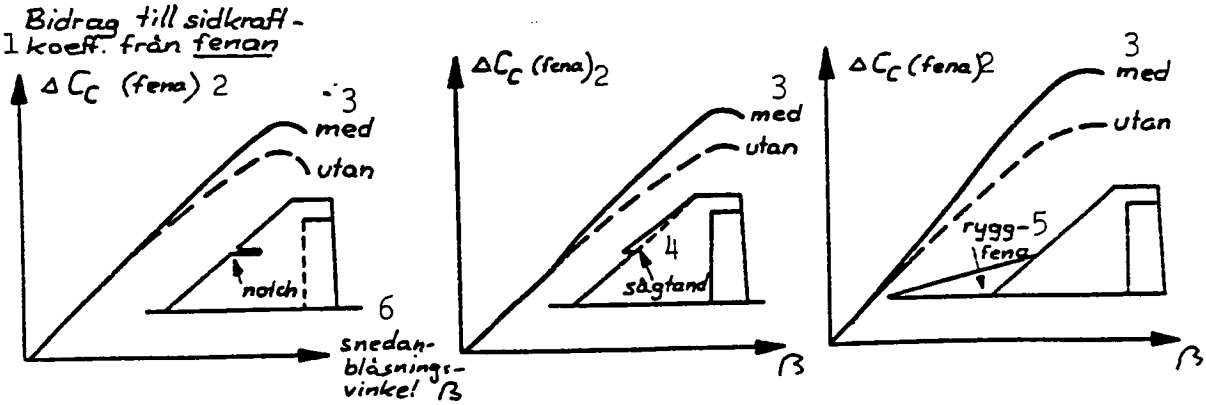

Fig. 82. Key: 1. Contribution to the coefficient of the component force from the tail fin.
2. ΔC_C (tail fin).
3. With / Without (a notch).
4. ... a sawtooth.
5. ... a dorsal fin.

The effect of the "dorsal fin" is due to the fact that an increased upsweep over the upper portion of the tail fin is created by a flow type, resembling a vortex, at the same time as it is possible to prevent the boundary layer of the fuselage from disturbing the flow around the tail fin by a favorable design of the tail fin. It is a disadvantage that the attack point of the component force is moved forward so that the yaw moment is lost. Thus, in practice, the efficiency of the tail fin is reduced at narrow angles of an oblique air flow. In addition, the changed design of the tail fin affects the interference between wing and tail fin as well as that between the bow of the fuselage and the tail fin. /68

4.7 Efficiency of the Tail Fin of FPL 37 - Effect Exerted by the Canard

The interaction between the bow of the fuselage, the canard and the wing of FPL 37 has been utilized in order to create yaw resistance up to wide angles of attack and obliquely approaching air flows. The canard/tail fin interference dominates among the interactive contributions in respect to FPL 37 due to the fact that the vortices generated by the canard pass close

to the tail fin. Since the elevated position of the canard vortices is forced down by the vortices generated by the main wing, the yaw resistance is hardly at all disturbed by the canard.

If this interaction did not exist, the relatively elevated position of the canard on this aircraft would be unfavorable. How delicate this interaction is for the interference can be demonstrated by the improvement in the effect of the tail fin, achieved by a reduction in the V-position of the canard from +10° on the test plane to 0° on the serialized plane. The V-position was introduced at a stage of the project when air jet flaps were still valid and constituted one method for achieving an acceptable longitudinal stability. When the slotted flap was accepted, the necessity for holding on to the V-position for the sake of longitudinal stability disappeared. Therefore the V-position was abandoned when, for the sake of yaw resistance, it became necessary to improve the efficiency of the tail fin of the aircraft.

Fig. 83. Key: see p. 98

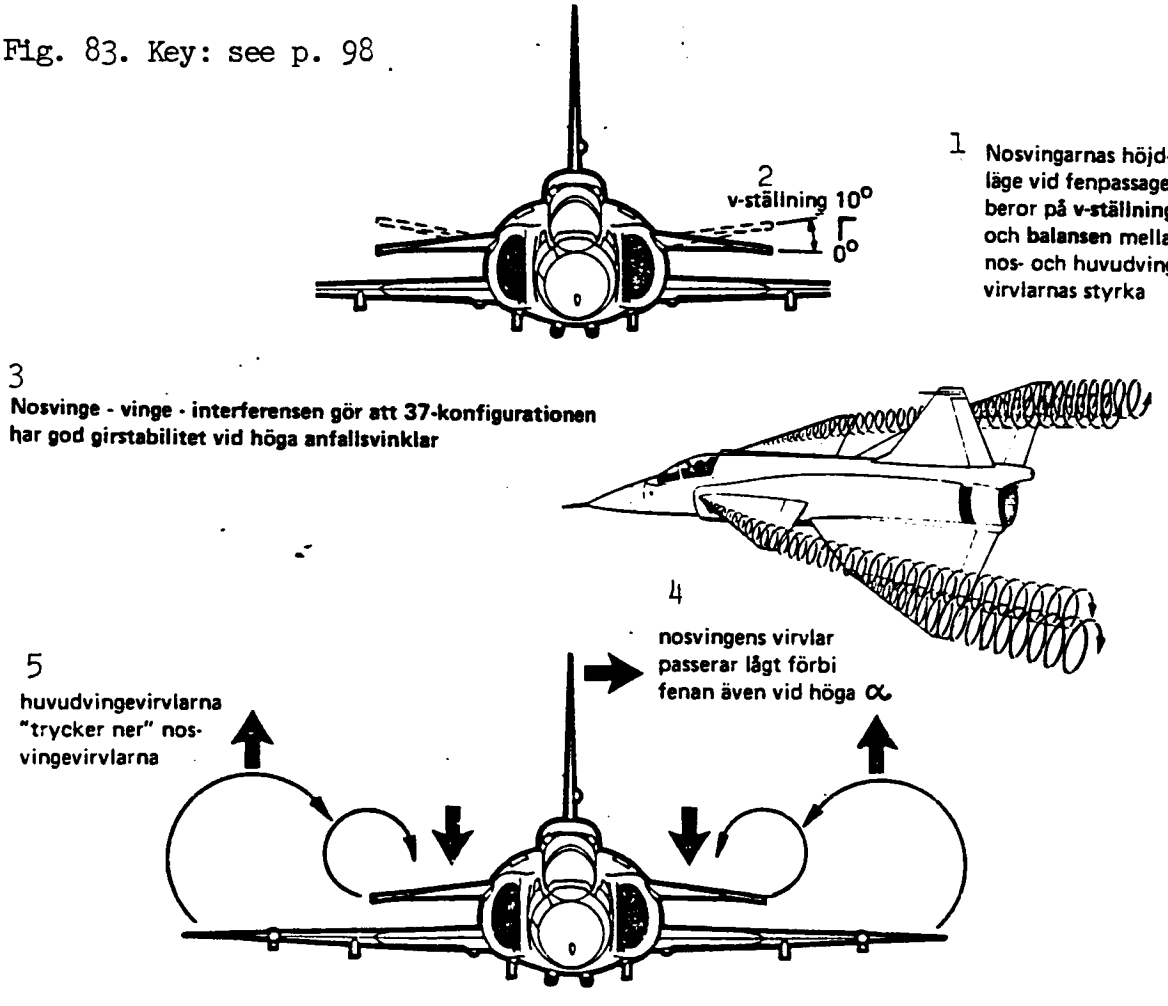

Key to. Fig. 83:

1. The vertical position of the canard for the passage of the tail fin depends on the v-position and the balance between the force of the vortices of the canard and the main wing, respectively.
2. V-position, 10°.
3. The interference between the canard and the wing of FPL 37 provides this configuration with a favorable yaw resistance at wide angles of attack.
4. The canard vortices pass the tail fin at a low position also at wide angles of attack.
5. The vortices generated by the wing "press down" those generated by the canard.

4.8 Asymmetric Forces During Extreme Angles of Attack and Symmetric Oblique Air Flow

/69

Component forces constitute a special effect pertaining to slender aircrafts and occurring at very wide angles of attack and an oblique airflow at 0°. Due to the mutual interference between the vortex layers of the fuselage and the canard, an unstable equilibrium occurs at a certain range of angles of attack. See Fig. 84. One vortex layer (of the fuselage) affects the other so that the layers come to assume an asymmetric position, one farther away from the fuselage than the other. The result is that a component

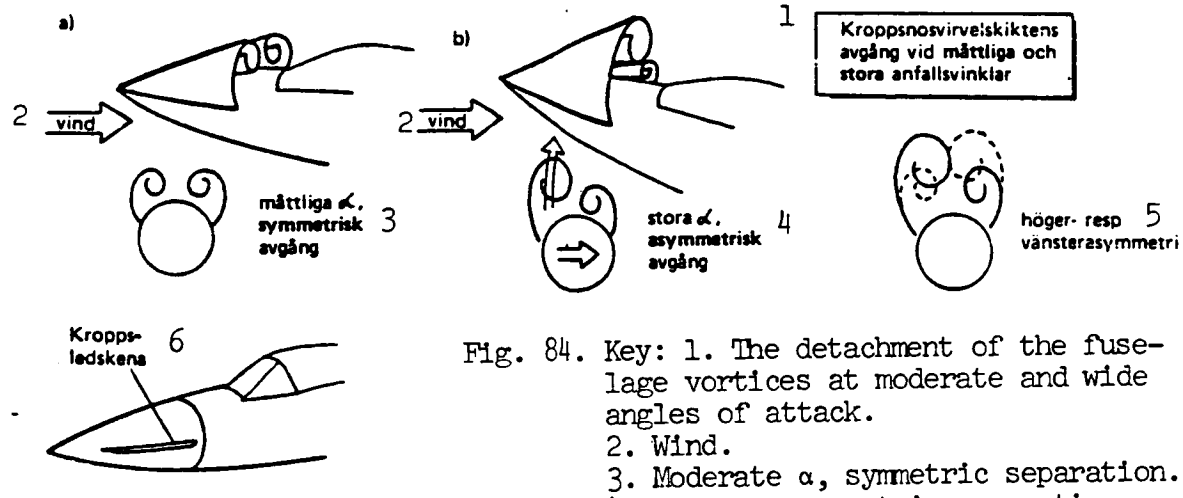

Fig. 84. Key: 1. The detachment of the fuselage vortices at moderate and wide angles of attack.
2. Wind.
3. Moderate α, symmetric separation.
4. Wide α, asymmetric separation.
5. Right-hand and left-hand assymetry, respectively.
6. Body strake.

force is induced on the fuselage and the tail fin. The wing as well is subjected to asymmetric forces. Asymmetry at angles of attack between 40° and 80° occurs in the case of FPL 37. The alternation between left-hand and right-hand asymmetry gives rise to changes in the load on the tail fin when entering into a stall accompanied by a high load factor and associated with periodic separation of the flow close to the tip of the tail fin. Changes in load, occurring within a narrow range of angels of attack around +40°, make themselves felt so that the tail fin starts to flutter. This is not critical although such a state of flight should be avoided. The characteristics of the component force have been measured in a wind tunnel (Fig. 85).

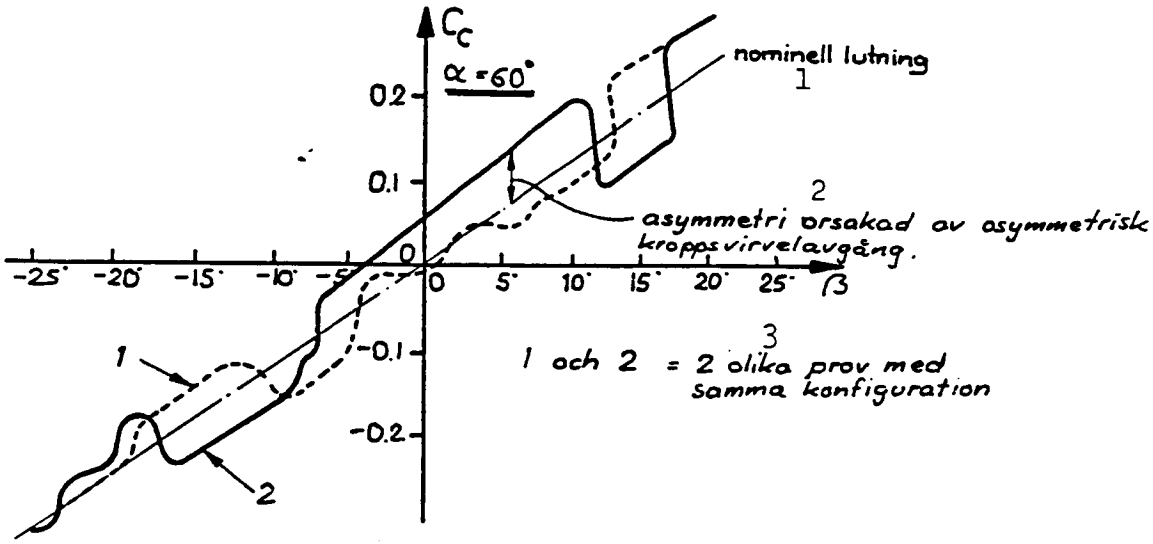

Fig. 85. Key: 1. Nominal gradient; 2. asymmetry caused by asymmetric detachment of fuselage vortices, 3. 1 and 2 = two different tests made with the same model.

Such a disturbance occurs at positive as well as negative angles of attack and varied in an arbitrary manner during the wind tunnel experiments between dextral and sinistral asymmetry. The asymmetry has been "remedied" by placing body strakes on the sides of the fuselage of foreign aircrafts.

4.9 Characteristics of the Component Force and the Yawing Moment of FPL 37 at Low Speed /70

a) Component Force

The derivative of the component force at low speed has the following appearance in respect to FPL 37 according to Fig. 86.

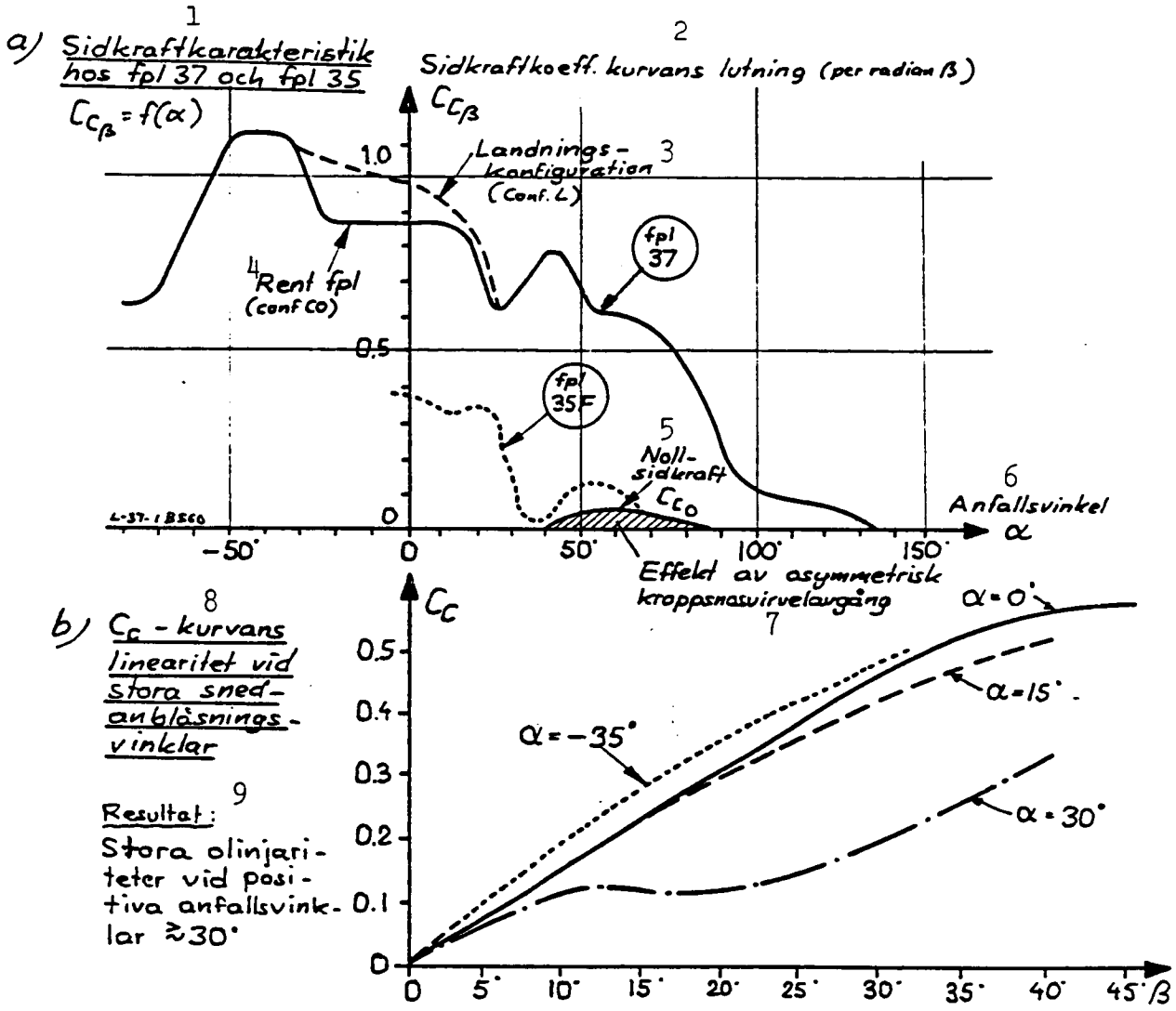

Fig. 86. Key: 1. a) Characteristics of the component force of FPL 37 and FPL 35.
2. Gradient (per radian of β) of the coefficient of the componentforce.
3. Landing configuration (conf. L.)
4. Aircraft without external load (conf. CO)
5. Aero component force.
6. Angle of attack.
7. Effect of asymmetric detachment of fuselage vortices.
8. b) The linearity of the C_C graph at wide angles of an oblique air flow.
9. Result: Great non-linearities at positive angles of attack $\gtrsim 30^\circ$

Figure 86 illustrates also how the component force C_C varies in relation to the angle of oblique air flow, β, at some wide angles of attack. The reduction in C_{C_β} at extremely wide angles of attack, shown in Fig. 86, depends

mainly on the fact that the tail fin was "in the shadow". It is evident from the figure that the tail fin is most efficient at negative angles of attack.

The high level of component force during start and landing is caused mainly due to the effect of the landing gear. An increase in component force of a similar magnitude is present when the aircraft flies with external armament. The most powerful component force occurs when an extra fuel tank is mounted on girder C 7 (i.e., is centrally positioned) and there are external loads at other girder positions as well.

b) Yawing Moment /71

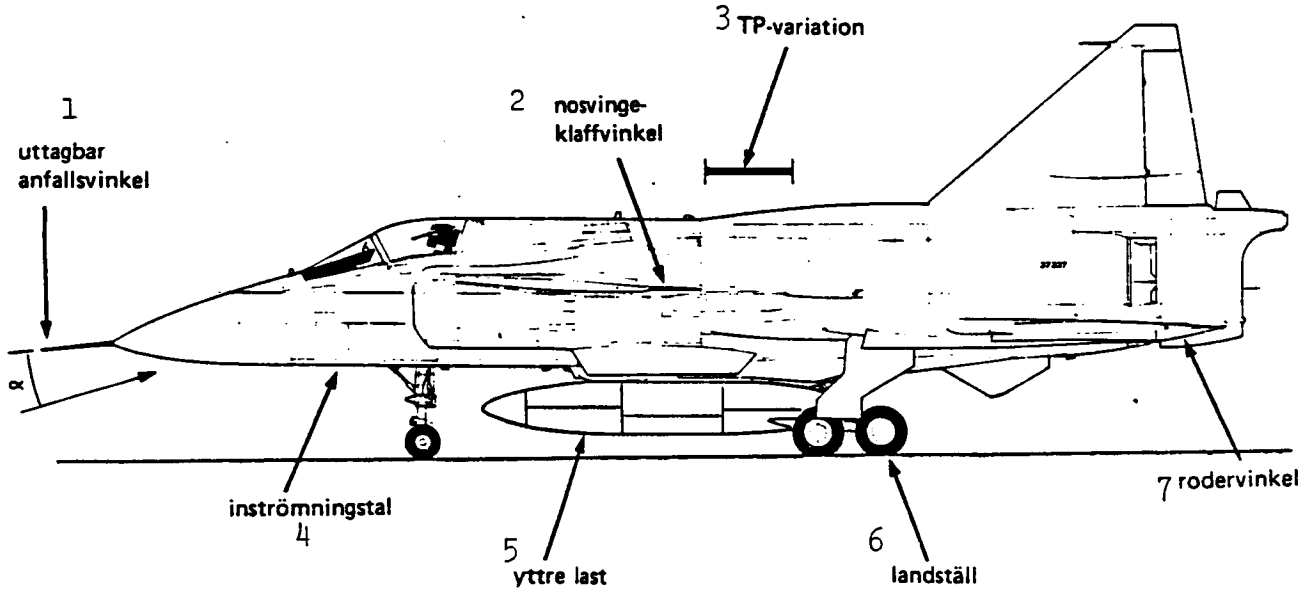

Fig. 87. Factors affecting the magnitude of the yawing moment.
Key: 1. Angle of attack applicable.
2. Flap of canard.
3. Variation in the point of gravity.
4. Air intake factor.
5. External load.
6. Landing gear.
7. Angle of aileron.

The size of the tail fin and, thus, also the level of the yaw resistance of FPL 37 are determined so that the actual requirements on the specifications for flight characteristics of military aircrafts shall be fulfilled. The destabilizing factors which must be controlled while retaining the standards of yaw resistance are:

- o an external load, mounted on the fuselage;
- o effects of interference between wing and tail fin, aileron and tail fin as well as flap and tail fin; and
- o high air intake factors (in analogy with the case of the pitching moment).

The aircraft must also be resistant to yawing up to the widest angles of attack occuring. Other requirements dimensioning the yaw resistance of an aircraft are:

- o acceptable yaw resistance at high supersonic speed;
- o a margin for effects on the yaw resistance at trans-sonic speed; and
- o acceptable maximum oblique air flow when banking within the entire range of speed.

It is therefore difficult to determine the final dimensioning value during the design stage. Series of alterations of the tail fin design of well known aircrafts illustrate that mistakes occur easily. Experience shows that, in general, a $C_{n\beta}$ of the magnitude 0.10 - 0.15 for the basic aircraft is a suitable value. This is what approximately distinguishes the 37 configuration.

An additional demand on FPL 37 (which is able to fly at very low speed) is that it must master the wide angles of oblique airflow (up to 20°) which can occur in combination with wide angles of attack. Among the three principal methods used for improving the efficiency of the tail fin, i.e.:

- o an increase in the component force contribution of the tail fin; /72
- o an increase in the moment of the tail fin; and
- o a utilization in the most favorable manner of the interference effect,

the last possibility has been selected for FPL 37 especially in order to limit the volume of the tail fin and, thus, reduce its weight and drag.

This has resulted in a relatively tall tail fin with a moderate aspect ratio and a moderate sweep-back of its leading edge. Due to the fact that the vortex system of the canard is forced by that of the wing to pass the tail fin at a low level (cf. above), a favorable yaw resistance is obtained

at wide angles of attack as well. The importance of the interference is shown, among others, by the fact that moving the tail fin rearward certainly provided more leverage but gave also rise to a more elevated passage of the canard vortices, i.e., to a collapse of the yaw resistance at wide angles of attack. The present position and shape of the tail fin has resulted in the most satisfactory compromise in this respect.

As far as the training version of FPL 37 is concerned, it became necessary to increase the efficiency of the tail fin following the testing. This was accomplished in part by making the tail fin taller, in part by improving the characteristics of the component force of the tail fin at wide angles of an oblique air flow by introducing a sawtooth on the leading edge of the tail fin as well.

The reason for the improvement of the yaw resistance which was necessary for the training version was the unfavorable position of the point of gravity in combination with the increase in the destabilizing contribution from the fuselage and the addition of a "DK" hood. The effects were especially noticeable since this aircraft always flies with an extra fuel tank, mounted centrally and externally.

The previously mentioned effects of the interference from the canard as well as the asymmetric properties at wide angles of attack are especially noticeable in respect to the yaw resistance (due to the counteracting contributions from the fuselage and the tail fin).

The yaw resistance at low speed of FPL 37, expressed as $C_{n\beta}$, is illustrated in Fig. 88. This figure shows also how the yawing moment, C_n, varies in relation to the angle, β, of an oblique air flow at some different angles of attack.

Contrary to what has been stated concerning the derivative of the component force in Fig. 86, the derivative of the yaw resistance is strongly reduced in relation to an increasing angle of attack in order to change sign and become negative at ca. 27°. In part, the yaw instability depends on the fact that the tail fin is "in the shadow" of the fuselage, the wing and the canard, in part on the fact that there is interference from the vortices

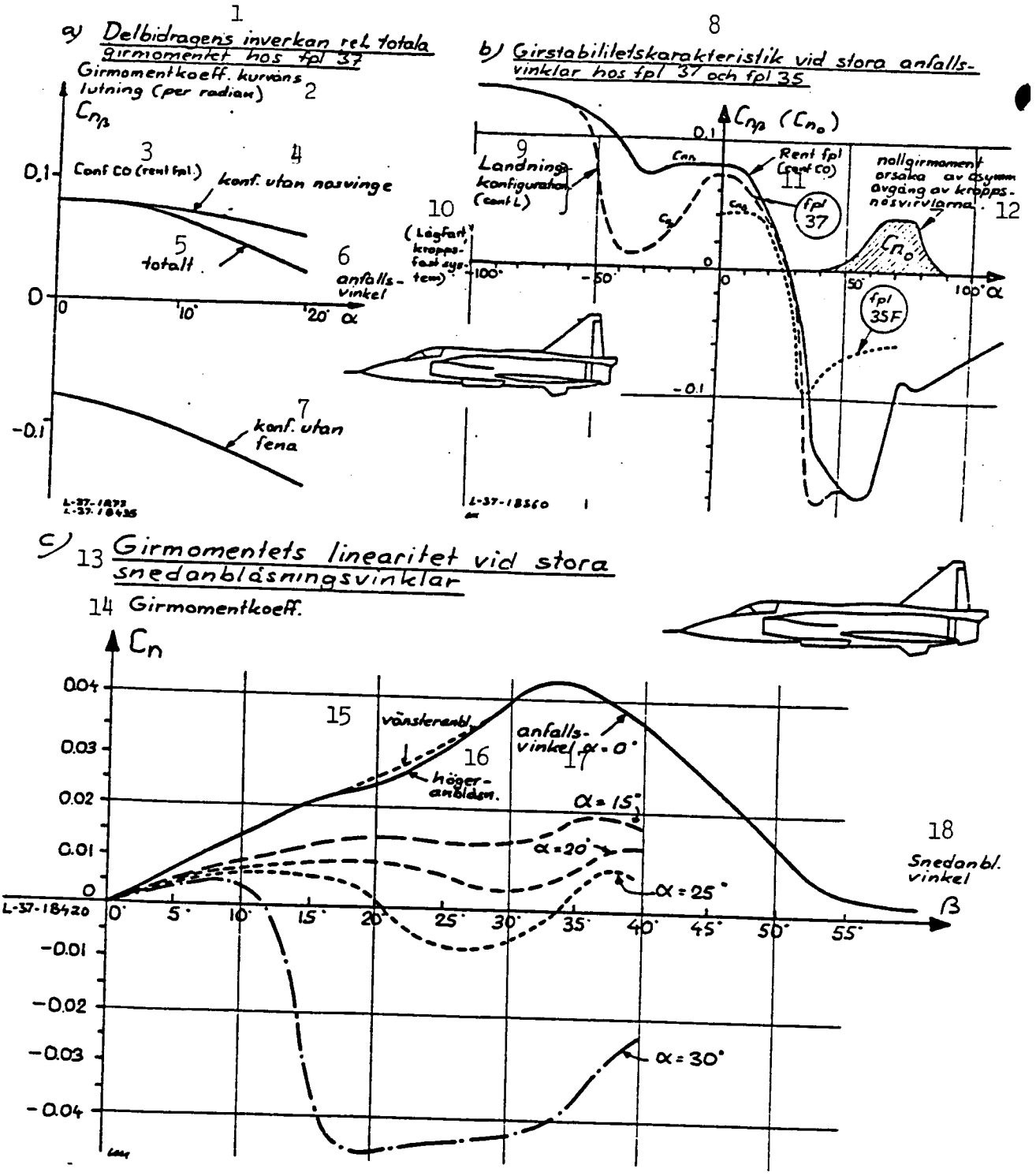

/73

Fig. 88. Key: 1. a) Effect of the joint contributions on the total yawing moment of FPL 37.
2. Gradient (per radian) of the graph illustrating the coefficient of the yawing moment.
3. Conf. CO (aircraft without external load)
4. Configuration without a canard.

[cont. p. 105]

Key to Fig. 88, cont.:

5. In total.
6. Angle of attack.
7. Configuration without a tail fin.
8. b) Characteristics of yaw resistance at wide angles of attack in respect to FPL 37 and FPL 35.
9. Landing configuration (conf. L).
10. (Low speed, fuselage related system)
11. Aircraft without external load (conf. CO).
12. Zero yawing moment caused by asymmetric detachment of the canard vortices.
13. c) The linearity of the yawing moment at wide angles of oblique air flow.
14. Coefficient of yawing moment.
15. Air flow approaching from the left.
16. Air flow approaching from the right.
17. Angle of attack, $\alpha = 0°$.
18. Angle of oblique air flow, β.

---

of the canard on the tail fin (the windward vortex "changes side"). At narrow and moderate angles of attack the vortices of the canard are kept down by those of the wing. When the flow across the outer portion of the wing starts to collapse at angles of attack above 25°, the "down-forcing" effect is reduced which, in analogy with the principle shown in Fig. 77, results in a rapid deterioration of the yaw resistance. The vortices generated by the bow of the fuselage are taken care of by the canard and this effect cannot be clearly distinguished in the case of FPL 37. The contribution of the interference between the canard and the tail fin is, therefore, the actually dominating contribution to this rapid deterioration of the stability.

The effect of a deflection of the flap of the canard can also be seen in Fig. 88a. Due to the fact that the total lift of the canard increases, the force exerted by the vortices of the canard increases at the same time as their vertical and longitudinal position at the trailing edge of the canard is altered. At narrow angles of attack the vortices of the canard are powerful in relation to those of the wing. The "down-forcing" effect of the main wing will be less prominent and alters, consequently, the yaw resistance only to a minor extent in respect to an aircraft without an external load (the reduction shown is due mainly to the landing gear). At an increasing

angle of attack the difference in relative force between the vortices generated by the canard and those of the wing becomes less marked. The canard vortices, - the definitely stronger ones, - and their somewhat depressed position cause the level of yaw resistance to increase in the case of an aircraft without the flap of the canard deflected. The final break-down of the yaw resistance occurs more suddenly during the landing configuration due to the fact that the canard, then more heavily loaded, gives up at a somewhat lower angle of attack and loses a larger portion of its lifting power. /74

The "shadow" effect, mentioned above, is also evident from Fig. 88a, since an aircraft without external load has a better yaw resistance at negative angles of attack than at positive ones. The large difference between an aircraft without an external load and the landing configuration at wide, negative angles of attack may depend on interference from the canard, although this has not been fully elucidated. It is, however, of no practical importance since there is no "stationary" flying within that area.

In addition to its large tail fin, FPL 37 is equipped with a small fin (a "belly-fin") below the tail of the fuselage. Its effect toward improving the yaw resistance is, however, small (on the same order of magnitude as the difference between an aircraft without external load and a landing configuration at narrow angles of attack). The advantage of the "belly-fin" is that "shading" can be avoided at wide angles of attack when the tail fin loses its efficiency.

4.10 Effect of External Load

An external load, mounted on the fuselage of FPL 37 has a generally detrimental effect on the yaw resistance. In the worst case one half of the yaw resistance at narrow angles of attack disappears. This depends not only on the position of the external load in front of the point of gravity and on the diameter of the frontal portion of the load, but is also a consequence of the fact that the belly fin is shaded. This is valid especially in respect to equipment alternatives with a centrally mounted tank to be jettisoned.

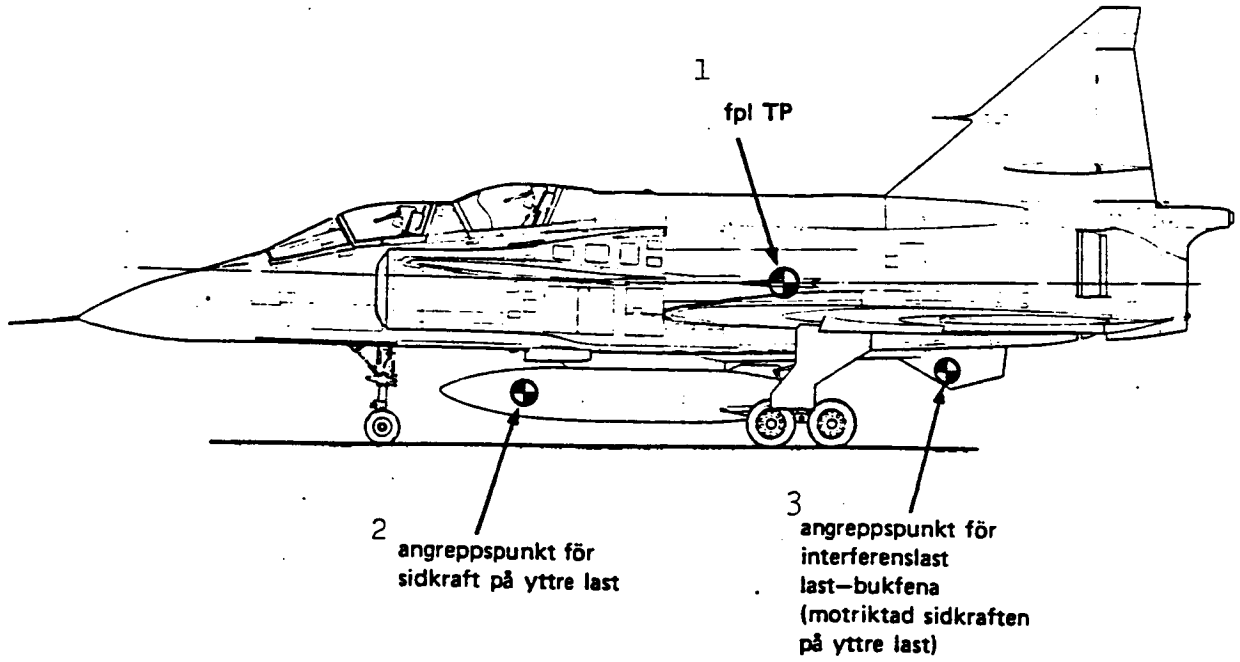

Fig. 89. Key: 1. Point of gravity of the aircraft.
2. Point of attack of the component force on the external load.
3. Point of attack of the load interfering between the external load and the belly fin (opposite to the component force on the external load).

In that case the entire contribution of the belly fin to the yaw resistance disappears in the form of interference and, thus, the belly fin is totally without any function. This depends in part on the mounting of the belly fin in the "wake" of the extra tank, in part on vortices detached from this tank at large angles of attack in an obliquely approaching air flow. The /75
local increase in oblique air flow at the site of the extra equipment, induced by the fuselage, is another reason why the external load, mounted on the fuselage, affects the yaw resistance so powerfully. It is also one of the reasons why equipment, mounted below the wing (i.e., placed behind the point of gravity of the aircraft) does not result in any major compensation for the reduction in yaw resistance, caused by the equipment mounted on the fuselage. The worst case of yaw resistance in respect to all alternatives of AJ-37 is the one where the extra tank is attached to position C 7 and the combat armament to the S 7 girders.

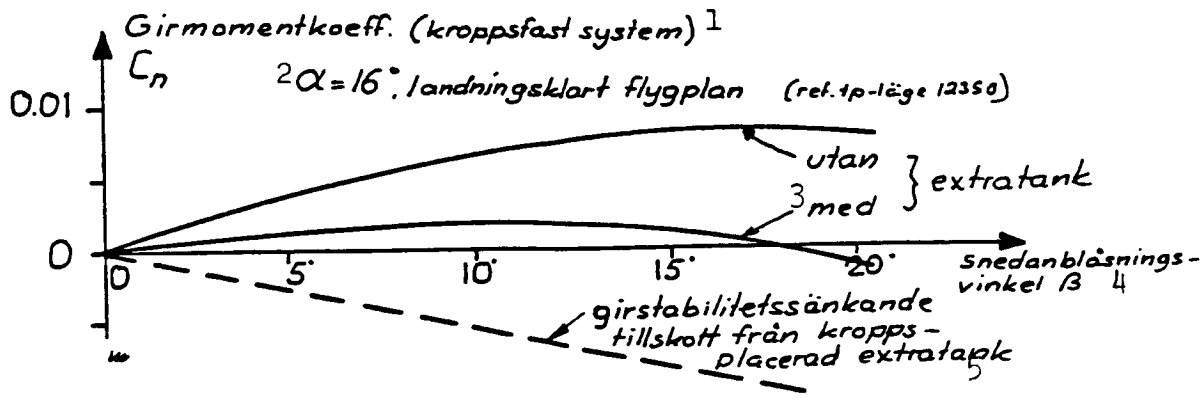

Fig. 90. Effect of the extra fuel tank on the yaw resistance of FPL 37.
Key: 1. Coefficient of yawing moment (fuselage-related system).
2. $\alpha = 16°$, aircraft prepared to land (position of reference point 12350).
3. Without/with an extra tank.
4. Angle of oblique air flow, β.
5. Contribution lowering the yaw resistance due to the position of the extra fuel tank on the fuselage.

4.11 Yaw Resistance of FPL 37 in Comparison with that of Other Aircrafts

How does the yaw resistance of FPL 37 compare to that of other, similar aircrafts? A comparison of the fuselage-related derivative of yaw resistance in relation to the angle of attack in the case of FPL 37 and some other aircrafts is illustrated in Fig. 91. Since different magnitudes of reference are used, the yaw resistance at a zero angle of attack has been standardized to the same value.

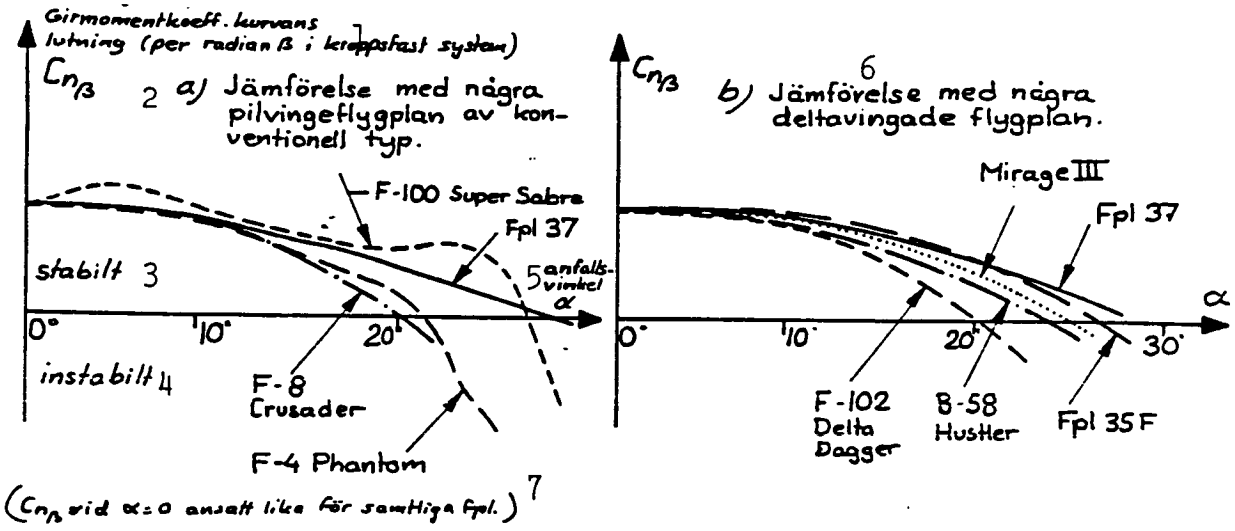

Fig. 91. Yaw resistance of FPL 37 in comparison with that of other aircrafts.
Key: see p. 109.

Key to Fig. 91:

1. Gradient (per radian β in a fuselage-related system) of the graph illustrating the coefficient of the yawing moment.
2. a) Comparison with some aircrafts with swept-back wings of conventional type.
3. Stable.
4. Unstable.
5. Angle of attack.
6. b) Comparison with some delta-winged aircrafts.

Evidently FPL retains its yaw resistance up to wider angles of attack than other types of aircrafts belonging to the same class. The fact that FPL 37 is so superior to B 58 and F 102 depends on that its air intakes and the root of its wing affect the vortices generated by the fuselage and prevent them from passing the tail fin at a high level. /76

4.12 Rudder Effect

The aerodynamic properties of FPL 37 assure that a satisfactory effect of the rudder is retained up to wide angles of attack. Fig. 92 illustrates the effect of the rudder at low speed.

In order to nullify the lateral force resulting from a 20° oblique air flow, a 10° deflection of the rudder (at 16° angle of attack and low speed) is necessary. In reality, this deflection cannot be achieved because a lateral force is generated by deflecting the aileron (see below). The large coefficient of the lateral force of FPL 37 in combination with a satisfactory rudder effect makes it feasible to fly at an angle of side slip already at relatively moderate speeds. This is occasionally applied during demonstrations.

4.13 Yaw Damping, Dynamic Yaw Resistance

The dynamic yaw resistance of an aircraft corresponds in principle to the dynamic pitch resistance although instead the rotation around the vertical axis of the aircraft is considered. Like in the case when attenuating the pitching, the characteristics of the dynamic yaw resistance can also be distinguished into two joint contributions: /77

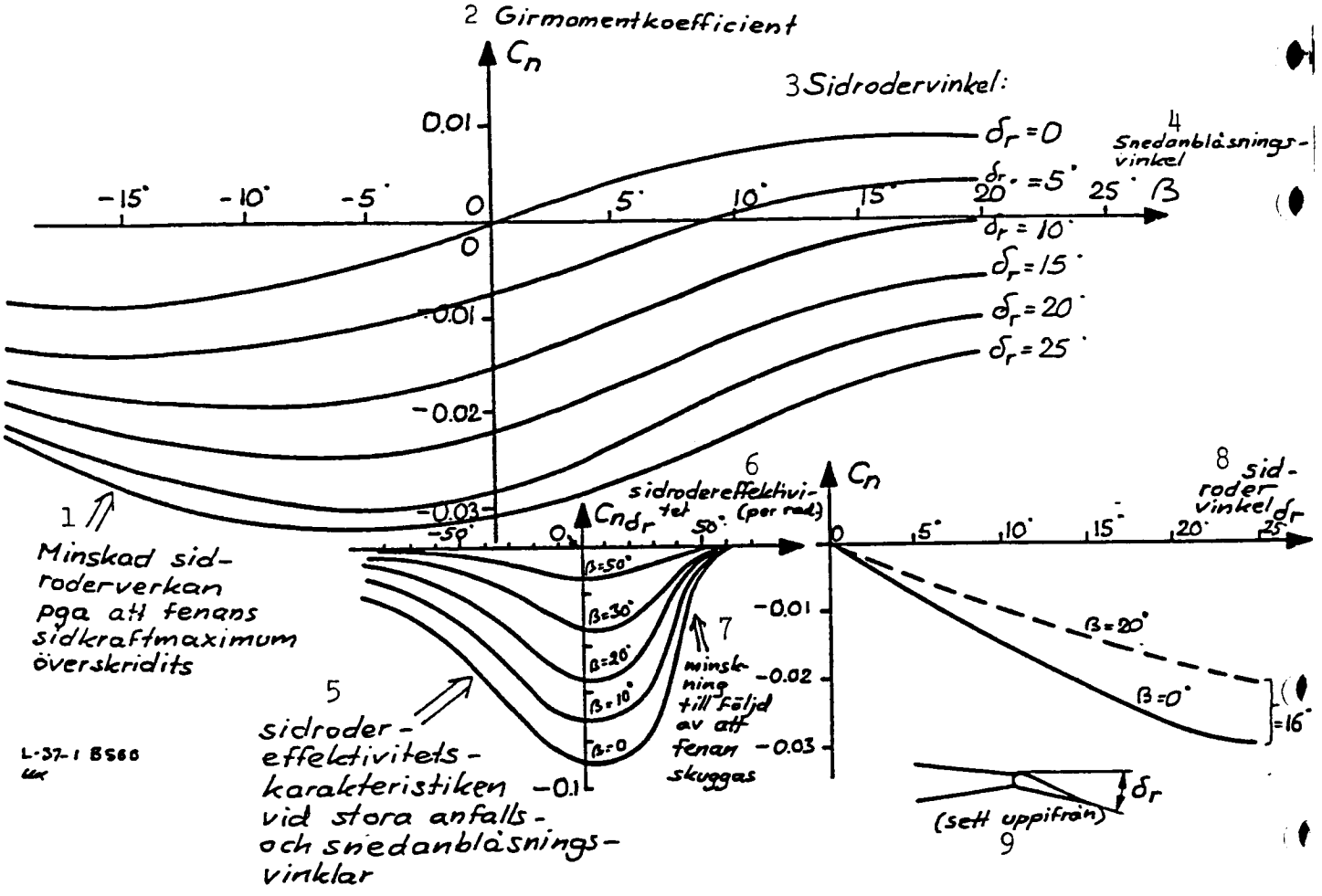

Fig. 92. Key: 1. Reduced effect of the rudder when the maximum lateral force of the rudder is exceeded.
2. Coefficient of the yawing moment.
3. Rudder angle.
4. Angle of ovlique air flow.
5. The efficiency characteristic of the rudder at wide angles of oblique air flow and attack.
6. Efficiency of the rudder (per radian).
7. Reduction due to shading of the tail fin.
8. Angle of rudder, δ_r.
9. Seen from above.

- C_{n_r} (actual yaw damping); and
- $C_{n_{\dot{\beta}}}$ (contribution due to delaying effects during rapidly altered oblique air flow).

Conventions regarding symbols require that the dynamic yaw resistance shall be written:

$$C_{n_r} - C_{n_{\dot{\beta}}}$$

When viewed from the side, an aircraft is dominated by the rudder placed far behind the point of gravity. Due to this long lever arm, the rudder delivers a correspondingly major contribution to C_{n_r}. The contribution from the bow of the fuselage acts jointly with that of the rudder in contrast to what is the case in respect to C_{n_β}, where the contributions of the fuselage and the rudder counteract each other.

The effects of time delay play a considerably lesser role in the direction of yawing than that of pitching. In the case of FPL 37, $C_{n_{\dot\beta}}$ is only 6 - 7% of the C_{n_r}.

The characteristics of yaw damping at low speed of FPL 37 is shown in Fig. 93.

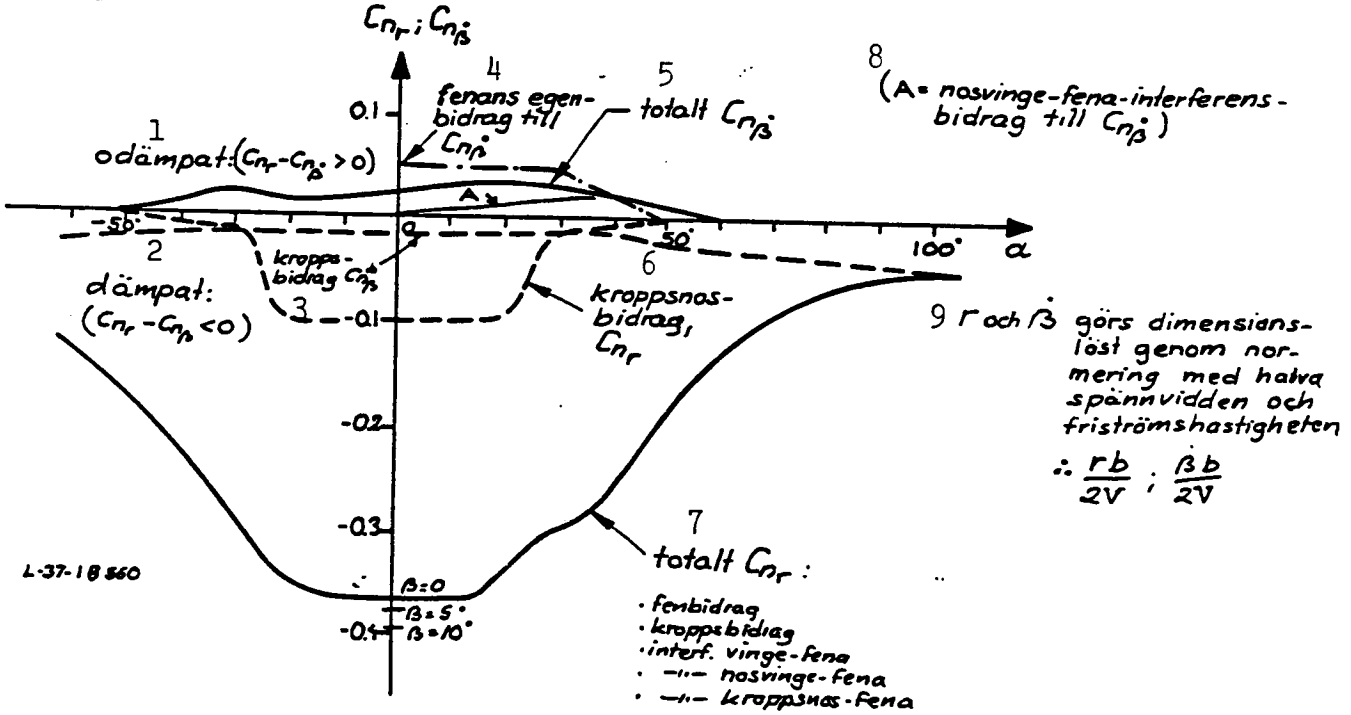

Fig. 93. Yaw damping; FPL 37.

Key: 1. Not damped:...
2. Damped:...
3. Contribution from the fuselage.
4. Contribution of the tail fin itself.
5. Total $C_{n_{\dot\beta}}$.
6. Contribution from the bow of the fuselage.
7. Total C_{n_r}: contributions from:
   - o the tail fin
   - o the fuselage
   - o interference wing/tail fin
   - o " canard/tail fin
   - o " bow/tail fin.
8. A = contribution of interference between canard and tail fin to the $C_{n_{\dot\beta}}$.
9. r and β are made non-dimensional by standardizing them by half of the wing span and the speed of free flow: thus, $\frac{rb}{2V}$ and $\frac{\beta b}{2V}$.

The aerodynamic yaw damping is in the case of FPL 35 ca. 25% lower than that of FPL 37, because when seen from the side FPL 35 has a more slender bow and a proportionally lesser surface of its tail fin. FPL 32 has approximately the same yaw damping properties as FPL 35 (-0.25 in respect to FPL 32 against -0.27 in respect to FPL 35 when expressed as $C_{n_r} - C_{n_{\dot{\beta}}}$). Conventional delta-winged aircrafts, e.g., the Mirage, belong also to this class.

5. ROLLING MOMENT, ROLL RESISTANCE /78

5.1 General

Roll resistance is of interest in respect to the flight characteristics of an aircraft, especially concerning its relation to yaw resistance ("dutch roll" characteristics).[1] It is desirable that the aircraft shall develop increased lift of the windward wing in comparison with the leeward one during an oblique air flow. This corresponds to a negative gradient of the $C_l(\beta)$ graph. CF. Figs. 74 and 75. In addition, the roll resistance and the yaw resistance should be favorably related to each other in order to produce satisfactory characteristics in the case of a dutch roll. A too great resistance to rolling in combination with moderate or unsatisfactory yaw resistance should therefore be avoided.

The main contribution to the roll resistance originates from the wing and depends, among others, on the planar shape of the wing and its vertical position in relation to the fuselage.

5.2 Effect of Sweep-back Angle

In the case of an aircraft with swept-back wings, the windward wing has a lesser sweep-back angle in relation to an oblique air flow and is, thus, less effective when producing lift. The opposite condition prevails in respect to the other wing. The rolling moment induced by the wings is therefore strongly dependent on the angle of attack (Fig. 94).

---

[1] See also: G. Strang: "Aircraft 37, aviation mechanics and flight characteristics."

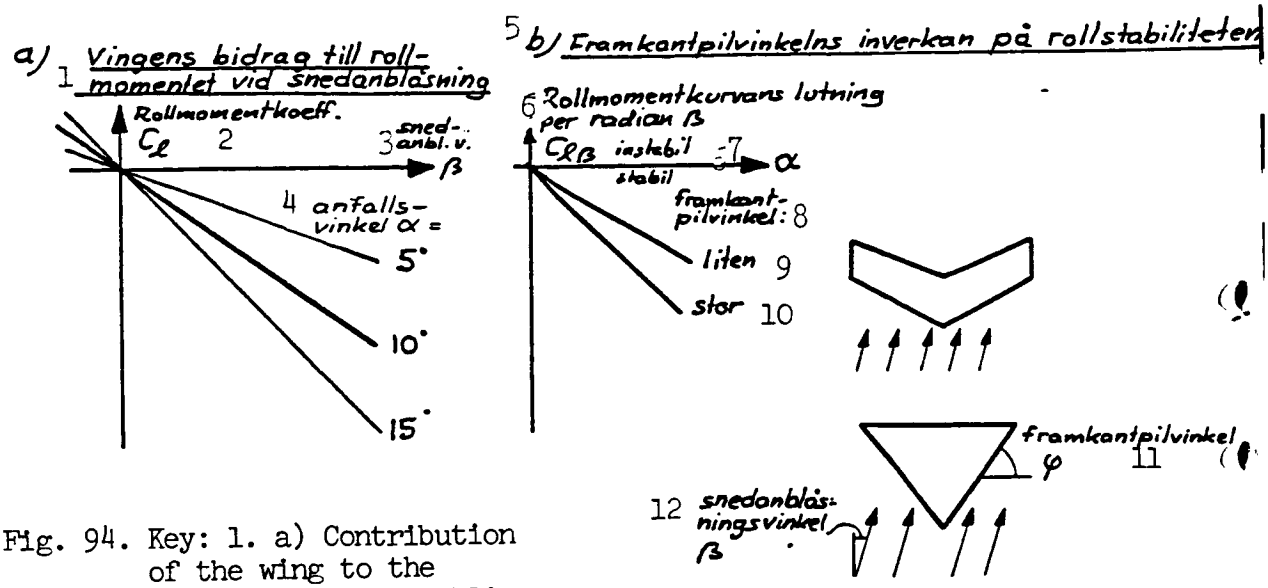

Fig. 94. Key: 1. a) Contribution of the wing to the rolling moment at oblique air flow.
2. Coefficient of the rolling moment.
3. Angle of oblique air flow.
4. Angle of attack.
6. b) Effect of the sweep-back of the leading edge on the roll resistance.
7. Gradient per radian β og the graph of the rolling moment.
7. Unstable/stable
8. Angle of sweep-back.
9. Narrow.
10. Wide.
11. = 8
12. Angle of oblique air flow.

The larger the sweep-back angle, the more pronounced is the contribution of the wing to the roll resistance as long as the flow is adhering. The difference between the effective aspect ratios of the windward and the leeward wings in an oblique air flow increases with increased sweep-back. In addition there is also an increased effect due to the "shading" caused by the fuselage, especially when the wing span is limited; see below. This is the reason why delta-winged aircrafts as such are very resistant to spinning so that other tricks must be resorted to in order to decrease the roll resistance. This is contrary to the case of aircrafts, e.g., like the HFB Hansa with its wings swept forward for which measures were taken for increasing the roll resistance among others by providing the wings with a positive V-shape.

5.3 Effect of Fuselage/Wing Interference

/79

A certain stabilizing effect due to the "shading" of the leeward wing occurs already in the case of a straight-winged aircraft at wide angles of

an oblique air flow. During normal flight, this contribution is of minor importance. However, the fuselage exerts a generally weakening effect on the contribution of the sweep-back angle to the roll resistance due to the fact that the fuselage tends to straighten out the air flow, i.e., to reduce the angle of the oblique flow above the wing.

The most important effect of the fuselage is, however, seen in respect to an upper or a lower position of the wings. The effect is evident from Fig. 95.

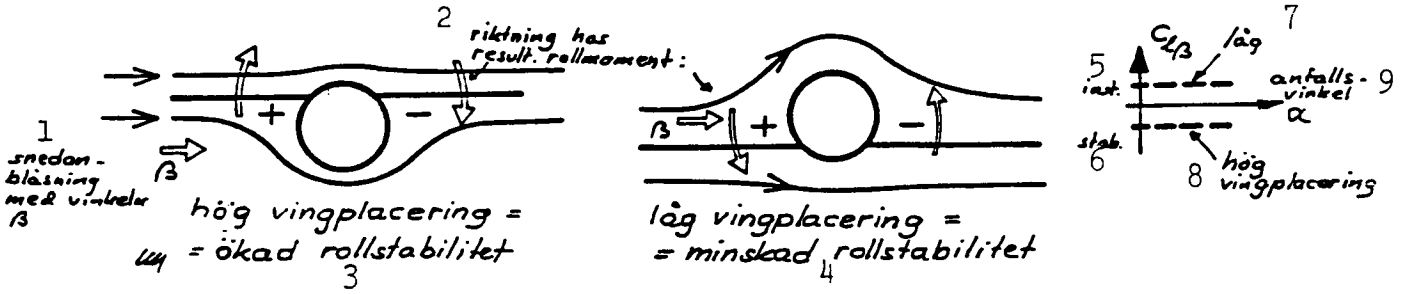

Fig. 95. Effect on the roll resistance of an upper or a lower position of the wings.
Key: 1. Oblique air flow at an angle of β.
2. Direction of rolling moment resulting.
3. Wing in an upper position = increased roll resistance.
4. Wing in a lower position = decreased roll resistance.
5. Stable.
6. Unstable.
7. Low ...
8. high position of the wings.
9. Angle of attack.

The resulting disturbance of the pressure, caused by the fuselage in an oblique air flow, furnishes a roll-destabilizing moment when the wings are placed low down, while wings placed at an elevated position provide a roll-stabilizing moment. A corresponding difference can also be noticed when the stabilizer of conventional aircrafts is placed in a lower or an upper position, respectively.

The contribution of the fuselage/wing interference to the rolling moment increases at increasing angles of an oblique air flow but is, on the other hand, relatively independent of the angles of attack at normal angles.

5.4 Effect of the V-positioning of the Wing

A similar effect like that of an upper or a lower position of the wings can be achieved by giving the wings a positive or a negative V-position (Fig. 96).

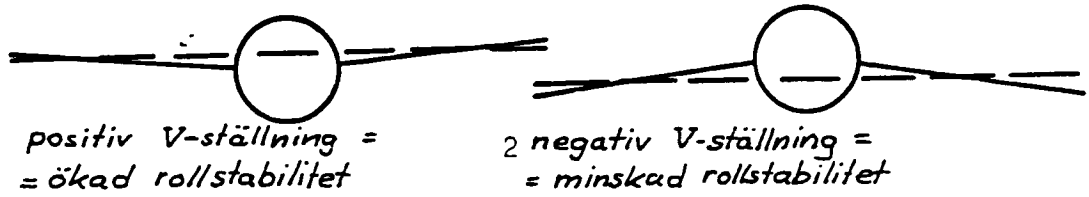

Fig. 96. Effect on the roll resistance of the V-positioning of the wings.
Key: 1. Positive V-position = increased roll resistance.
2. Negative V-position = decreased roll resistance.

The filed of air flow resulting produces increased lift on the windward wing at a positive V-position just like an upper position of the wings and, thus, it delivers a contribution to the roll resistance, the character of which reminds of the contribution due to the upper position of the wings. A negative V-position constitutes a frequently applied method toward compensation for the large inherent roll resistance of a strongly swept-back wing or a delta wing. /80

5.5 Contribution of the Wing to the Roll Resistance at Wide Angles of Attack

As long as the air flow adheres the roll resistance increases in a largely linear manner in relation to the angles of attack (just like the lift does). However, as soon as angles of attack near the separation limit are approached, this trend is broken. In the case of a swept-back- or a delta-winged aircraft, the windward wing has a tendency to separate the air flow before the leeward wing does (cf. the variation in pitch-up limit in relation to the sweep-back angle). This results in a strong disturbance of the rolling moment. The course of the characteristics of the angle of attack of the roll resistance calls to mind an inverted characteristic of lift. Local "kinks" in the characteristic of the pitching moment (cf. Fig. 40) can also appear in the form of a disturbance of the rolling moment and are frequently considerably more noticeable as a derangement of

the rolling moment rather than the pitching moment.

Fig 97

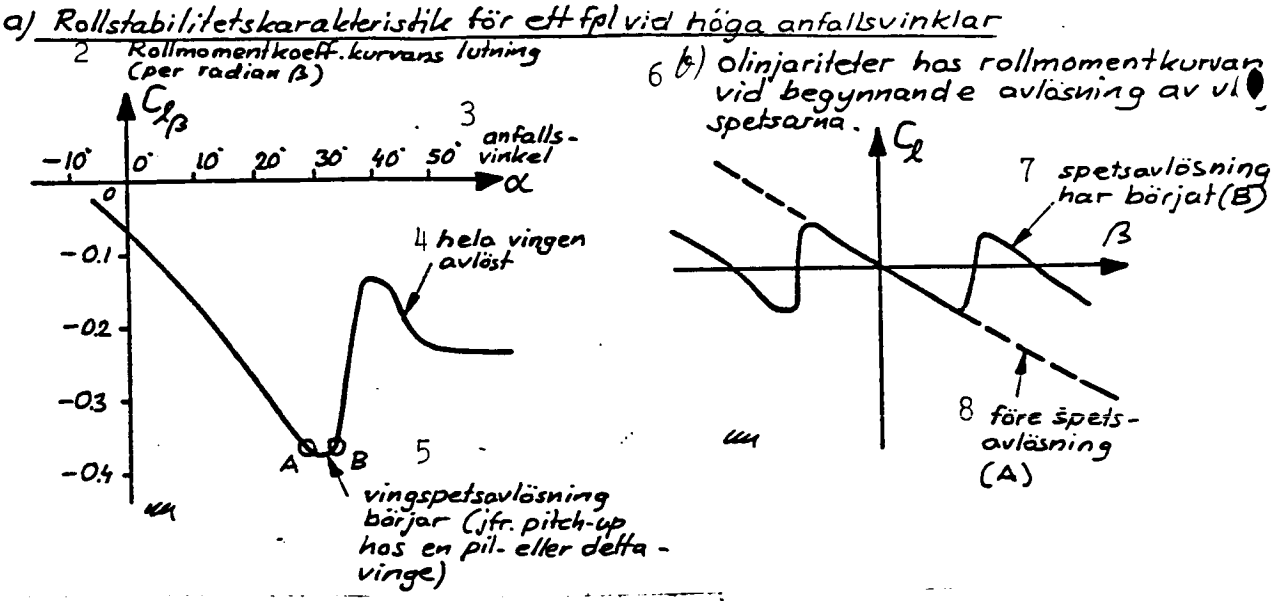

Fig. 97. Key: 1. a) Characteristic of the roll resistance of an aircraft at wide angles of attack.
2. Gradient (per radian β) of the graph illustrating the coefficient of the rolling moment.
3. Angle of attack.
4. The entire wing detached.
5. Separation starts at the wing tip (cf. pitch-up of a swept-back wing or a delta wing).
6. Non-linearity of the graph of the rolling moment at beginning separation of the wing tips.
7. Tip-separation has started (B).
8. Before tip-separation (A).

The variation of the rolling moment in relation to the angle of attack in an oblique air flow can then appear like in Fig. 97 b (cf. FPL 35 at a mach .. number of 0.5 and ca. 15° angle of attack). This is an additional reason for trying to attain a linear graph of the pitching moment, free of kinks, which is preferable both when an external load is present or not present below the wings.

5.6 Effect of Ground Interference

The contribution to the roll resistance from the wings of a delta-winged aircraft is reinforced when close to the ground level. This is noticeable

in respect to FPL 35 as well as FPL 37 and can affect the characteristics of a dutch roll of the aircrafts since the yaw resistance is largely unaffected by the presence of the ground nearby (Fig. 98). When increased due to the ground interference the roll resistance is associated with an increase in longitudinal stability as well as an increase in lift (cf. section 2.7).

/81

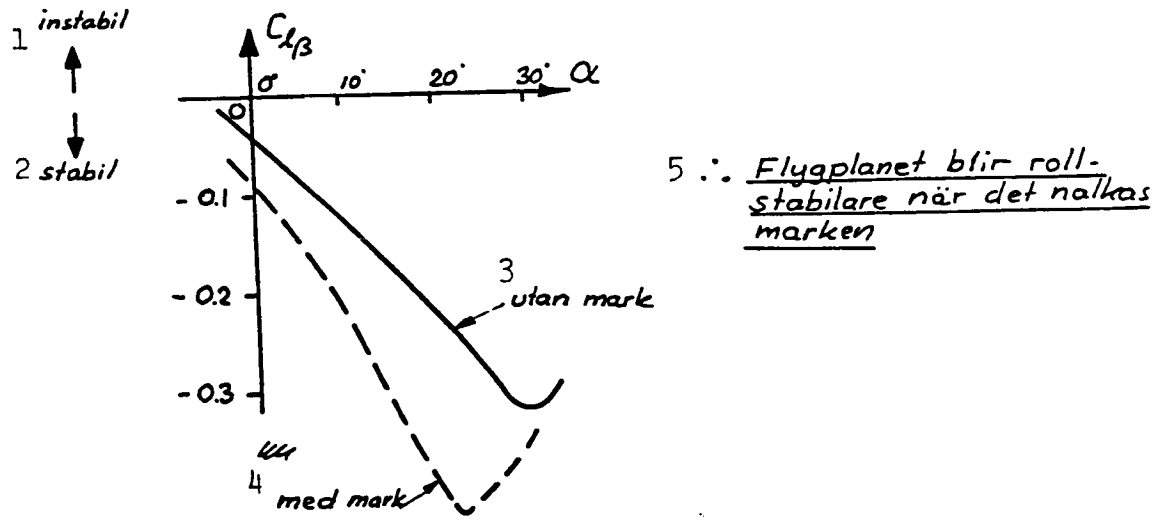

Fig. 97. Effect of ground interference on the roll resistance.
Key: 1. Stable.
2. Unstable.
3. Without presence of ground nearby.
4. In presence of ground nearby.
5. Thus, an aircraft is more roll resistant when approaching the ground.

5.7 Contribution of the Tail Fin

An oblique air flow approaching the tail fin furnishes a directly destabilizing effect on the rolling moment. Unfortunately -, or, perhaps, fortunately from the point of view of a dutch roll,- a large portion of the contribution causing a tail fin/wing interference disappears in the case of FPL 35 and FPL 37. The low pressure area on the leeward side of the tail fin will spread out over the wing and results there in a moment reversely directed to the one which can be directly referred to the suction force of the tail fin. Which of these moments will "dominate" depends on the configuration (i.e., the size of the tail fin and its longitudinal position in relation to the wing). As far as FPL 35 and FPL 37 are concerned, the

interfering moment reduces to a considerable extent the total rolling moment because of the large wing surface, which is affected by this interference. The principle is illustrated in Fig. 99.

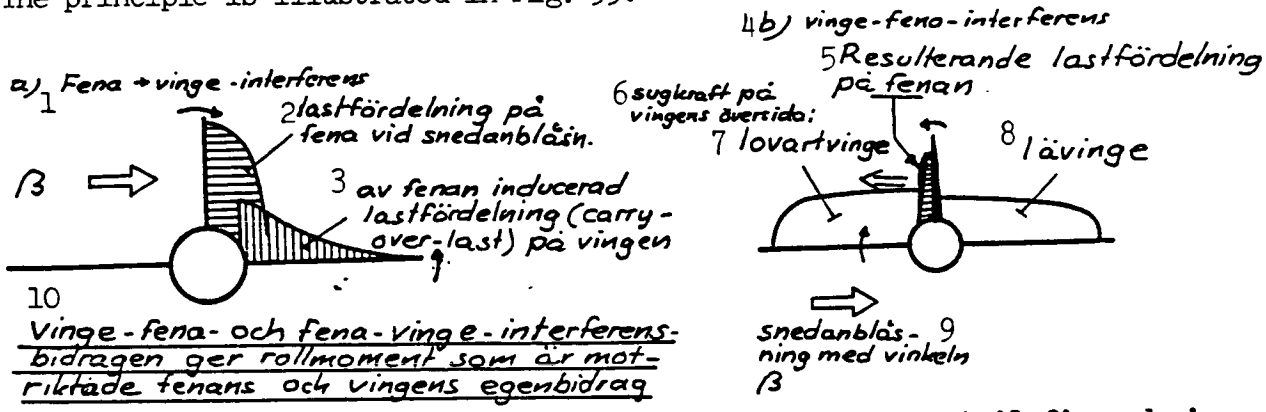

Fig. 99. Interference between wing and tail fin and between tail fin and wing.
Key: 1. a) Tail fin/wing interference.
2. Load distribution on the tail fin during oblique air flow.
3. Load distribution (carry-over load) on the wing, induced by the tail fin.
4. b) Wing/tail fin interference.
5. Load distribution resulting on the tail fin.
6. Suction force on the upper side of the wing.
7. Windward wing.
8. Leeward wing.
9. Oblique air flow at an angle of β.

/82

There is, in addition, a contribution from the wing and the tail fin which depends on the angle of attack due to the fact that the distribution of the load above the wing differs between the leeward and the windward sides in an oblique airflow. The vortices generated by the fuselage affect, similarly, the rolling moment via the tail fin at large angles of attack and an oblique air flow. Usually the last-mentioned contributions produce a destabilizing effect on the rolling moment. The entire contribution from the tail fin to the rolling moment is small in comparison with that delivered by the wing.

The total contribution to the roll resistance, delivered by the tail fin of FPL 37 is evident from Fig. 100, both in respect to a fuselage-related system and a wind-related one.

It is evident from the figure that the canard, too, has a certain effect on the roll resistance.

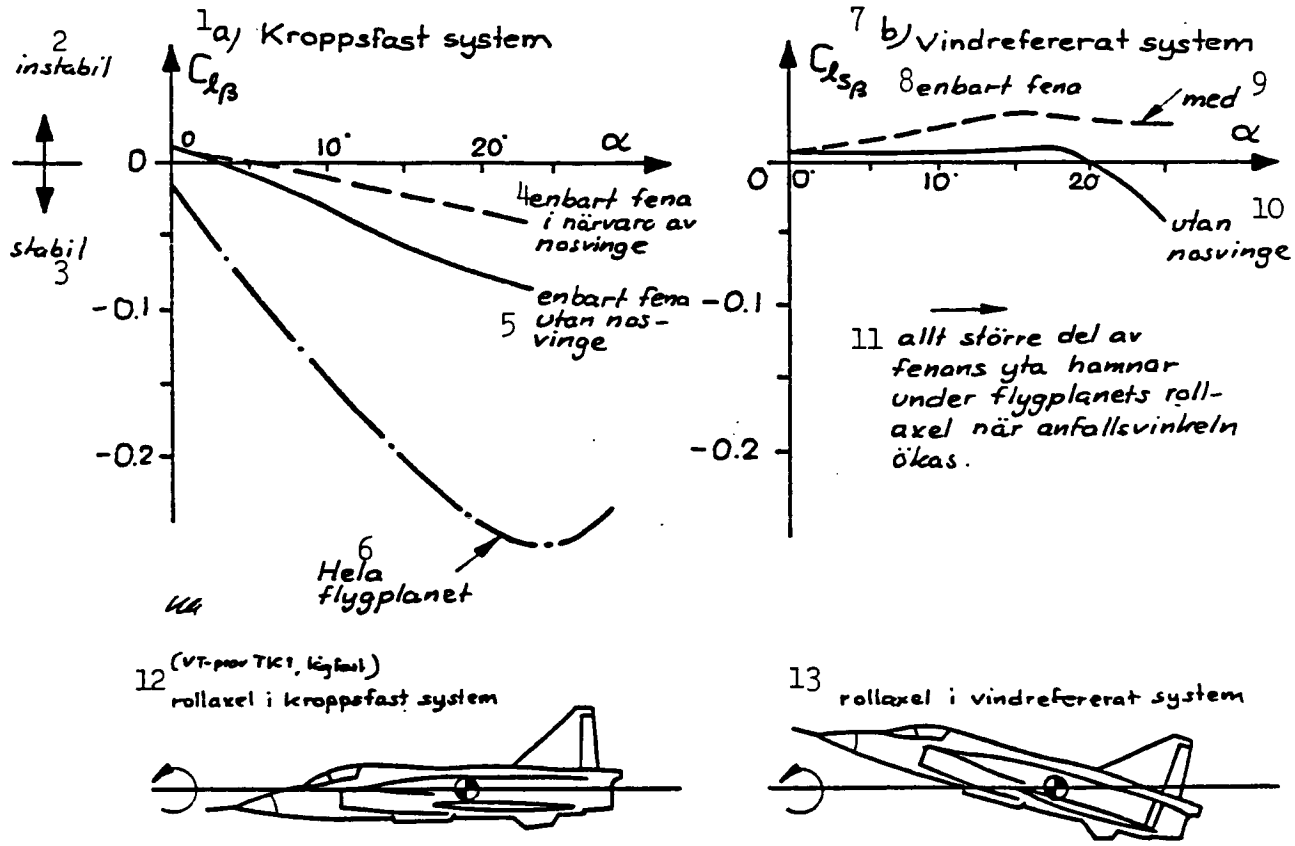

Fig. 100. Contribution of the tail fin to the roll resistance at low speed; FPL 37.

Key: 1. a) Fuselage-related system.
2. Unstable.
3. Stable.
4. Tail fin alone in the presence of a canard.
5. Tail fin alone without a canard present.
6. The entire aircraft.
7. b) Wind-related system.
8. Tail fin alone.....
9. in the presence of a canard.
10. without a canard present.
11. increasingly large portions of the surface of the tail fin fall below the roll axis of the aircraft when the angle of attack widens.
12. (Wind-tunnel test TK 1, low speed). Roll axis of fuselage-related system.
13. Roll axis of wind-related system.

The contribution from the tail fin depends on how the axial system is defined. At wide angles of attack the tail fin will be placed below the roll axis of a wind-related system. The effect of this is illustrated in Fig. 100.

5.8 Contributions of Stabilizer, Canard, Etc., to the Roll Resistance of FPL 37.

/83

There are additional contributions to the roll resistance of the aircraft from other kinds of its horizontal airfoils. Just like an upper position of the wings produces increased roll resistance, a greater roll resistance can be achieved by placing the stabilizer in a raised position (e.g., on a T-tail) in contrast to placing the stabilizer in the conventional low position. Thus, e.g., the negative V-position of the wings of FPL 105 (SK 60) is a consequence of the fact that the combination of wings in an upper position plus a T-tail results in a greater roll resistance than desirable from the point of view of flight characteristics.

The contributions to the roll resistance of the stabilizer and the canard themselves can be derived in the same manner as that of the wing. However, the smaller surface and the shorter extension of the wing span of the canard make these contributions correspondingly smaller than that of the wing. In general, interferences between the wing and the stabilizer, the fuselage and the stabilizer as well as the tail fin and the stabilizer must also be added and complicate the course of event.

As far as FPL 37 is concerned, the interference between the canard and the wing is of interest and of a considerably greater importance than the contribution from the canard itself. Because the "leading edge vortices" of the canard interfere rear-ward with the wing, a distribution of the load above the wing develops, the result of which is a long lever arm and, thus, easily causes extensive rolling moments during changes in the angle of an oblique air flow. Simultaneously the flow type is stable even at relatively wide angles of attack just like we have seen above. Interference from the canard leads, thus, to that:

- o the roll resistance increases strongly in relation to the angle of attack; and that
- o the saturated angle of attack (i.e., the one where the roll resistance is at its maximum) becomes wider (just below 30° in the case of FPL 37).

The maximum value of the roll resistance is therefore very large. If the air circulation around the canard is increased (i.e., its lift is increased), e.g., be deflection of its flap, the increase in roll resistance becomes even further accentuated. Fig. 101 illustrates how the canard and its flap affect the roll resistance of AJ 37 at low speed.

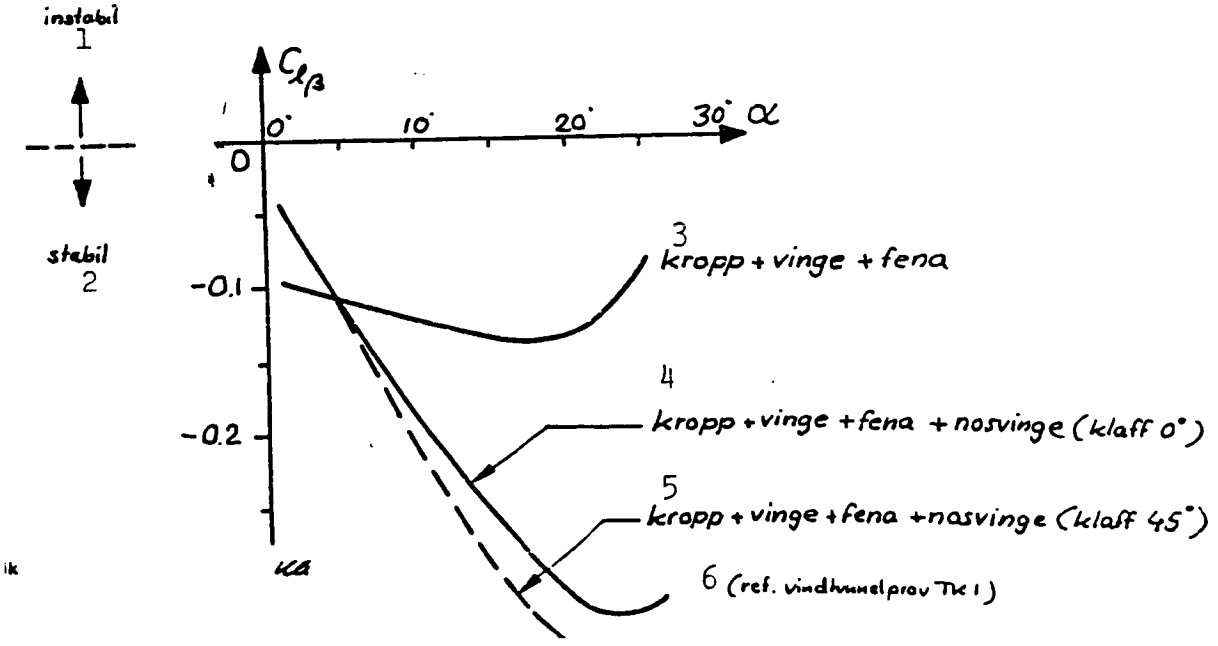

Fig. 101. Effect of the canard on the roll resistance of FPL 37.
Key: 1. Unstable.
2. Stable.
3. Fuselage + wing + tail fin.
4. Fuselage + wing + tail fin + canard (flap at 0°)
5. Fuselage + wing + tial fin + canard (flap at 45°)
6. (ref.: wind tunnel test TK 1).

A review of the different contributions and their relative magnitudes is furnished in Fig. 102. /84

5.9 Comparison Between the Roll Resistance of FPL 37 and That of Other Aircrafts

It should be evident from the discussion above that a rather considerable roll resistance is associated with the design of the canard, i.e., a large negative value of $C_{l\beta}$ exists. In order to "match" this value a satisfactory pitch resistance at large angles of attack is necessary. Among others, we have

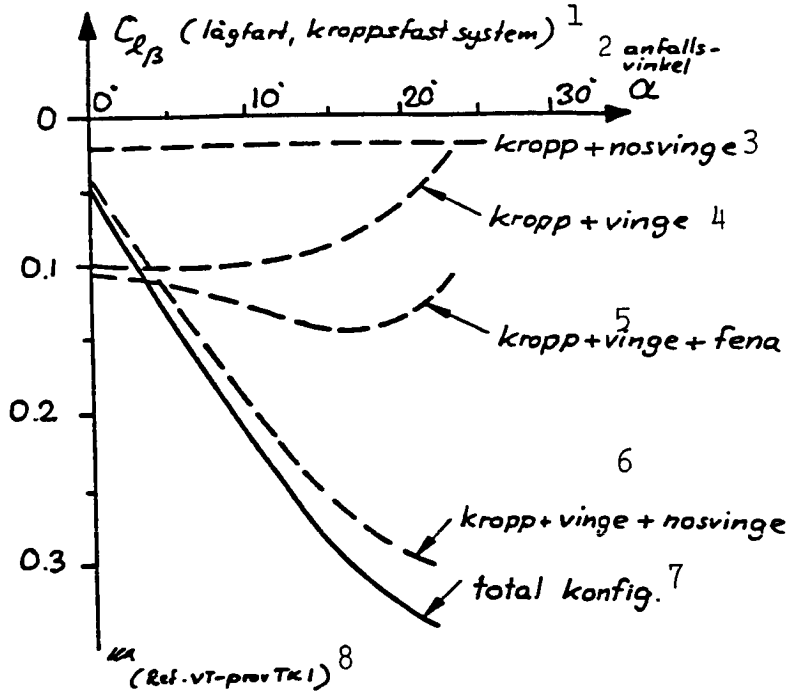

Fig. 102. Roll resistance and its partial contributions; FPL 37.
Key: 1. C_{l_β} (low speed, fuselage related system)
2. Angle of attack.
3. Fuselage + canard.
4. Fuselage + wing.
5. Fuselage + wing + tail fin.
6. Fuselage + wing + canard.
7. Total configuration.
8. (ref: wind tunnel test TK 1).

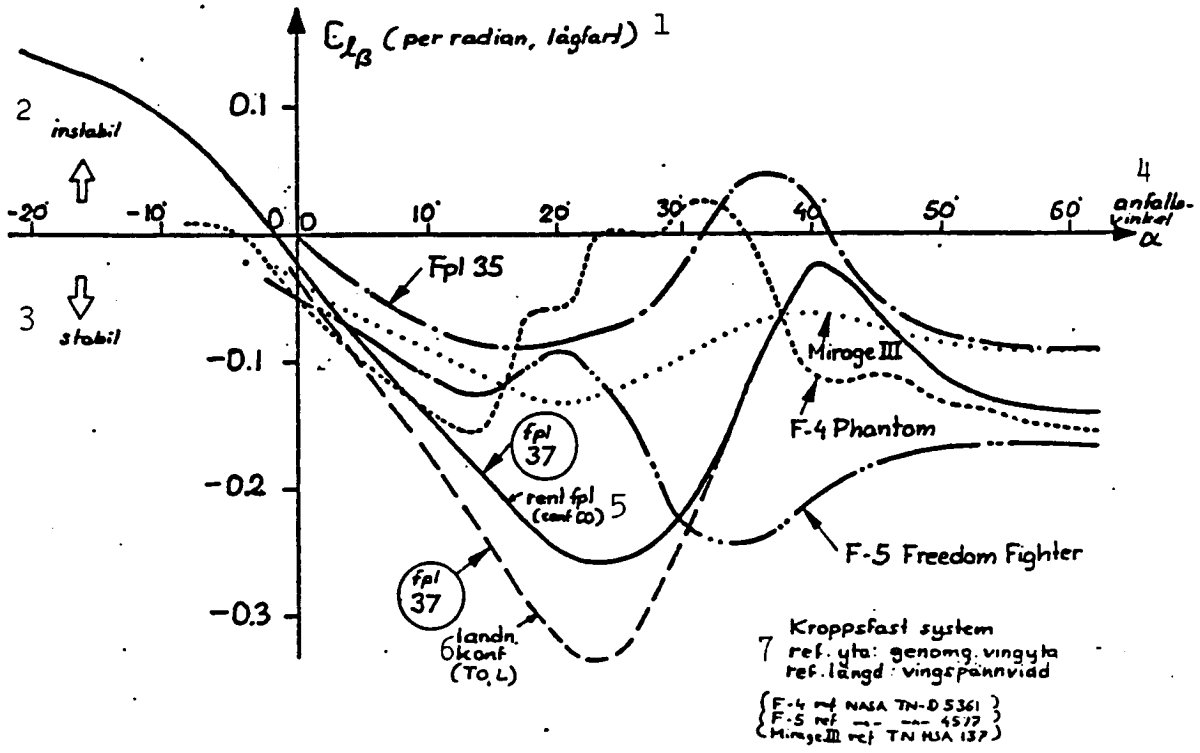

Fig. 103. Characteristics of the roll resistance of FPL 37 in comparison with that of other aircrafts.
Key: 1. C_{l_β} (per radian, low speed)
2. Unstable.
3. Stable.
4. Angle of attack.
5. No external load (conf. CO).
6. Landing config. (conf. TO,L).
7. Fuselage-related system. Ref. surface: total wing syrface. Ref. length: total wing span.

utilized the advantages offered by placing the wing in a low position. It is evident from Fig. 103 what the roll resistance of FPL 37 looks like in comparison with that of other aircrafts with similar performance characteristics.

The linearity of the $C_l(\beta)$ graph (cf. Fig. 83) is more satisfactory in /85
respect to FPL 37 than in the case of both FPL 35 and the F4. The latter aircraft displays in particular unruly rolling moments at angles of attack above 12°. FPL 35 manages without difficulties up to 15° but at low speed FPL 37 behaves satisfactorily at angles of attack as wide as 25°.

5.10 Roll Resistance in Relation to External Load

The most noticeable effect results from an external load mounted on the fuselage, both when it is placed far below the point of gravity of the aircraft and when it acts in the same manner as if the position of the wing was raised in relation to the fuselage. At narrow angles of attack the latter kind of interference contributed by the armament and the wing dominates. However, at wide angles of attack this contributions almost disappear and the destabilizing contribution from the external load itself will determine the magnitude of the additional effect. See Fig. 104.

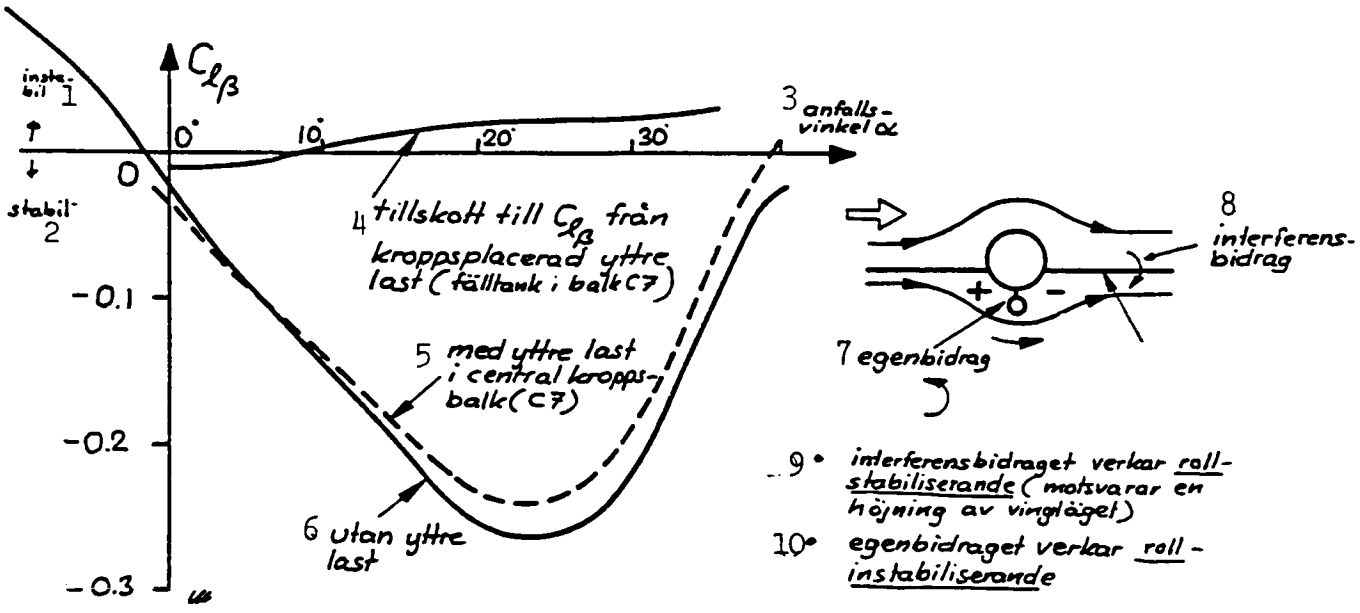

Fig. 104. Effect on the roll stability of FPL 37 caused by an external load mounted on the fuselage.
Key: see p. 124.

Key to Fig. 104:

1. Unstable.
2. Stable.
3. Angle of attack.
4. Contribution to C_{l_β} from an external load mounted on the fuselage (e.g., a tank mounted on girder C 7, and to be jettisoned).
5. Interference of an external load, mounted centrally on girder C 7.
6. Without any external load.
7. Contribution from the load itself.
8. Contribution due to interference.
9. The contribution from the interference is roll-stabilizing (corresponds to an elevation of the wing position).
10. The contribution from the load itself is roll-destabilizing.

An external load placed on the wings produces no apparent contribution when it is symmetrically mounted. An increase in roll resistance, caused by interference of the armament on the wing, can be felt only when such a bulky load as missile Rb 04 is suspended below the wing. Just like the contribution from the wing itself, this contribution due to interference depends on the angle of attack (Fig. 105).

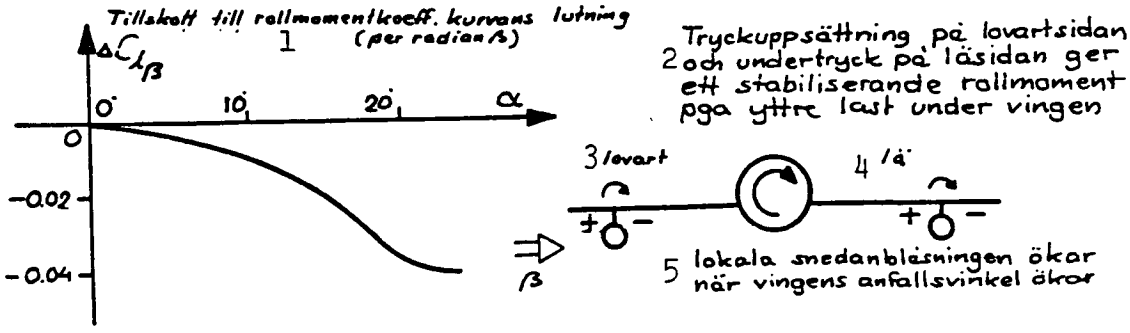

Fig. 105. Effect on the roll resistance of an external load, suspended below the wings.

Key: 1. Contribution to the gradient (per radian β) of the graph illustrating the coefficient of the rolling moment.
2. Pressure increase on the windward side and a low pressure on the leeward side result in a stabilizing rolling moment due to external load below the wing.
3. Local oblique air flow increases with increasing angle of attack.

In the case of a single missile or other external load, mounted asymmetrically, a roll-stabilizing effect results, corresponding to about 0.6 - 0.7 times the effect of two missiles or some similar load, when mounted askew on the fuselage. In respect to a load, suspended below the wing, the /86

contribution toward the roll resistance is halved if only one girder is loaded. The difference depends on the mutual interference between the arms.

An external load, asymmetrically mounted, especially if suspended below the wing, will also produce a zero contribution to the rolling moment which is independent of β but linearily dependent on the angle of attack. This contribution is especially noticeable in the case of a load suspended below the wing and it interacts with the gravity-induced rolling moment of the arms. At high speed the contribution of the aerodynamic zero-rolling-moment dominates. This effect is typical of all delta-winged aircrafts.

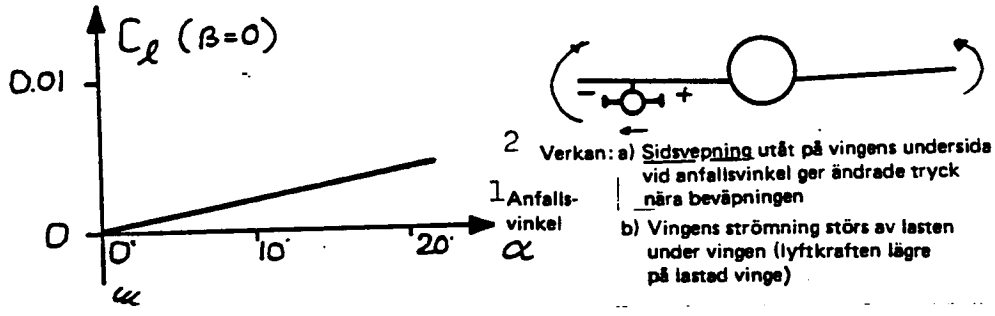

Fig. 106. Aerodynamic rolling moment due to an asymmetrically suspended external load below the wing.
1. Angle of attack.
2. Effect: A side-sweep outward across the lower surface of the wing at an angle of attach produces a change in pressure close to the armament.
b) The flow around the wing is disturbed by the load below the wing (the lift of a loaded wing is lower).

5.11 Effect of the Ailerons

Usually the flaps of the trailing edges of the wing are used both as ailerons and elevators in the case of airplains without a tail. In.practice this is accomplished in respect to both FPL 37 and 35 so that the deflection of the aileron is superimposed on that of the elevator and, thus, similar surfaces for steering are used.

The ailerons operate primarily so that a rolling moment is produced which varies in proportion to the magnitude of the deflection. The efficiency is usually expressed by the symbol $C_{l_{\beta a}}$, which is a measure, describing the variation of the rolling moment in relation to the deflection of the aileron.

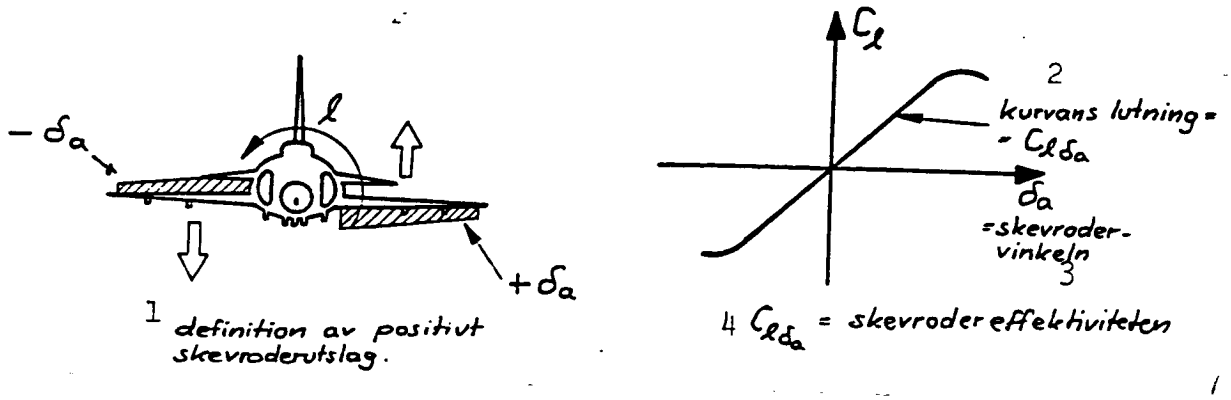

Fig. 107. Rolling moment due to deflection of the aileron.
Key: 1. Definition of a positive deflection of the aileron.
2. Gradient of the graph.
3. = angle of the aileron.

Just like the effect of the elevator the effect of the aileron , i.e., /87
$C_{l_{\beta a}}$, varies only insignificantly in relation to the angle of attack. As far as FPL 37 is concerned, it is satisfactory up to very wide angles of attack. At a high value of elevator deflection, a reduced aileron effect can be achieved already by minor deflections of the latter while saturating the effect of the stabilizer. This is, however, of little practical importance.

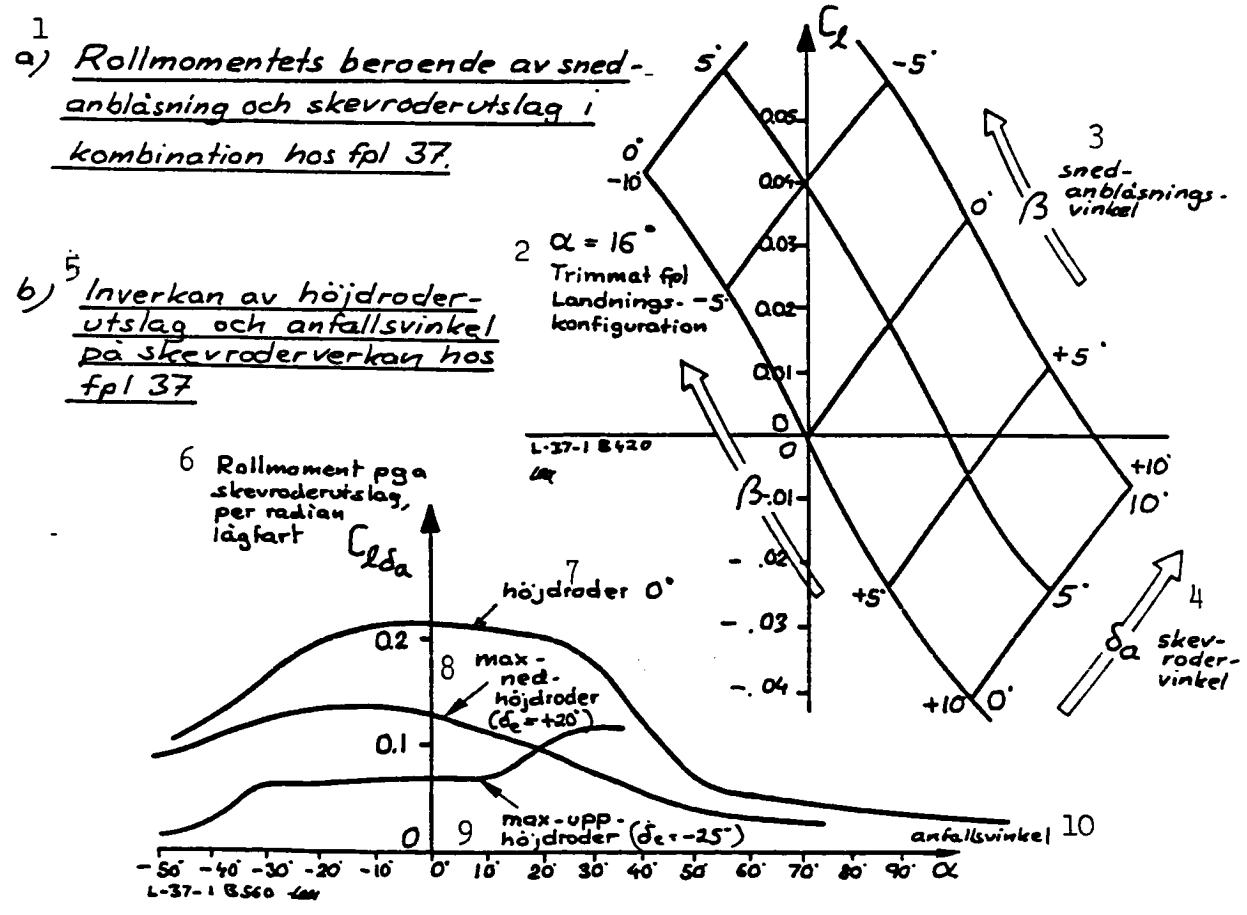

Fig. 108. Key: see. p. 129.

Key to Fig. 108:

1. a) Dependency of the rolling moment of FPL 37 on a combination of oblique air flow and deflection of the aileron.
2. $\alpha = 16°$, trimmed aircraft, landing configuration.
3. angle of oblique air flow.
4. angle of aileron, δ_a.
5. b) Effect of elevator deflection and angle of attack on the efficiency of the aileron of FPL 37.
6. Rolling moment due to aileron deflection, per radian, low speed.
7. Elevator at 0°.
8. Maximum deflection downward of elevator ($\delta_e = + 20°$).
9. Maximum deflection upward of elevator ($\delta_e = - 25°$).
10. Angle of attack.

The position of the tail fin on delta-winged aircrafts like FPL 35 and 37 constitutes a complication. In part, this results in a somewhat less satisfactory $C_{l\delta_a}$ due to interference, in part in a considerable yawing moment. The interference phenomenon is evident from Fig. 109.

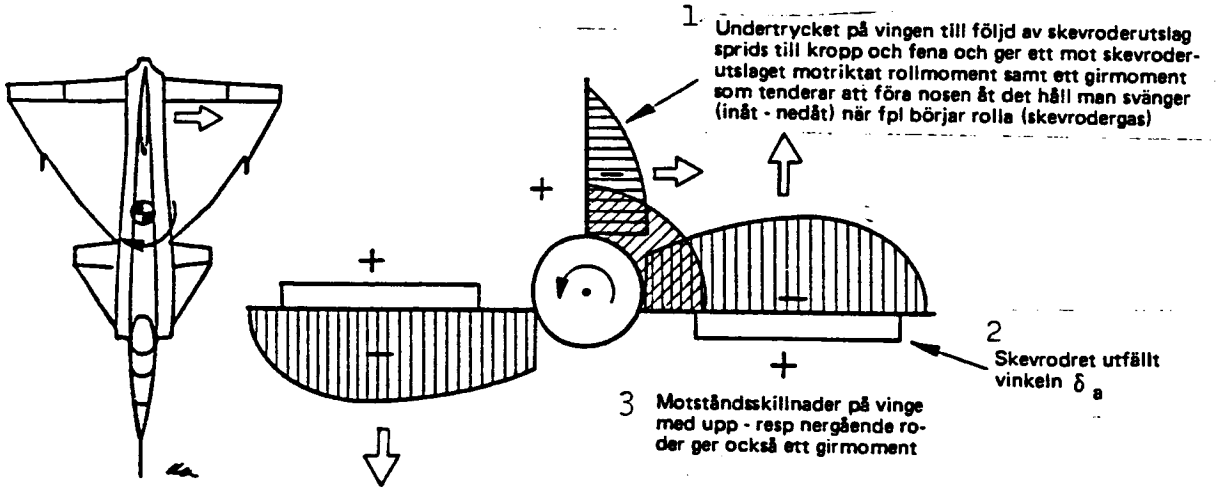

/88

Fig. 109. Effects of interference during deflection of the aileron.
Key: 1. The low pressure above the wing due to deflection of the aileron spreads out over the fuselage and the tail fin, producing a rolling moment, directed opposite to that of the aileron deflection, as well as a yawing moment, which tends to push the bow into the direction banked (inward - downward) when the aircraft starts to roll ("aileron gas").
2. Aileron deflected at the angle δ_a.
3. The difference in drag on the wing in relation to a flap deflected upward or downward will also produce a yawing moment.

The yawing moment developed attempts to direct the bow into the direction banked ("aileron gas"). This is a tendency opposite to that of a conventional aircraft with a large aspect ratio, where the contribution of the yawing moment due to deflection of the aileron is to a large extent produced by the increase in the contribution from the drag when the aileron is lowered on the lifting wing ("aileron brake"). In the case of FPL 37, there is also a less dominant contribution from the drag to the yawing moment, induced by the aileron. This explains the characteristics of the yawing moment of FPL 37 during deflection of its aileron.

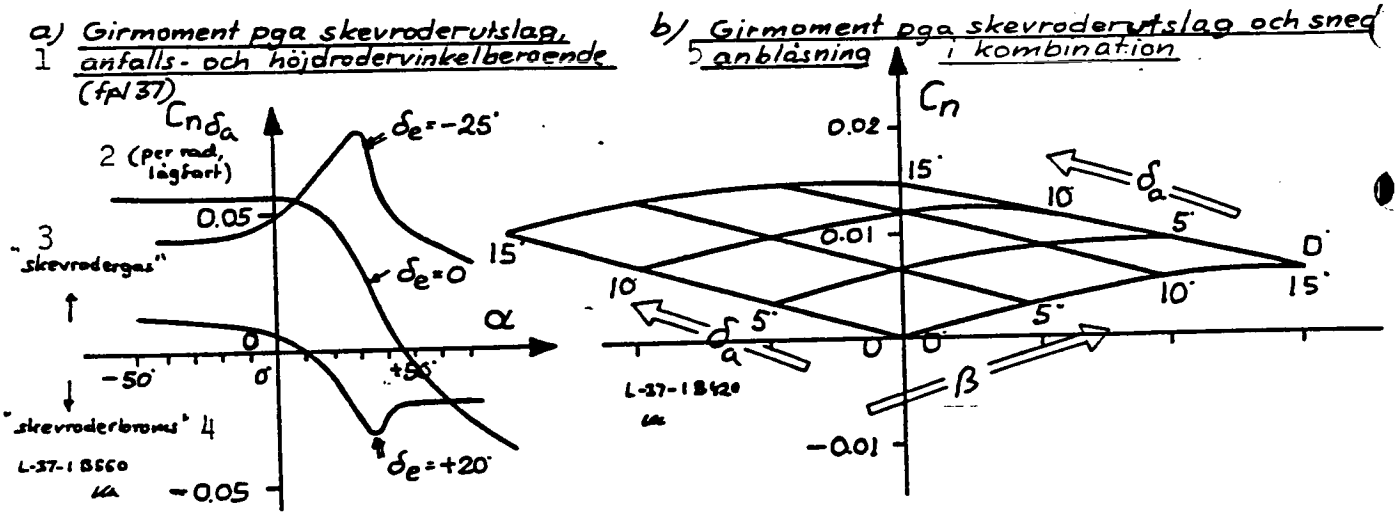

Fig. 110. Key: 1. a) Yawing moment due to deflection of the aileron, depending on the angles of attack and elevator; (FPL 37).
2. (per radian, low speed)
3. "Aileron gas".
4. "Aileron brake".
5. b) Yawing moment due to deflection of the aileron in combination with an oblique air flow.

The interference acting on the side of the fuselage and the tail fin as a consequence of the deflection of the aileron creates a component force as well, but this is in practise of minor inportance.

5.12 Dynamic Roll Resistance - Roll Damping

/89

When an aircraft spins, a resistance to the rolling moment develops due to the increasing angle of attack of the wing lowered and the decreasing angle of attack of the wing raised. The difference in lift gives rise to a rolling moment

which usually tends to counteract the rolling movement. As a measure of this counteraction, the term roll damping or C_{l_p} is used, where p means the angular speed of the rolling moment).

The correlation between roll damping and aileron effect determines how fast an airplane can roll and this is important for judging the value of the plane during combat.

When rolling, a yawing moment similar to that due to aileron deflection develops. The wing directed downward will have an increased angle of attack and the suction force on its topside will grow stronger. A corresponding suction force can be felt on the tail fin and it counteracts almost completely its own contribution. The gradient of the $C_n(p)$ graph, written as C_{n_p}, can be used as a measure of the yawing moment due to banking.

Both C_{l_p} and C_{n_p} of FPL 37 are illustrated in Fig. 111.

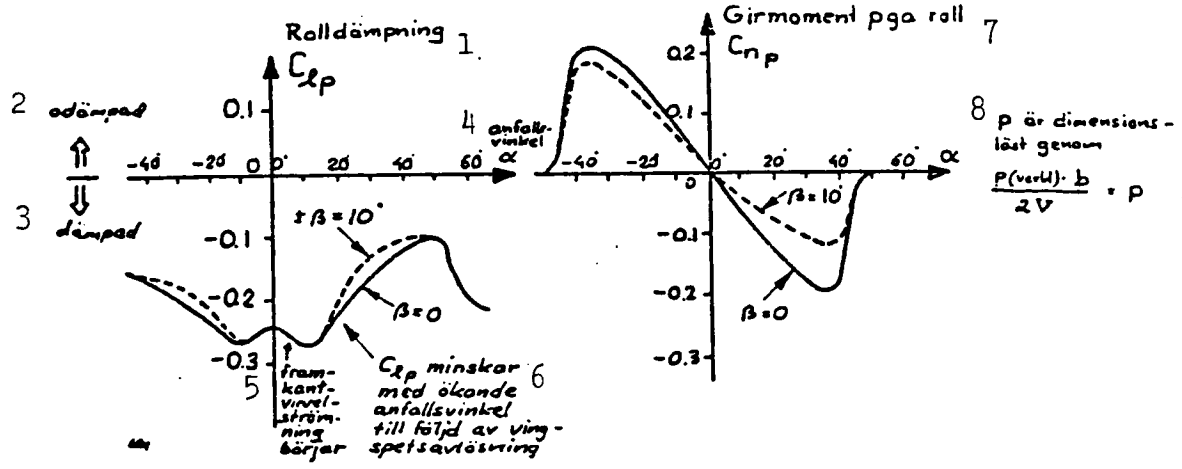

Fig. 111. Roll damping and yawing moment induced by banking of FPL 37 as a consequence of the angle of attack.

Key: 1. Roll damping.
2. Not damped.
3. Damped.
4. Angle of attack,
5. Vortex flow starting at the leading edge.
6. C_{l_n} ir reduced in relation to increasing angles of attack as a consequence of separation at the wing tip.
7. Yawing moment due to banking.
8. p is non-dimensional through $\frac{p(actual) \cdot b}{2V} \cdot p$.

When banking, the vortex system of the wing directed downward becomes relatively stronger in relation to that of the canard. Thus, its effect, forcing the vortices generated by the canard downward, is reinforced on that side, while the opposite takes place on the wing, pointing upward. Figure 112 illustrates how this phenomenon affects the roll damping and the yawing due to banking.

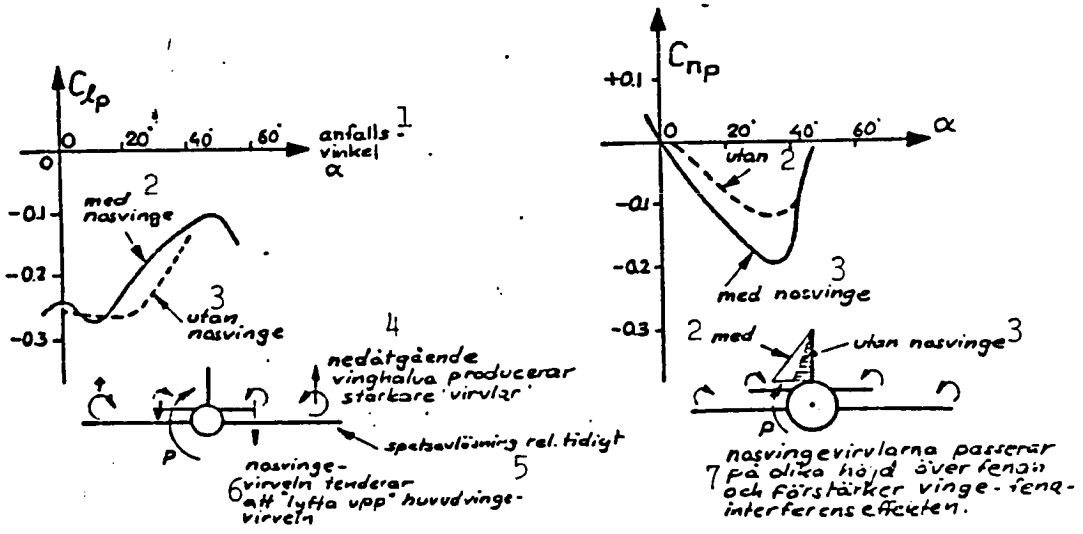

Fig. 112. Effect of the canard on the rolling and yawing moments induced due to rolling.
Key: 1. Angle of attack.
2. Canard present.
3. Canard not present.
4. The downward-directed half of the wing produces more powerful vortices.
5. Separation at the tip starts relatively soon.
6. The vortex of the canard tends to "elevate" the vortex of the wing.
7. The vortices of the canard pass the tail fin at various elevations and reinforce the effect of the wing/tail fin interference.

The detachment from the wing tip starts at a narrower angle of attack /90
on aircrafts with a canard since the vortex of the wing is simultaneously elevated by that of the canard. At narrow angles of attack the contribution of the canard to the roll damping is increased because the canard produces an up-sweep acorss the outer portion of the wing.

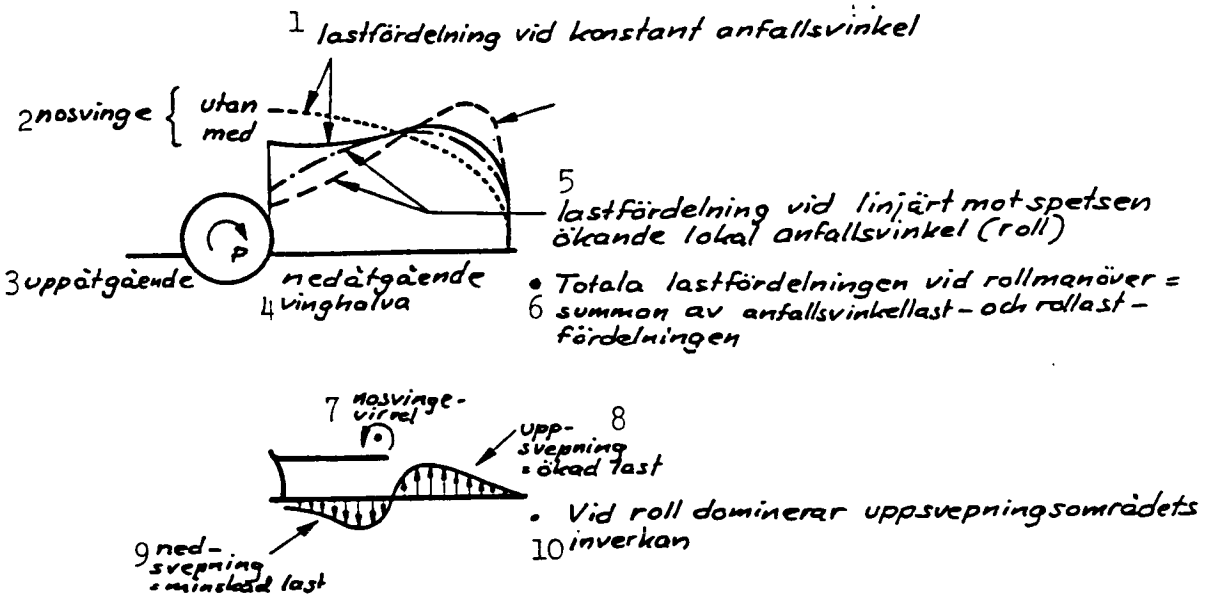

Fig. 113. Distribution of load when banking: effect of the canard.
Key: 1. Distribution of load at constant angle of attack.
2. Canard present (not present)
3. Wing half pointing upward.
4. " " " downward.
5. Distribution of the load at a local angle of attack increasing linearily toward the tip (a roll).
6. o Total distribution of load during a rolling maneuver= the sum of the distribution of the load due to the angle of attack + the rolling moment.
7. Vortex of the canard.
8. Up-sweep = increased load.
9. Down-sweep = decreased load.
10. When banking the effect of the up-sweep area dominates.

The reverse is valid for the opposite (upward-pointing) half of the wing. This phenomenon is responsible for the fact that the capacity for maneuvering when rolling at large angles of attack, e.g., when landing, is considerably improved in relation to an ordinary delta-winged aircraft. The dependency of the C_{n_p} on the angle of attack is great due to the fact that the vortices, generated by the canard, are kept low just as is evident from Fig. 108.

Figure 114 illustrates the C_{l_p} and the C_{n_p} of FPL 37 in comparison with those of some other aircrafts.

According to the data available, the roll damping and the C_{n_p} of a conventional swept-back aircraft varies in general less in relation to the angle of attack than they do in the case of a delta-winged aircraft. It is evident from Fig. 114 that FPL 37 behaves largely like an aircraft with a 60° delta wing. /91

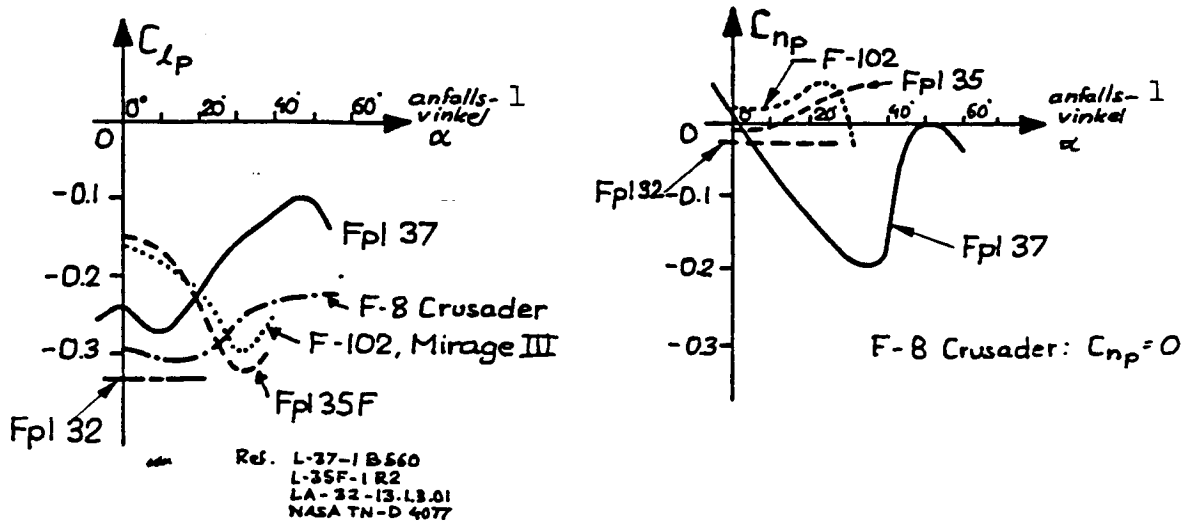

Fig. 114. Rolling and yawing moments induced by rolling; comparison with other aircrafts.
Key: 1. Angle of attack, α.

The C_{n_p} of most aircrafts is small. FPL 37 holds a special position because of its large C_{n_p} at wide angles of attack.

During a yawing moment and additional type of contribution to the rolling moment develops, because the wing meets with a curving field of air flow; cf. Fig. 115.

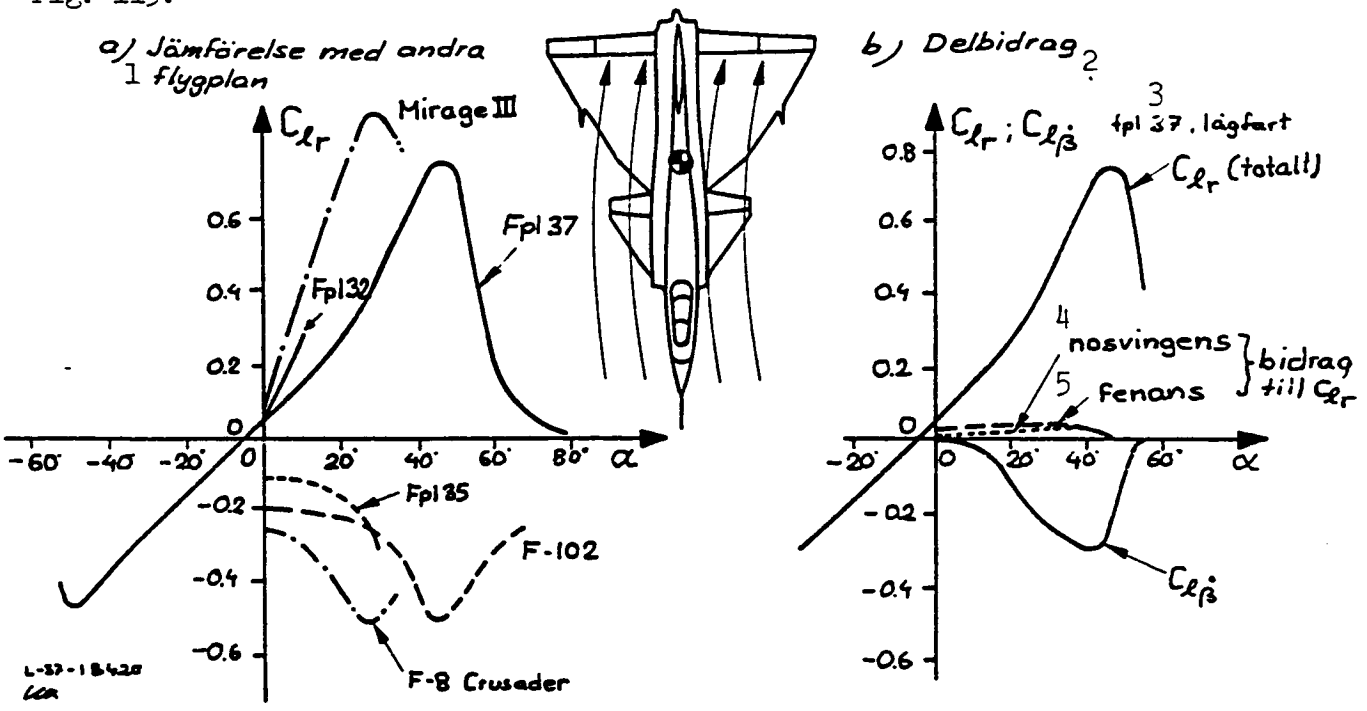

Fig. 115. Rolling moment due to yawing moment; FPL 37.
Key: 1. a) Comparison with other aircrafts. 2) Partial contributions. 3. FPL 37, low speed. 4. Contribution to C_{l_r} of the canard. 5. Contribution to the C_{l_r} of the tail fin.

In the case of FPL 37 the rolling moment due to yawing ($C_{l_r} - C_{l_{\dot{\beta}}}$) is small at narrow angles of attack but grows quickly larger at increasing angles of attack. The main contribution to C_{l_r} comes from the wing. The characteristics in relation to varying angles of attack can take different form in respect to different aircrafts and depends on the difference between the characteristics of the normal force of the aircraft ($C_{N_{(\alpha)}}$) and that of the angle of attack in relation to the gradient of the graph illustrating the normal force, C_{N_α}. This can lead to that C_{l_r} at wide angles of attack can vary within wide limits from being negative like in the case of FPL 35 or the F 8 or being strongly positive like in the case of the Mirage III. Other contributions to C_{l_r} (that of the tail fin itself and those of the interferences between the wing and the tail fin, the tail fin and the wing as well as the canard and the tail fin) cannot be ignored at narrow angles of attack. It results also in great differences between the various kinds of aircrafts. Just like in respect to C_{l_β} factors such as the vertical position of the wings and their sweep-back angle are effective.

The other contribution (i.e., the time lag contribution)= $C_{l_{\dot{\beta}}}$ can be ignored in respect to FPL 37 at narrow angles of attack. It tends to interact with C_{l_r} at wide angles of attack. Figure 115 illustrates both what C_{l_r} and $C_{l_{\dot{\beta}}}$ appear like at various angles of attack in respect to FPL 37 as well as a comparison between C_{l_r} of FPL 37 and that of other current aircrafts. /92

In general it is valid for the derivatives of the yawing/rolling moments and other so-called "cross-over derivatives" that they are difficult to determine directly by testing or calculating and, thus, they are comparatively unreliable.

SELECTED REFERENCES

a) Aerodynamics of FPL 37; Reviews. /93

1. Behrbohm, H., Aerodynamiske grundvalar foer FPL 37 [Aerodynamic basics of FPL 37], SAAB L-37-1 R4 (1963).

2. Holme, O., Den aerodynamiska bakgrunden till Viggens vingsystem [The aerodynamic background of the wing system of the Viggen]. In: Kosmos (1968).

3. Rooed, Aa., Development of the SAAB 37 Viggen. In: Le Ingenieur, No. 23, (1972).

b) System of Symbols, Etc.

4. Straeng, G., Foerslag till ett foer SAAB gemensamt aerodynamiskt- och flygmekaniskt beteckningssystem [Suggestions toward a common SAAB system of symbols for aerodynamics and aviation mechanics]. SAAB L-0-1 R8.

c) Aerodynamic Data and Solutions of Problems

5. Ingelman-Sundberg, M., Vindtunnelundersoekning av flygplan type 32. Del 1. 3- ech 6-komponentvaegningar (vid laaga hastigheter], [Wind tunnel experiments with FPL 32. Part 1. Weighting of 3 and 6 components (at low speed)]. FFA-AU-185:2 (1952.

6. Eklund, K. and Skoglund, K.-E., Vindtunnelundersoekning av schematiskt "ank"-flygplan med klaffblaasning paa nosvingen, [Wind tunnel tests of a schematic "duck"-aircraft with air jet flaps on the canard]. FFA-AU-I-482 (1983.

7. Eklund, K. and Skoglund, K.-E., Aerodynamiska stabilitetsderivator foer flygplan 32, [Aerodynamic stability derivatives in respect to FLP 32]. SAAB LA-32-13, 1.3.01.

8. Karling, K. et al., Aircraft 35 F^{II} Flight Simulator. Chapter 0. Aerodynamic data. SAAB L-35-F-1 R2 (1966).

9. Elvemär, P. and du Rietz, U., Stabilitets and styrningsunderlag foer flygplan 105, [Stability and control basis of FPL 105]. SAAB L-105-1- R5 (1965).

10. Karling, K., Data for Flight Simulator Design a/c AJ 37. SAAB L-37-1 B420; 2nd. revision, (1971).

11. Karling, K. Elvemar, P. et al., Aerodynamiska data foer FPL 37 i grundversionen (AJ37) utan yttre last, [Aerodynamic data of FPL 37 in tis basic version (AJ37) without external load]. SAAB L-37-1 R77 (1975).

12. Karling, K. and Elvemar, P., Aerodynamic tillskotts effecter p g a yttre last foer FPL 37 i AJ-, JA-, SK-, SH- och SF-version, [Aerodynamic effects due to contributions of an external load in respect to FPL 37, the AJ, JA, SK, SH and SF versions]. SAAB L-37-1 R82 (1977).

13. Karling, K., Problem i samband med foerbaettring av nosvingens lyftkraft, FPL 37, [Problems relating to improved lift of the canard; FPL 37]. SAAB L-37-1 B30 (1963).

14. Bennich, G., Bestaemning av dynamiska stabilitetsderivator foer typkonfiguration 1, FPL 37, genom vindtunnelfoersoek med paatvingad rotation, [Determination of dynamic stability derivatives in respect to type configuration 1 of FPL 37 via wind tunnel tests in combination with forced rotation]. SAAB L-37-1 B88 (1964).

15. Karling, K., Panel forces on aircraft SAAB 37. SAAB L-37-1,B129 (1964). /94

16. Karling, K., Panel forces on aircraft SAAB 37. Part 2. Side force derivatives. SAAB L-37-1 B139 (1964).

17. Bennich, G., Orienterande vindtunnelundersoekning av nosvingeflygplans superstallegenskaper, [Orienting wind tunnel tests of the superstall characteristics of aircrafts with a canard]. SAAB L-0-1 B51 (1964).

18. Rooed, Aa., Laengdstabilitet FPL 37 - en oeversikt oever kvarvarande problem, [Longitudinal stability of FPL 37 - a review of the problems remaining]. SAAB L-37-1 B301 (1966).

19. Rooed, Aa. and Karling, K., Girstabilitet FPL 37 - en oeversikt oever kvarvarande problem, [Yawing resistance of FPL 37 - a review of the problems remaining]. SAAB L-37-1 B303 (1966).

20. Holm, L.-Aa., Vindtunnelundersoekning av typkonfiguration 4 av FPL 37 vid laaga hastigheter och stora anfallsvinklar (superstall), [Windtunnel investigation of type configuration 4 of FPL 37 at low speed and wide angles of attack (superstall)]. SAAB-SCANIA L-37-1 B435 (1969).

d) Foreign Sources

21. Earnshaw & Lawford, Low-speed Wind Tunnel Experiments on a Series of Sharp-edged Delta-wings. RAE TN aero 2780 (1961).

22. Anglin, E. I., Relationship between magnitude of applied spin recovery moment and ensuing number of recovery turns. NASA TN D-4077 [no date].

23. Heffley & Jewell, Aircraft Handling Data. NASA CR 2144 (1972).

24. Wilson, R., Analytical Investigation of Spinning Behavior and Recovery from the Developed Spin on A 60 deg. Delta Wing Aircraft (Mirage III). W.R.E. TN HSA 137 (1968).

APPENDIX No. 1

Geometric Data of FPI. 37.

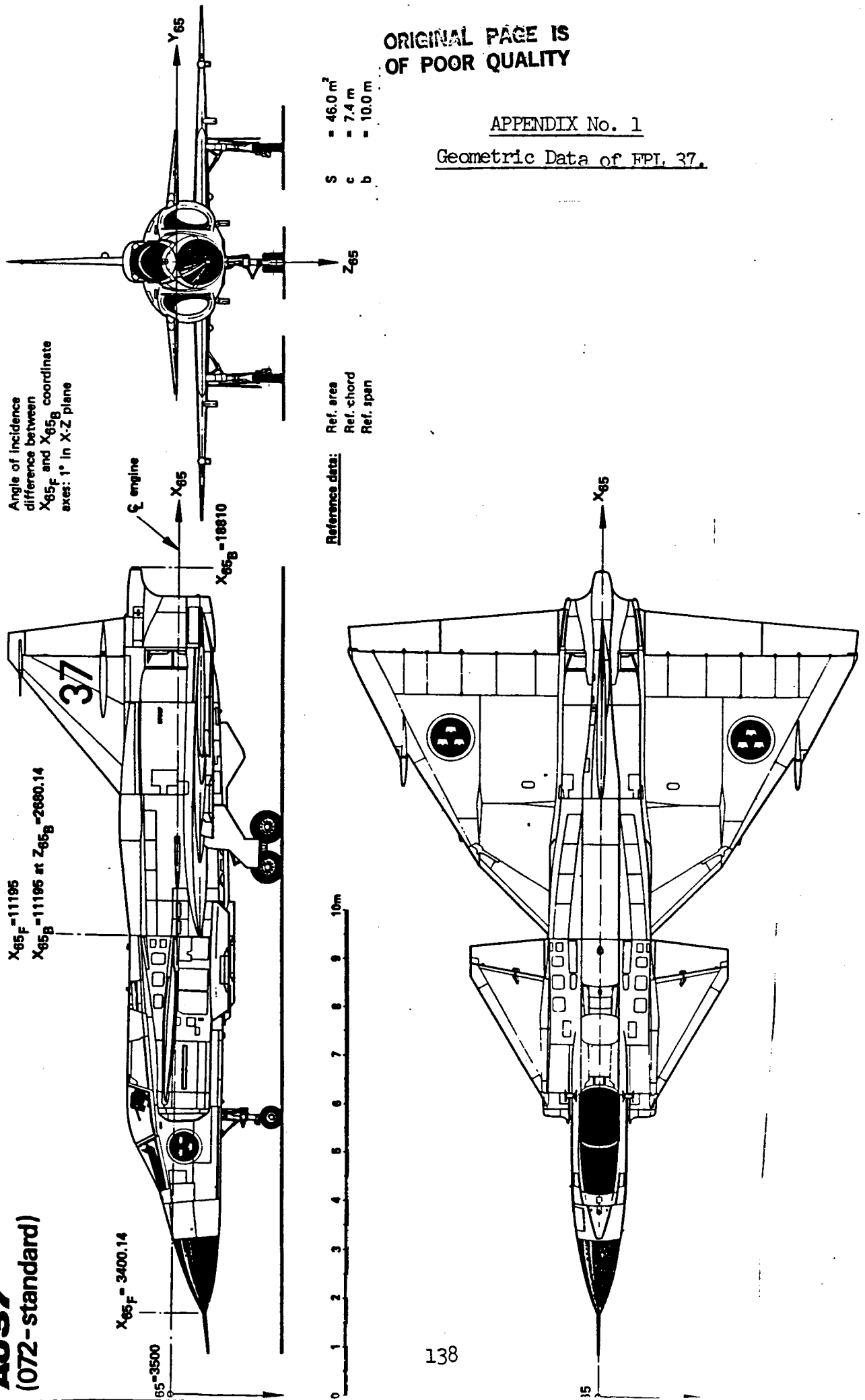

APPENDIX No. 2.

Key: 1. Definitions of positive directions of forces, moments and angles.

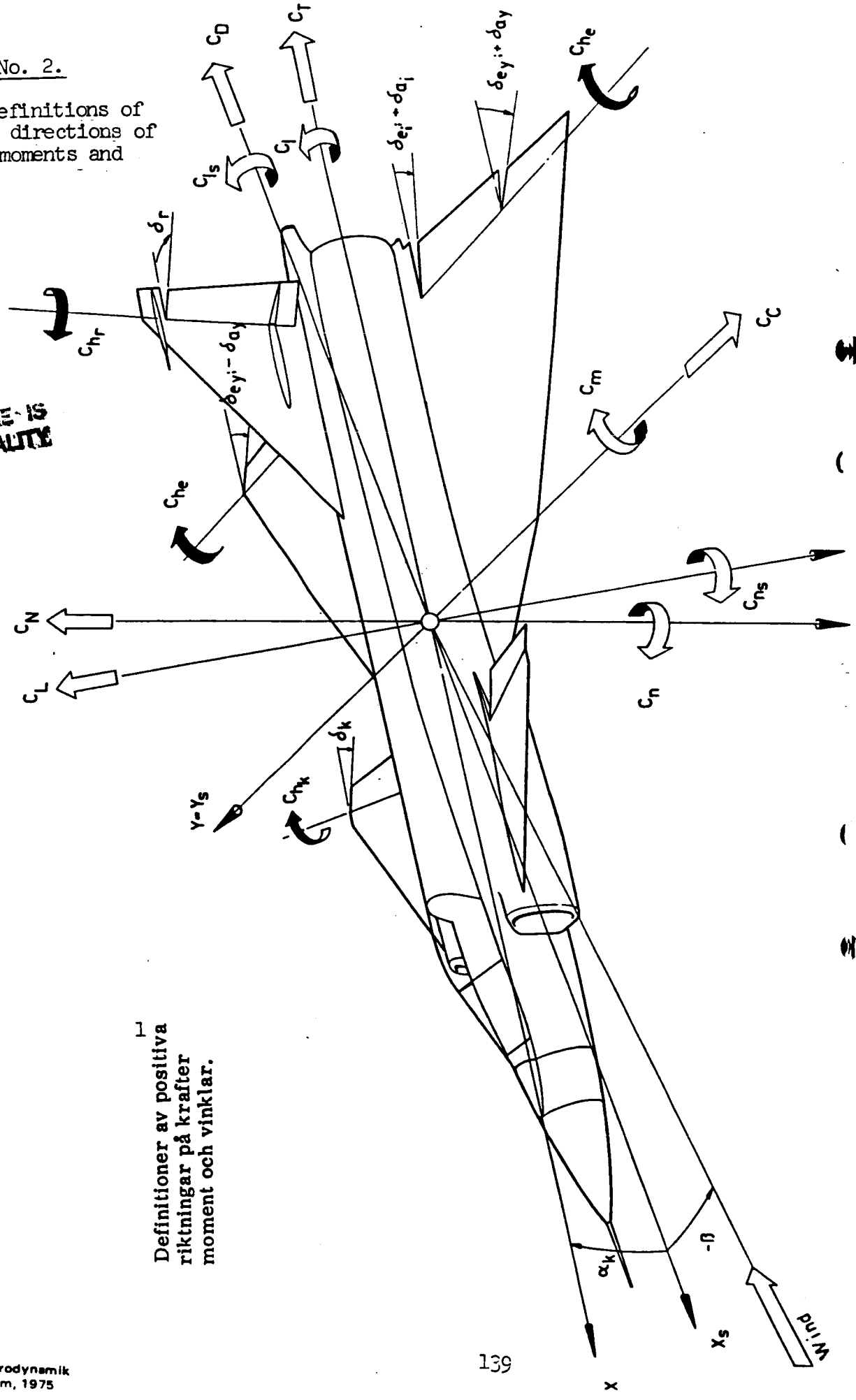

1 Definitioner av positiva riktningar på krafter moment och vinklar.